EXPERIMENTAL AND ANALYTICAL INVESTIGATION OF THE SHEAR STRENGTH OF UNSTIFFENED TAPERED STEEL MEMBERS

By:

Nicholas A. Redmond

Thesis submitted to the faculty of the

Virginia Polytechnic Institute and State University

in partial fulfillment of the requirements for the degree of

MASTER OF SCIENCE

In

CIVIL ENGINEERING

APPROVED:

Dr. Thomas M. Murray, Chairman

Dr. Finley A. Charney

Dr. W. Samuel Easterling

November 28, 2007

Blacksburg, Virginia

EXPERIMENTAL AND ANALYTICAL INVESTIGATION OF THE SHEAR STRENGTH OF UNSTIFFENED TAPERED STEEL MEMBERS

By
Nicholas A. Redmond

Thomas M. Murray, Chairman
Civil and Environmental Engineering

ABSTRACT

Tapered beams and columns are often used in single story gable framed steel buildings for reasons of economy. By varying the resistance to bending in similar proportion to the bending moments, more economical structures can be obtained. The beam and column connection, or knee area, is generally subject to the greatest bending moments. It is therefore comprised of the deepest sections of the tapered members, which also possess the least resistance to shear buckling.

The web element's stress distribution in this region of relatively complicated geometry is unknown. For this reason, web stiffening plates are commonly used to brace the slender web elements against elastic shear buckling. The design and proper installation of these relatively small elements, while proven to be effective, is also costly. Because it is desirable to remove the stiffeners, the shear behavior of unstiffened tapered members near the moment connection was the primary focus of this study. Four knee area specimens were tested to failure under simulated gravity load conditions.

The specimens were analyzed according to the AISC shear provisions for prismatic members. The appropriateness of a modified shear force, which accounts for the influence of inclined flanges, and the role of initial web imperfections were examined as well. Finally an analysis method which most consistently produces conservative results is proposed.

ACKNOWLEDGEMENTS

I would like to express my sincere thanks to Dr. Thomas M. Murray for his influence and patience throughout the course of this project. His insight and guidance in the experimental and analytical phases of this study and finally the writing of this thesis were invaluable. I would also like to thank Dr. Finley A. Charney and Dr. W. Samuel Easterling for their thoughtful review of this work while serving on my advisory committee.

I would like to thank American Buildings Company for sponsoring this investigation, and thereby financing a portion of my studies. I am also grateful to Mrs. Marion Via, for her generous support of the Charles E. Via, Jr. Department of Civil Engineering, and to the Via Endowment Program administrators for their expressed confidence in me through the Via Research Fellowship. I am grateful to have been given the opportunity to study and work at Virginia Tech.

I have benefited form the advice and experience of Mr. Brett Farmer, Mr. Dennis Huffman and Mr. Clark Brown, and their practical contributions to the experimental phase of this project are gratefully acknowledged. Working along side so many industrious and talented people at the Structures and Materials Lab has been a pleasure, and I sincerely appreciate their assistance during the experimental portion of this study. I would like to thank Jon Bagwell, Josh Boggs, Adam Bowland, Eric Crispino, Brad Davis, Ben Dymond, Hunter Hodges, Bryan Loflin, Chris McGill, Jim Ordija, Andres Sanchez, Mike Seek and Pratik Shah for their help and good company.

I am grateful to all of my family for their support throughout my studies, and most especially my wife Leah. Her confidence and friendship are my most valuable possessions. Finally I am grateful to the Creator of the natural laws, the material resources, and the inquisitive human minds that have made this study possible.

TABLE OF CONTENTS

LIST OF FIGURES

Figure Page

LIST OF TABLES

Table | Page

CHAPTER 1

BACKGROUND

1.1 General

Tapered beams and columns are often used in single story gable framed steel buildings for reasons of economy. By increasing the resistance to bending in similar proportion to the increased bending moments, more economical structures can be obtained. The presence of varying bending moment is always accompanied by shearing stresses. While the design of members with variable cross-section for the resistance of flexural stresses has been thoroughly investigated, the design of tapered members for resistance to shear has not. The current design practice for sizing such structural elements for shear loads is to treat them as non tapered elements and employ established methods for prismatic beams.

While the resistance of an I-shaped member to flexural stresses is generally increased as the web height increases, the opposite is true of a slender web's resistance to shear buckling. The connection details of such structures typically account for full moment continuity at the deeper end, and the narrow ends are in the locations of lowest moment. The beam and column connection, or knee joint, is made through the use of bolted moment end-plates, allowing for individually built-up welded beams and columns to be shop fabricated, with only bolt connections required during construction, which is also economical. This knee area of the frame is subject to the greatest bending moment, and therefore comprised of the deepest sections of the tapered members, which also possess the least resistance to shear buckling.

The actual shear capacity of the web elements in this region of relatively complicated geometry is unknown. For this reason, web stiffening plate elements are commonly used to brace the web against shear buckling. The design and proper installation of these relatively small elements, while proven to be effective, can be costly.

The elastic shear buckling strength of the webs of tapered members near the moment connection was the primary focus of this study. Four gable frame knee area sub-assemblies were tested to failure under simulated gravity loads. The shear forces in the webs were determined in two different ways. The first is simply the applied shear force at the cross-section of interest, and is called the unmodified shear force. A modified shear force was also determined which

assumes that the inclined flanges reduce the shear force carried by the web. These results were compared to the current AISC design provisions for prismatic member shear design.

This study addresses the appropriateness of a modified shear force and the possible influence of initial web imperfections on the shear performance of slender unstiffened tapered steel members. The predicted strengths are compared to the modified and unmodified experimental shear forces, and an analysis method which most consistently produces conservative results is proposed.

1.2 Literature Review

1.2.1 Tapered Members

The use of tapered members was first formally proposed by Amirikian (1951) under the title "Wedge-Beam Framing", for the purpose of assuring "appreciable savings in weight and economies in the cost of construction". This is achieved through imposing hinges at the midspan of beams and base of columns – the narrow ends of the wedge, and fixed connections at wider ends of the wedge – the beam/column interface. In this way the flexural stresses are controlled by means of connection detailing, and the members were sized with a variable cross-section to efficiently accommodate these stresses.

Analysis methods for the resulting indeterminate structures were given, as well as several design examples. As a design aid general deflection expressions were provided for various types of tapered members, including doubly tapered members which vary in both depth and width, under various loadings conditions by way of virtual work. Furthermore, Amirikian provided tables to facilitate the solution of simultaneous equations, in which the interaction of adjacent bays could be accounted for. He then introduced simplifying approaches in an effort to make the solutions to indeterminate frame analyses more amenable to slide rule calculations.

In 1966 a joint committee of the Structural Stability Research Council and the Welding Research Council was formed to deepen the understanding of and formulate design criterion related to tapered steel members. Under the sponsorship of the Metal Building Manufacturers Association (MBMA), the American Institute of Steel Construction (AISC), the American Iron and Steel Institute (AISI), and the Naval Facilities Engineering Command (NFEC), research studies were carried out at the State University of New York at Buffalo (SUNY) under the principal direction of Professor George C. Lee.

Design of Single Story Rigid Frames (Lee *et al*. 1981) is a published summary of more than a decade of research work undertaken at SUNY, and offers a discussion on indeterminate frame analysis, descriptions of tapered member behavior under various loading conditions, as well as extensive design examples. It is claimed that tapered members are used in construction both to provide an aesthetically pleasing frame outline, and also to achieve comparatively large reductions in weight. It also stated that tapered members are best designed according to elastic rather than plastic analysis, due to the fact that plastic design assumes that inelastic yielding and plastic rotation occur locally, after which bending stresses are redistributed. The design of tapered members is motivated by a desire to develop elastic yield stresses in a more uniform manner, by closely matching the member's flexural resistance to the demand. Thus areas of low bending stress do not exist to safely allow the redistribution of stress associated with a plastic hinge mechanism.

Several Welding Research Council (WRC) Bulletins were published from the work conducted at SUNY, which addressed the analytical and experimental results of investigations into various stress conditions of web tapered, welded steel I-shaped members. The first and foremost of these papers dealt with the theoretical axial and bending stress analyses of tapered members, and then proposed design formulas for adequate proportioning of I-shaped tapered members. The design formulas were extensions of the then governing AISC-ASD provisions for prismatic members, algebraically modified to account for the tapering geometry (Lee *et al*. 1972). Other WRC Bulletins concerned various aspects of tapered member design. The essential approach taken throughout the SUNY body of work was to use prismatic member provisions, applied with an adjusted tapered beam length and section properties associated with the critical cross-section for the load type under consideration.

These adapted provisions, first codified as a supplement (AISC 1974) to the *Specification for the Design, Fabrication and Erection of Structural Steel Buildings* (1969), endured relatively little revision until finally being removed entirely from the 2005 AISC *Specification for Structural Steel Buildings* (AISC 2005a). Throughout the tapered member provisions' tenure in the AISC Specifications, treatment of both shear design and concentrated forces were referenced to the applicable provisions for prismatic members.

1.2.2 Theoretical Shear Buckling

The first practical analytical solution to the shear plate buckling problem is attributed to Timoshenko by Bleich in his compendium *Buckling Strength of Metal Structures* (Bleich 1952). Timoshenko derived a critical shear buckling stress for a rectangular plate, simply supported on all four edges, as an approximate solution to St. Venant's differential equation describing the deflection of thin plates loaded at their mid-plane (Bleich 1952). Timoshenko's critical elastic shear buckling stress is:

$$\tau_{cr} = \frac{k\pi^2 E}{12(1-\nu^2)}\left(\frac{t}{h}\right)^2 \tag{1-1}$$

Where:
k = plate buckling coefficient
E = Young's Modulus, 29000 ksi
ν = Poisson's ratio
t = plate thickness
h = plate width

Timoshenko also proposed a plate buckling coefficient for small values of aspect ratio which is the ratio of the length of the rectangular panel to its depth. The value of the plate buckling coefficient is determined from the aspect ratio of the plate and the boundary conditions along the edges of the plate. Plate buckling coefficient solutions are available for combinations of boundary conditions and aspect ratios varying from one to infinity. Based on these solutions, Bleich proposed an approximate parabolic form for the plate buckling coefficient, using the pinned edge condition. This approximation is given in Equation (1-2), which varies with the aspect ratio, and intersects the two known extreme values for infinite aspect ratio and square aspect ratio.

$$k = 5.35 + \frac{4}{\left(\frac{a}{b}\right)^2} \tag{1-2}$$

Where:
a = panel length
b = panel depth

By this formulation, it is assumed that the longer plate dimension is always "a". However in plate girder design it is convenient to let "h" represent the girder depth, and "a" the length of the panel. In this case Equation (1-1) is rewritten in the form:

$$\tau_{cr} = \frac{k\pi^2 E}{12\left(1-\nu^2\right)\left(\frac{h}{t_w}\right)^2} \tag{1-3}$$

Where: h = girder web height
t_w = web panel thickness

With this form the aspect ratio can take values less than unity, and as such Equation (1-2) requires a new formulation. The plate buckling coefficients for plate girders are:

$$k = 4.00 + \frac{5.34}{\left(\frac{a}{h}\right)^2} \qquad \text{for} \left(\frac{a}{h}\right) \le 1 \tag{1-4a}$$

$$k = 5.34 + \frac{4.0}{\left(\frac{a}{h}\right)^2} \qquad \text{for} \left(\frac{a}{h}\right) \ge 1 \tag{1-4b}$$

Where: h = girder web height
a = panel length between transverse stiffeners

These plate buckling coefficients were derived for a web plate that is simply supported at all four edges. Though not true for built up plate girder webs, this formulation has been generally accepted as sufficient for design purposes, and the treatment of the web as simply supported at the flanges is a conservative estimate. While the use of this conservative simplification is a matter of some contention, the codified standards for steel design still make this assumption (AISC 2005a). It is also generally assumed that for relatively slight tapering angles, the rectangular plate shear buckling relationships are adequate.

1.2.3 Experimental Shear Strength of Plate Girders

The current codified design of plate girders for shear effects has its empirical base in work conducted at Lehigh University from 1957 to 1960 by Konrad Basler and Bruno

Thurlimann. The purpose of the investigation was to more quantitatively determine the influence of post-buckling strength observed in stiffened plate girders, for which plate buckling theory had been unable to account. Experimental results were published in a Welding Research Council Bulletin, and analytical results were published as three separate papers concerning independently the strength of plate girders in bending (Basler and Thurlimann 1961), shear (Basler 1961a), and the combined effects thereof (Basler 1961b). Although the studies were primarily directed at stiffened plate girders, the design for shear forces in unstiffened members has been influenced by results of Basler (1961a).

The interaction between shear and flexure is certainly of interest in the study of shear force effects in tapered members, due to the fact that a member may not be loaded in shear without the presence of flexural load effects. Also the compressive web stresses due to flexure may act to destabilize the web, while tensile stresses might have a stabilizing effect with regard to shear buckling. These interactions are however not supported by any analytical evidence, and the interaction of flexure and shear as defined by Basler (1961b) is an empirical relationship based on stiffened web panel tests which include the effects of a post buckling tension field. As such, the flexure and shear interactions in tapered unstiffened members cannot be explicitly denied, nor can they be applied ad hoc to the current study without further investigation.

1.2.4 Determination of Shear Forces

The determination of shear forces which a tapered member must be designed to resist is still a matter of some controversy. Clearly the most basic and conservative approach would assume that all of the internal shear forces, required by equilibrium to balance the externally applied shear loads, be supplied by the web which is the case with prismatic members. Several rational methods for the unique treatment of web shear forces in members of variable cross-section have been proposed in the literature. All of these recommendations offer effectively the same advice, with varying degrees of simplification, and will be generally referred to as modified shear.

Williams and Harris (1957) offered possibly the first discussion of the influence of inclined flanges on the web shear forces. Figure 1-1 shows the authors' description of flange forces due to flexural stresses. The motivation for the proposed orientation of flange forces was that the principal stresses at the extreme fibers of the cross-section are parallel to the edge of the

flange. By this argument, the normal force due to bending stresses is a component of the flange force.

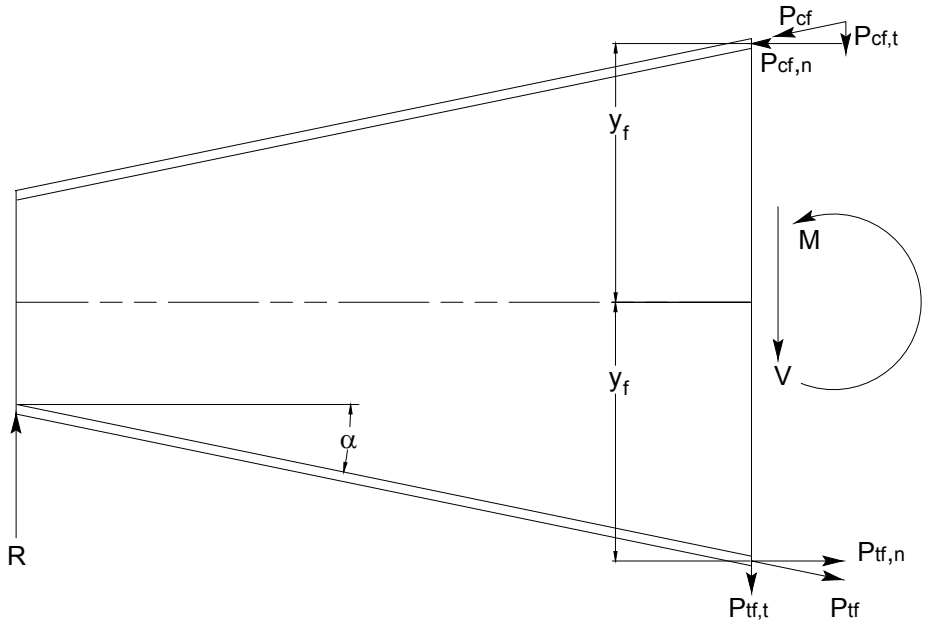

Figure 1-1 Flange Stresses Due to Bending

They proposed that under an elastic flexural stress distribution, the compression flange axial force, P_{cf} could be closely approximated by the following:

$$P_{cf} = \frac{A_f M y_f}{I \cos(\alpha)} \tag{1-5}$$

Where: P_{cf} = axial compression flange force
A_f = area of the flange plate, (b_f x t_f)
y_f = distance from section neutral axis to flange center of gravity
I = moment of inertia of the cross-section computed with flange plate area

This is an approximate solution because the moment of inertia has been simplified. This moment of inertia is computed using the flange plate area, A_f rather than the more precise flange area normal to the cross-section, $A_f/\cos(\alpha)$ where α is the angle that defines the taper of the flange. The authors claimed that the calculation of transverse flange stresses can be accurately

based on a simplified moment of inertia when a large concentration of the cross-section is contained in the flanges. The transverse component of this force, parallel to the cross-section, is:

$$P_{cf,t} = P_{cf} \sin(\alpha) \tag{1-6}$$

The transverse force component of the tension flange force, $P_{tf,t}$ is found similarly. Finally, the modified shear force resisted by the web is:

$$V_w = V - P_{cf,t} - P_{tf,t} \tag{1-7}$$

Another of the first attempts to describe the stresses in tapered members was given by Bresler et al. (1968) which was first published in 1960. The authors suggested that for any element in a cross-section, radial stresses could be resolved into normal and shearing stress components. It is suggested that the integration of these shear stresses on the cross-sectional area, added to the tangential shear stresses, are equal to the external shear force acting on the cross-section. This concept is shown graphically in Figure 1-2.

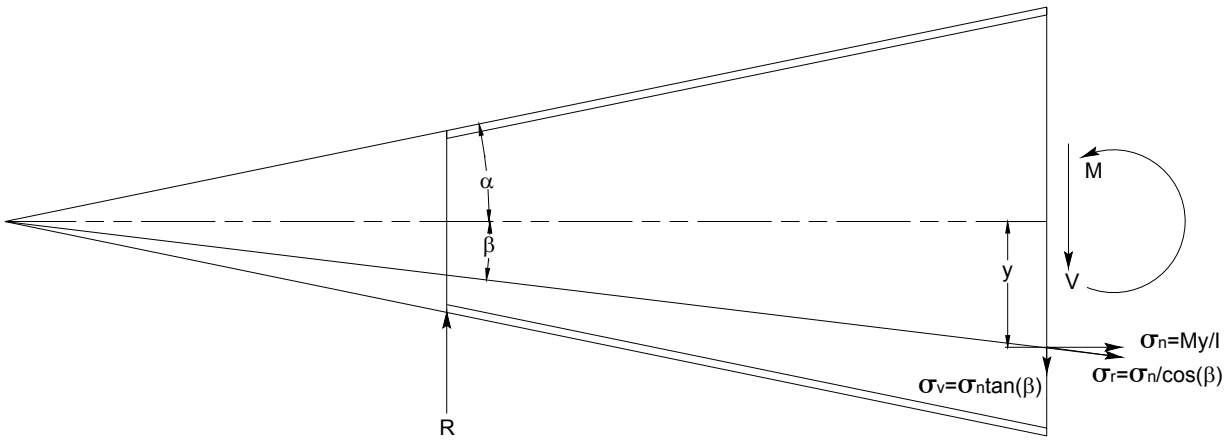

Figure 1-2 Bresler et al. Modified Shear

In this case, the sum of the shear force components resulting from the radial stresses acting on the cross-section is:

$$V_r = \int \sigma_v dA \tag{1-8}$$

Where: σ_v = shear component of radial stress, $\sigma_v = \sigma_r (\sin(\beta)) = \sigma_n (\tan(\beta)$
σ_n = normal flexural stress, My/I
σ_r = radial stress, $\sigma_n /(\cos(\beta))$
β = angle to area element; varies from 0 at neutral axis to α at extreme fibers

The remainder of the shear force required for equilibrium is made up of what the authors call tangential shearing stresses acting on the cross-section. It is recommended that the effect of these tangential stresses be approximated by:

$$\tau = V_t Q / It \tag{1-9}$$

Where: τ = tangential shear stress
V_t = force that produces τ, $V_t = V - V_r$
V = total shear force on the cross-section
I = cross-section moment of inertia
t = cross-section element thickness
Q = first area moment

Equilibrium is then satisfied by:

$$V = V_r + V_t \tag{1-10}$$

In this way the shear force that a prismatic beam would be required to resist, V_t is reduced by the transverse components of forces from radial flexural stresses. Identical recommendations were presented by Tall (1974).

Blodgett (1966) proposed a determination of web shear forces very similar to that of Williams and Harris (1957), with the simplifying assumption that all of the bending stresses are concentrated in the flanges. These stresses are then resolved into components normal and

parallel to the transverse cross-section. Figure 1-3 provides reference for the following compression flange transverse force:

$$P_{cf,t} = \frac{M}{d}\tan(\alpha) \tag{1-11}$$

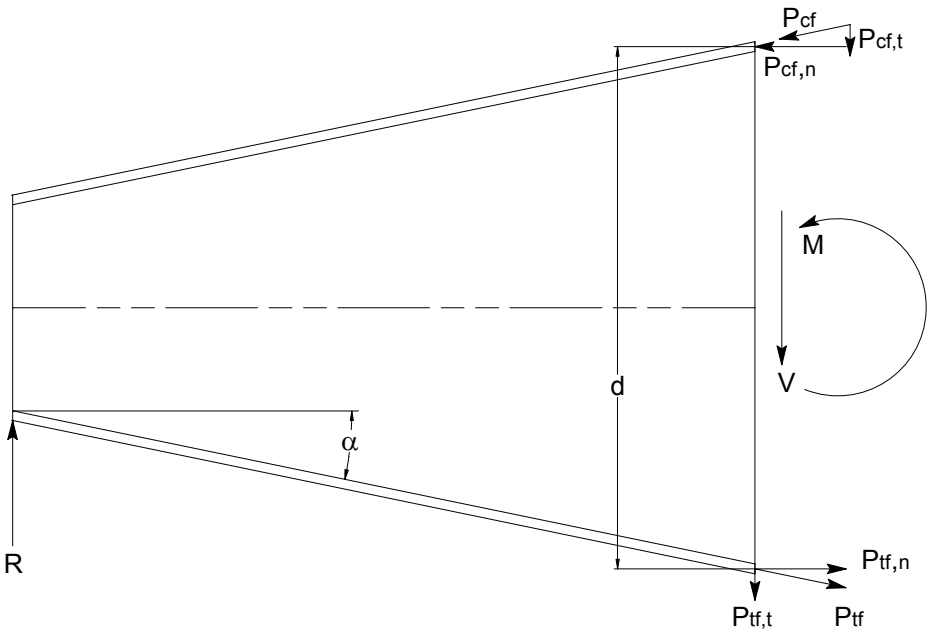

Figure 1-3 Blodgett's Modified Shear (Reduced Web Shear)

For this case of loading, the following equilibrium of vertical forces must be satisfied, which reduces the shear resistance required of the web:

$$V = V_{web} + P_{fc,t} + P_{ft,t} \tag{1-12}$$

Where:
V = applied shear force at cross-section
V_{web} = shear resistance provided by web
$P_{fc,t}$ = compression flange contribution = (M/d)tan(α)
$P_{ft,t}$ = tension flange contribution = (M/d)tan(α)

Blodgett warns that care must be taken when applying this modified shear approach because the influence of the flanges does not reduce the shear force in the web in all cases. The

orientation of the member and the correct sense of the internal forces must be properly identified. An example in which the flange contributes a force that increases the demand on the web beyond that which should be required for equilibrium is shown in Figure 1-4. In this case the effect of the negative bending moment in the flanges increases the web shear force required to satisfy equilibrium.

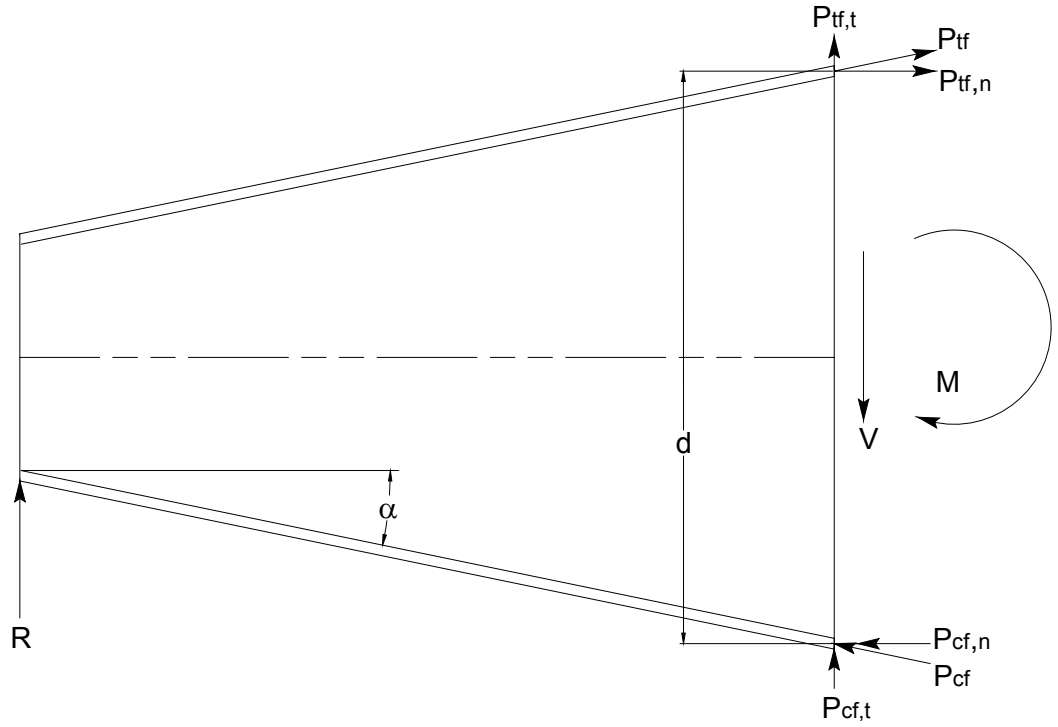

Figure 1-4 Blodgett's Modified Shear (Increased Web Shear)

The vertical equilibrium for the orientation shown in Figure 1-4 is given by:

$$V = V_{web} - P_{fc,t} - P_{ft,t} \tag{1-13}$$

Where: V = applied shear force at cross-section
V_{web} = shear resistance provided by web
$P_{fc,t}$ = compression flange contribution = (M/d)tan(α)
$P_{ft,t}$ = tension flange contribution = (M/d)tan(α)

It is noted that since the modified shear force proposed by Blodgett assumes the bending moment is resisted only by the flanges, a larger transverse flange component and lower web shear force results than if an elastic stress distribution is used.

1.2.5 Experimental and Analytical Studies of Tapered Plate Girders

Little has been done to verify that the provisions for prismatic girder shear design also apply to plate girders of variable cross-section. An experimental study of eight tapered member knee area specimens by Sumner (1995) found that while the AISC provisions for flexure in tapered steel members were quite accurate, the predicted shear strength of tapered plate girders fell short of the experimental values obtained, in some cases by as much as 50 percent. It was proposed that the conservative estimates were attributable to a tension field developed over the full length of the tapered member, providing a post buckling reserve of strength.

By applying the tension field action provisions for prismatic girders provided in AISC (1994), neglecting the upper limits on aspect ratios, and using the average panel depth to determine the aspect ratio, less conservative values were obtained. This analysis was then combined with a shear/flexure interaction provision for prismatic members. These results were however somewhat inconclusive because only one of the specimens failed in shear, making direct comparisons of predicted ultimate strength to actual shear capacity impossible. The lack of evidence that shear buckling occurred also makes the assumption of post buckling strength somewhat tenuous. The possible reduction in web shear forces due to the influence of inclined flanges, or modified shear, was not investigated.

Mirambell and Zarate (2004) presented recommendations for the treatment of tension field action as well as a shear and flexure interaction based on FEM analytical modeling. Prior to this work, Mirambell and Zarate (2000) presented a shear buckling coefficient and critical shear stress expression for web tapered members. A finite element model was created and parametric studies conducted to determine the relative influence of flange slenderness, angle of taper, and the ratio of flange width-greatest web depth, on the plate buckling coefficient.

One value of critical shear stress results from the proposed analysis, which is then applied to the analysis of the web at the narrow end of the member. Presumably in design the web thickness and aspect ratio would be determined such that the critical stress is not exceeded at the narrow end of the specimen, as this was considered the critical cross-section in the development of the plate buckling coefficients. This is somewhat counterintuitive, and one would expect the critical buckling section to be at the cross-section of greatest slenderness. The analysis does not include flanges of unequal thickness however, it might be reasonable to assume both flange

thicknesses equal to that of the thinner flange, as the effective restraint provided by the flange to web rotation would be conservative.

The authors note that the boundary conditions are appropriate for a panel located near the midspan of a stiffened member, and both ends of the panel are restrained against translation in the longitudinal direction. The narrow end flanges are allowed to rotate about an axis normal to the plane of the web, however the restraint against translation in the longitudinal direction essentially fixes the narrow end rotationally. This allows a moment to be resisted at the narrow end and is therefore inappropriate for end panels lacking the rotational restraint provided by adjacent panels. Analysis of the specimens used in the current study according to these provisions is inappropriate. However, the proposals by Mirambell and Zaraté show promise for intermediate panels of stiffened tapered specimens, and warrant a comparison with experimental data which cannot be offered here.

Prior to this study, a preliminary analytical investigation was conducted at Virginia Tech by Sullivan and Charney (2006), to assess the feasibility of removing transverse stiffeners from the knee area connection of gable and portal frames. The finite element model employed both material and geometric nonlinearity to determine the relative influence of transverse web stiffeners at the knee area of the frames. The study showed that removing the transverse stiffeners reduced the buckling strength by approximately 16 percent, and therefore their exclusion from the knee area was considered feasible.

Another Finite Element Method study of web tapered members was conducted by Shah (2007), in conjunction with the current investigation. Both material and geometric nonlinearities were accounted for in the models, and it was found that the predictions for ultimate loads were higher than experimentally observed failure loads by about 40 percent. This difference was attributed to idealized material response in the inelastic range, as well as to large measured initial web imperfections which were not completely captured by the computer models.

1.3 Scope and Purpose of Research

The purpose of this study was to determine the shear capacity of unstiffened, linearly tapered steel members with slender webs, and to recommend an efficient design method. These objectives are addressed in the following way. In Chapter 2 the experimental study is described in detail. The test assemblies and instrumentations used are described and a description and

interpretation of the results is given. Chapter 2 also contains a description of measurements made of the initial imperfections present in the webs. Finally the distributions of shear stresses determined form measured web shear strains are also presented. Chapter 3 contains a description of the analysis methods used. A modified shear force similar to that proposed by Williams and Harris (1957) and an unmodified shear force are used to describe the shear forces on the web. The web shear strengths were predicted according to AISC provisions for prismatic members. A comparison of the Experimental and Analytical results is presented in Chapter 4. Chapter 4 also contains a presentation of six additional knee specimens which were previously tested at the Virginia Tech Structures and Materials Laboratory, and were reevaluated with modified shear forces for this study. Final conclusions are made in Chapter 5, and recommendations are presented for future studies that might support and clarify the observations made in the current study. Full details of the experimental tests as well as sample calculations follow in appendices.

CHAPTER 2

EXPERIMENTAL INVESTIGATION

2.1 Scope of Testing

Four specimens with a diagonal knee connection area, typical of rigid gable frame metal buildings, were tested to study the significance of shear web buckling under negative moment bending. Negative moment bending is defined as the moment direction causing compressive stresses at the reentrant corner of the knee area, and is the condition which occurs under gravity loads acting on the roof. The tests were conducted at the Virginia Tech Structures and Materials Research Laboratory and were sponsored by American Buildings Company (ABC). Each test specimen consisted of a column and a portion of a rafter, the design of which was conducted by ABC. As shown in Figure 2-1, the column and rafter were bolt connected on a diagonal, with the flush moment end plates on both the rafter and the column oriented at an acute angle to their respective outside flange. This connection typically includes transverse web stiffeners also shown in Figure 2-1.

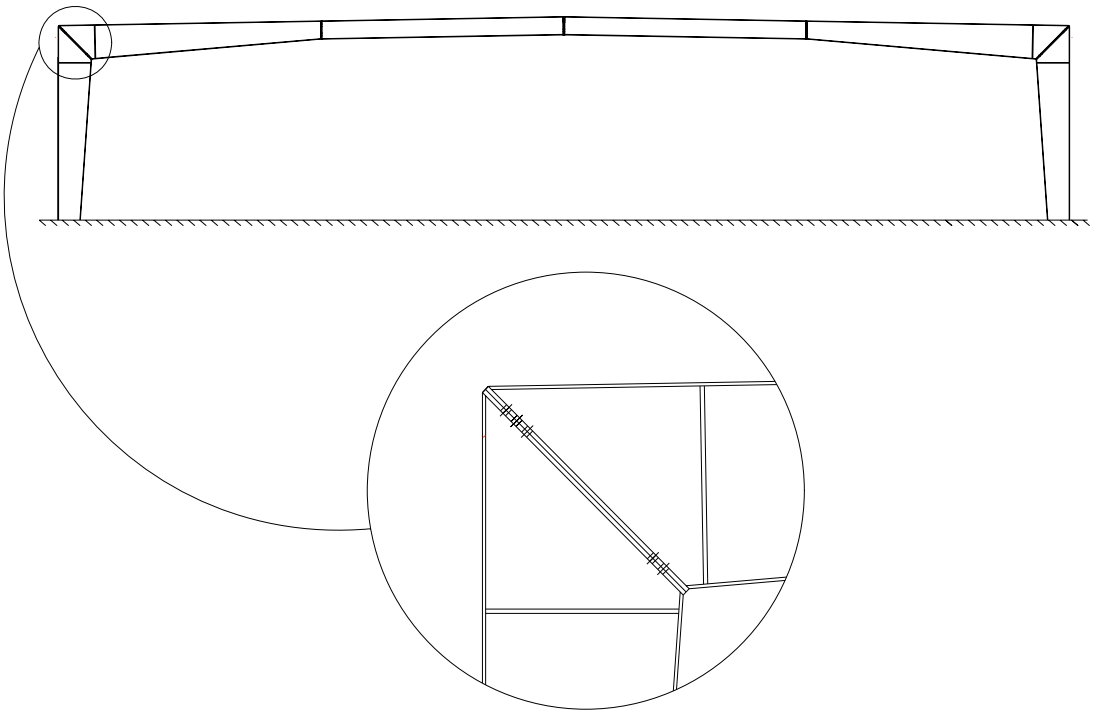

Figure 2-1 Typical Rigid Frame and Knee Connection Detail

The elastic shear buckling strength of the webs, in the absence of transverse stiffeners, was the focus of this investigation.

2.2 Test Specimens

Each test specimen was a sub-assemblage consisting of one column and a portion of the rafter of a particular rigid frame bent, with the rafter portion extending approximately to the first inflection point. The inflection point is the point of zero bending moment under the Allowable Stress Design (ASD) gravity load combination of 15.3 psf live load and 2.5 psf dead load. The column and rafter sections were tested in the orientation shown in Figure 2-2. The line of action of the applied load passed through the column base and the inflection point on the rafter section. In this way the axial, shear and moment in the knee area were representative of the internal forces present in the actual rigid frame, but the orientation and size of the test was more conducive to laboratory testing than a full scale specimen.

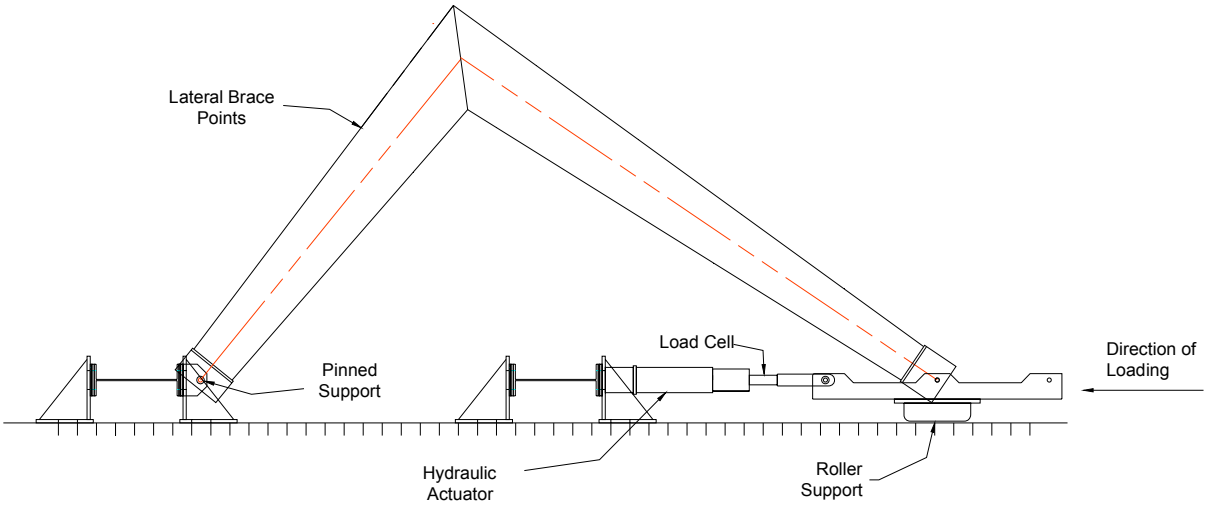

Figure 2-2 General Test Setup

Column and Rafter depths at the reentrant corners, along with connection details are found in Table 2-1. Further details and specimen dimensions are given in Appendices A through H. The test designations SH, MH and LH refer to the three sizes of tested specimens (Haunches) small, medium and large. The column and rafter built up sections were fabricated from steel plate and sheet material having nominal yield stresses of 50-55 ksi. The ASTM material specifications were ASTM A572 GR 55, with two exceptions: ASTM A529 GR 50/55 for the

small specimen flanges and end plates (SH-1 and SH-2), and ASTM A1011 GR 55 for the small specimen webs. These designations are from Material Test Reports furnished by ABC from independent testing agencies.

Table 2-1 Knee Connection Details

Specimen	*Depth of Column (in.)	*Depth of Rafter (in.)	No. of Bolts at Outside Flange/Total No.	Bolt Diameter (in.)	Bolt Type	End Plate Thickness (in.)
SH-1	22.00	22.13	6/10	3/4	A490	0.5
SH-2	22.81	22.13	6/10	3/4	A490	0.5
MH-1	35.94	35.63	12/18	3/4	A490	0.75
LH-1	59.50	59.75	10/18	3/4	A490	0.75 column 0.625 rafter

* Measured dimensions, otherwise nominal.
Note: Column and Rafter depth is measured perpendicular to outside flange, at reentrant corner

The flush moment end-plates were designed using snug tightened A325 bolts. However in an effort to insure that bolt failure would not inhibit the full development of the web shear capacity, A490 bolts were used. The target pretension was 50% of the specified minimum pretension for A325 bolts. Nominal dimensions for each specimen are in Table 2-2, with definitions given in Figure 2-3.

Table 2-2 Nominal Specimen Dimensions

Specimen	Column Flange Width (in.)	Column Flange Thickness (in.)	Column Web Thickness (in.)	Rafter Flange Width (in.)	Rafter Flange Thickness (in.)	Rafter Web Thickness (in.)
SH-1	6	0.375	0.131	6	0.375	0.131
SH-2	6	0.375	0.131	6	0.375	0.131
MH-1	8	0.5 outside 0.75 inside	0.25	8	0.5 outside 0.75 inside	0.25
LH-1	12	0.625	0.3125	12	0.625	0.3125

Details of each tested specimen, including measured dimensions and test data, can be found in Appendices A through H. The specimen designations include two fields. The first contains the haunch size of small (SH), medium (MH) or large (LH). The second is the specimen number, as there were two small haunches. A number of separate tests were conducted on several of the specimens and these are described in more detail in Section 2.6. In this section there is a third field in the specimen designation which represents the test number.

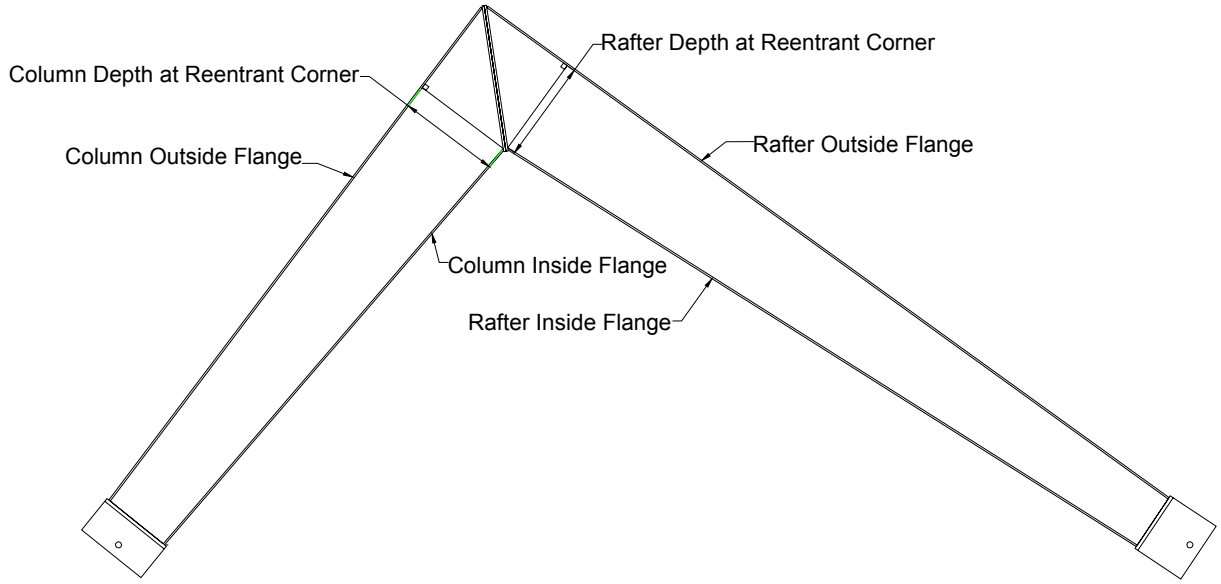

Figure 2-3 Test Specimen Nomenclature

2.3 Test Setup

All test setups were constructed by laboratory personnel. A pin connection was provided at the column end of the specimen and a pinned roller assembly at the rafter section end, as depicted in Figure 2-2. The load was applied using a 200 ton capacity, double acting hydraulic actuator (Enerpac RR200-13). The connection region of each specimen was whitewashed prior to loading so that the flaking of mill scale could be used as an indicator of local yielding during the test.

Lateral brace mechanisms were attached to the column and rafter section at locations specified by ABC. The lateral brace mechanisms were anchored to laboratory reaction frames, and prevented translation out of the plane of the webs, but permitted movement within this plane. Figure 2-4 is a representative photograph of the test setups.

2.4 Instrumentation

Instrumentation consisted of a load cell, displacement transducers, bolt strain gages, uni-directional strain gages and rectangular rosette strain gages. All instrumentation output was processed and collected using a PC based data acquisition system. The applied load was

measured using a 200 kip capacity load cell, which was calibrated prior to testing with a universal testing machine.

Figure 2-4 Typical Test Setup

Wire type displacement transducers were used to measure the displacement at both ends of the specimen, along the line of action of the force application. The difference between these measurements provided a deflection measurement of the roller end with respect to the pinned end, and is referred to as "chord displacement". LVDT type displacement transducers were used to measure out of plane displacement of both column and rafter webs adjacent to the moment end plates. These LVDT's were attached to fixtures which were supported by the flanges and end plates of the column and rafter. Three LVDT's were mounted over the web of both the rafter and the column, 2 in. from the cross-section containing the strain gages (gage line), as shown in Figure 2-5. There are three fields in the LVDT designations xPy where "x" represented rafter

(R) and column (C), P indicates a plunger type instrument, and "y" corresponds to the location along the gage line with A being nearest the outside flange, B at the middle of the web, and C nearest the inside flange. The web LVDT's were located on the north face of the specimens. The layout for the specimen SH-1 is shown in Figure 2-5, which represents the general arrangement for all test specimens except SH-2, which did not have strain gages on the webs or the inside flanges.

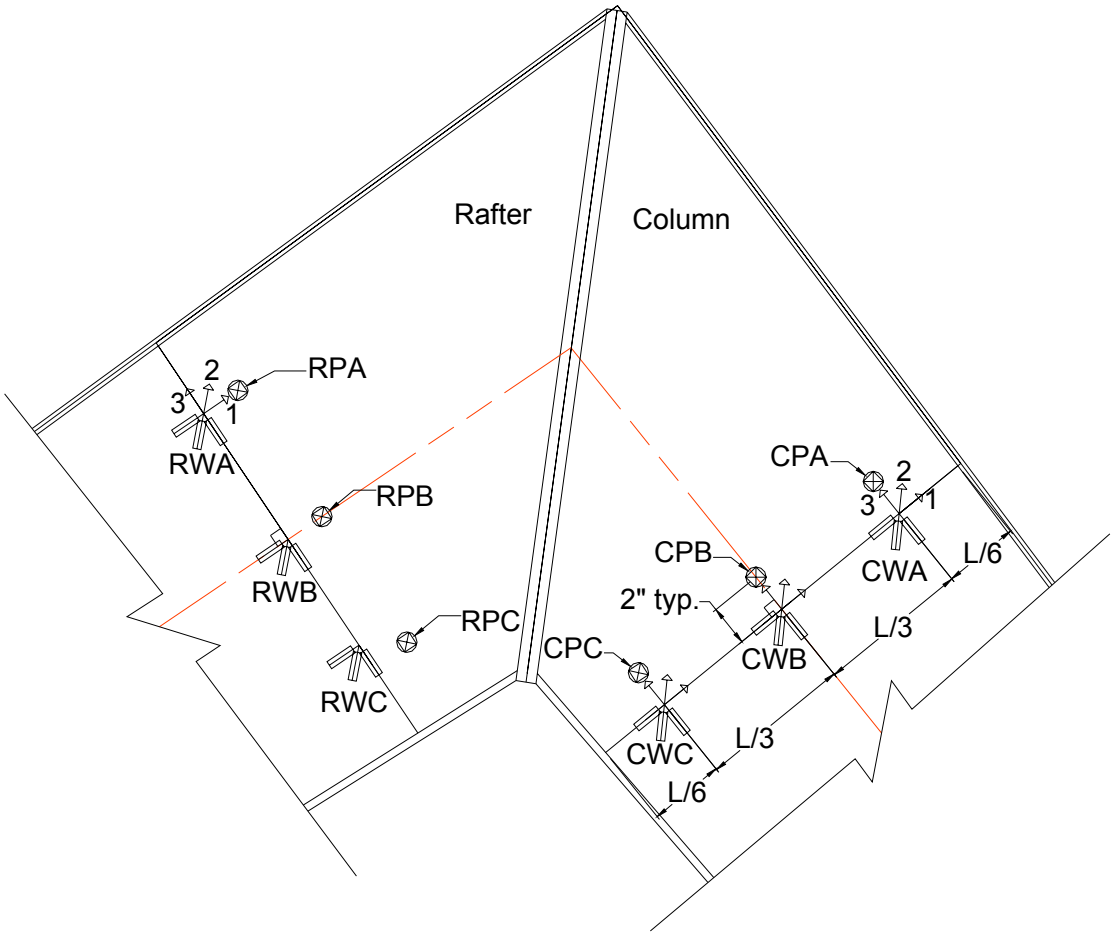

Figure 2-5 SH-1 LVDT's and Web Strain Gages as viewed from the North

Strain gage instrumented bolts were used in an alternating sequence in the tension side of the connection, as is shown in Appendices A through H. Bolt strain gages were installed in 2 mm diameter holes drilled through the bolt head into the unthreaded portion of the bolt shank. The bolts were calibrated up to the RCSC Specification AISC (2005b) minimum bolt pretension given for ¾ in. A325 bolts. This was done prior to testing using a universal testing machine, by establishing a factor by which the measured strain could be directly related to bolt force, so that

the proper specified pretension could be obtained. While the connections were designed using A325 bolts, A490 bolts were used in an effort to insure that premature bolt failure would not inhibit the full development of the web shear capacity. These bolts were treated as A325 bolts with regard to pretension procedures.

Uni-axial strain gages were installed on the flanges, and rectangular rosette strain gages were installed on the webs. The chosen cross-sections of interest, on which these gages and the web displacement transducers were installed, were determined from FEA buckling analyses (Shah 2007). The gages were placed at L/6, L/2 and 5L/6 from the inside flange, measured perpendicular to the geometric centerline with L being the web depth along the gage line. The general locations and orientation of all strain gages and displacement transducers are shown in Figure 2-6, with only the placement of the gage line relative to the connection varying among the specimens. The flange strain gages were labeled xFyz, where "x" designated column (C) or rafter (R); the second letter F was for flange; "y" designates the particular flange as indicated in Figure 2-6, and "z" represents the outside (1) or inside (2) face.

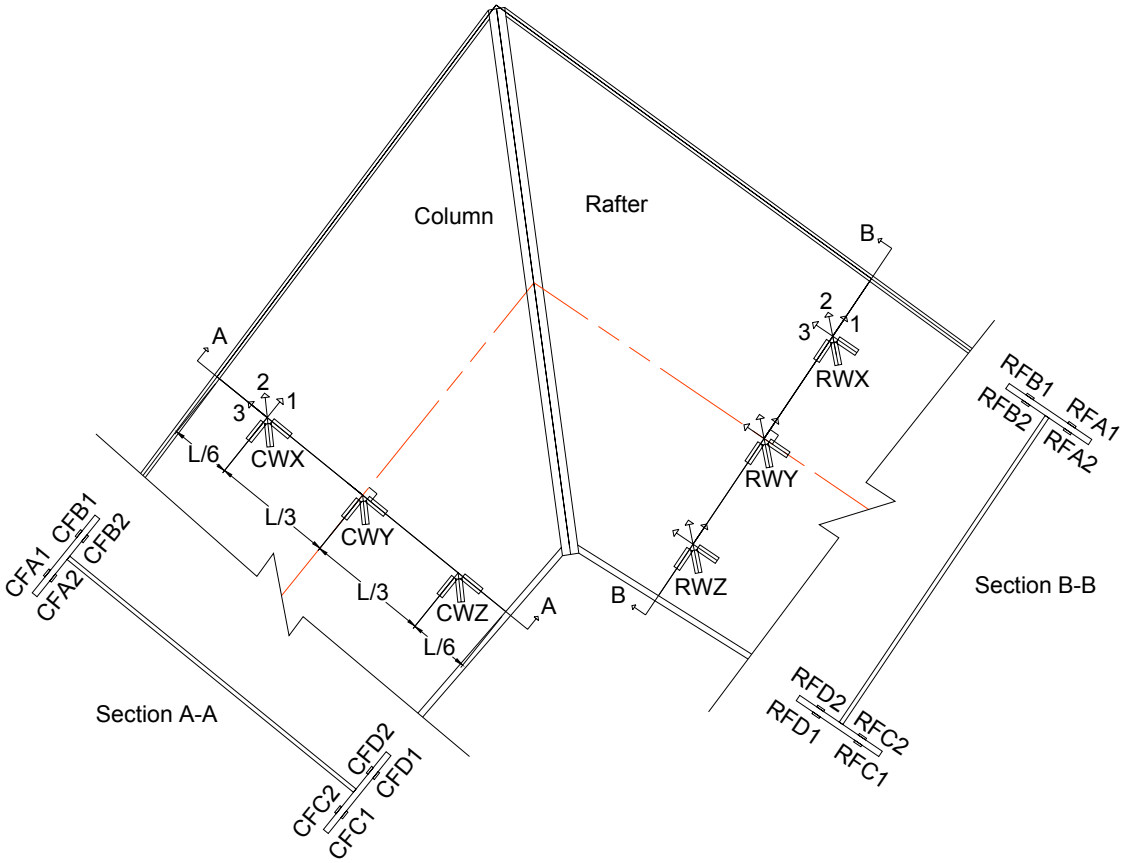

Figure 2-6 SH-1 Flange and Web Strain Gages as viewed from the South

The rosette strain gages were installed such that one grid was parallel to the geometric centerline and were labeled xWy with "x" representing rafter (R) or column (C), W indicating web gages, and the field "y" being a, b, or c for the North face, and correspondingly x, y and z on the South face. For example the gages "a" and "x" were installed directly mirrored to each other across the web so that bending stresses could be observed and related to web buckling. For further illustration, gage CWY in Figure 2-6 indicates a column web rosette at the L/2 or centerline location on the South face of the web. The determination of buckling behavior under transverse forces at this location would be obtained by comparing CWY grid 3 with CWB grid 1.

2.5 Testing Procedures

After the lateral bracing and loading mechanisms were put in place, the moment end-plate bolts were snug tightened to the pretension recommendation in AISC Design Guide 16, *Flush and Extended Multiple Row Moment End Plate Connections* (Murray and Shoemaker 2003). A pretension of 14 kips is recommended for ¾ in. A325 bolts. The instrumented bolts were monitored during the erection of the specimen so that the desired bolt tension could be obtained. Non-instrumented bolts were tightened by "feel" to approximately the same pretension as the instrumented bolts. Once the bolts were tightened, a load equal to approximately 20% of the predicted failure load for the specimen was applied in 0.5 kip increments to seat the specimen and check the instrumentation. The specimen was then unloaded incrementally.

The specimens were loaded in force increments until a yield plateau was developed, and then displacement control was initiated. At each load increment all instrumentation was recorded and the specimen was visually inspected periodically for signs of yielding. Ultimate loading was defined as significant loss of stiffness, marked by the leveling of the load vs. displacement curve. Several more data points were taken beyond this load, as well as during the incremental unloading of the specimen. As loss of stiffness first became evident, a displacement control was initiated, in which the hydraulic ram was used to impose an incremental displacement rather than an incremental measured force.

For several of the tests, the specimen was unloaded and reloaded in both positive and negative moment. Negative moment is defined as loading which produces compressive forces at the reentrant corner of the knee connection and positive moment is defined as loading which

produces tension at the reentrant corner of the knee connection. Specimen SH-1 was loaded four separate times, first in negative moment, second in positive moment, third in negative moment again, and fourth in negative moment with short transverse web stiffeners installed at the reentrant corner of the knee. MH-1 was loaded twice in negative moment loading, due to the slipping and realignment of a lateral bracing mechanism during the first test. All other specimens were loaded once only in negative moment.

2.6 Test Results

Results from the tests are summarized in Table 2-3. The following sections describe each test with supporting data found in Appendices A through H. Each Appendix includes the following: a test summary sheet; drawings of design dimensions and lateral brace locations produced by ABC; drawings of strain gage layout, designations and additional instrumentation (unless otherwise indicated in the following section); plots of applied load versus chord displacement, bolt strain versus applied load, applied load versus web deformation, and applied load versus strains at various gage locations; a picture of the test specimen connection area after yielding.

The applied load versus chord displacement plots include a theoretical stiffness based on linear elastic computer models created in Sap 2000 (CSI 2006), with cross-section geometry and nodal locations corresponding to those used in ABC's analyses. The stiffness models assume a structure discretized into short segments of prismatic elements, and the area within the knee connection was artificially stiffened by doubling the flange thicknesses to effectively double the moment of inertia in this region. This area is defined as the portion of the column and rafter beyond the reentrant corner.

Table 2-3 Test Results

Test Designation	Failure Load (kips)	Failure Mode
SH-1-1	26.48	rafter web buckling
SH-1-2	20.15	N/A
SH-1-3	25.04	rafter web buckling
SH-1-4	22.96	column web buckling
SH-2-1	26.08	column web buckling
MH-1-1	86.47	column web buckling
MH-1-2	77.48	column web buckling
LH-1-1	162.3	rafter/column web buckling

2.6.1 Test SH-1-1

Complete results for test SH-1-1 are found in Appendix A. The specimen was loaded to 5 kips to test instruments and then unloaded. Testing began in 0.5 kip increments and continued in a linear trend up to approximately 12.4 kips, at which time the specimen was unloaded to verify linear elastic behavior. No noticeable permanent set was observed. Testing was resumed and initial yielding behavior was observed in the Load vs. Deflection plot at approximately 18 kips (see Figure A-7). At approximately 23 kips the specimen was unloaded to check proper alignment of the rafter web displacement transducer RPB. A permanent set of 0.22 in. was observed at zero load. Testing was again resumed with significant leveling of the Load vs. Displacement curve at 25 kips, at which time displacement control was begun in 0.05 in. increments. No yield lines or whitewash flaking was observed, likely due to inadequate whitewashing. The specimen was finally unloaded when a slight loss of load was observed at approximately 3 in. chord deflection; however there was no visibly apparent failure or yielding. After the load was incrementally removed, there was a permanent chord deflection of 0.94 in.

The data points corresponding to the unloading phases of the test were removed from all plots except Figure A-7 for clarity. The maximum applied load was 26.48 kips and the controlling limit state was shear buckling in the rafter web. There was a snap through buckling shape observed in the Applied Load vs. Rafter Web Displacement plot (Figure A-9) which occurred at approximately 20 kips. This was closely followed by shear yielding behavior in the Applied Load vs. Rafter Web Transverse Strain plot (Figure A-15), at approximately 23 kips in gages RWY, RWA, and RWC. These gages exhibit compression yielding transverse to the specimen longitudinal axis.

The initial web buckling appears to propagate from the compression flange, evident in the fact that the shear strain gages RWC/RWZ, and CWC/CWZ are alternately positive and negative (see Figure A-15 and Figure A-16). These are the transverse web gages nearest to the compression flange for the rafter and column, respectively, and the opposite strain direction defines bending behavior, or buckling, which is propagated near the application of the component compressive force from the adjacent rafter or column flange. If not for the large out of plane movement of the center of the webs, this could possibly be considered web crippling.

2.6.2 Test SH-1-2

The SH-1 specimen was then loaded in positive moment; the complete results are found in Appendix B. The loading direction for this test was opposite that of all the other tests, and simulates positive moment on the connection, with tension at the inside flange, such as would result from wind loads on the windward wall. Loads and deflections were measured positive in the direction of imposed displacement, and so the sign convention has been reversed for this test. The specimen was loaded to 5 kips to check instrumentation and seat the specimen, and was then unloaded. Testing was begun in 0.5 kips increments to 10 kips. The stiffness observed in the Applied Load vs. Chord Deflection curve was significantly less than what was observed under negative moment loading (See Figure B-2). The end-plates at the inside flanges (tension flanges) showed significant separation. For this reason the specimen was unloaded through zero load to -10 kips, which corresponds to a negative moment loading, to verify that the differing stiffness was due to the loading condition. A permanent set of 0.27 in. was observed at zero load. At -5 kips the stiffness of the specimen began to follow the predicted stiffness more closely, likely corresponding to the re-closing of the end-plates. This difference in stiffness was attributed to the differing bolt patterns at the end-plate connection, with fewer bolts at the inside flanges or tension side during the positive moment test.

The specimen was again unloaded and reloaded in positive moment. No visible yield lines were observed during the test. The test was terminated when the gaged bolt nearest the tension flange reached its design strength. After the load was incrementally removed, there was a permanent chord deflection of 1.69 in.

The data points corresponding to the unloading phases of the test were removed from all plots except Figure B-2 for clarity. The maximum applied load was 20.15 kips and no failure mode was associated with this test, however there appears to be column web buckling as evidenced by the direction change in the web plungers (see Figure B-5). This behavior is supported by the differential strain across the web of the column in transverse web strain gages CWC/CWZ at the inside flange and CWA/CWX at the outside flange (see Figure B-11).

2.6.3 Test SH-1-3

The SH-1 specimen was then reloaded in negative moment; the complete results are found in Appendix C. The specimen was loaded in 0.5 kip increments to 17.75 kips. The structure exhibited less stiffness than was previously observed in negative moment up to approximately 10 kips. This was attributed to the closing of the end-plates at the inside flanges. The specimen was then unloaded incrementally and a permanent set of 1.04 in. was observed at zero load. The specimen was then reloaded and at 24 kips yielding became apparent in the Applied Load vs. Chord Deflection curve (see Figure C-2), and displacement control was initiated. The specimen was finally unloaded at a chord deflection of 4.55 in. as load loss occurred and web crippling became evident at the reentrant corner. The specimen was unloaded through zero in an effort to relieve the web crippling and facilitate installation of short web stiffeners. The permanent when passing through zero load was 2.1 in.

The data points corresponding to the unloading phases of the test were removed from all plots except Figure C-2 for clarity. The maximum applied load was 25.04 kips and the controlling limit state appears to be column web buckling near the connection. There is also a significant response in the column web at 10 kips (see Figure C-5) the load at which the end-plates came into contact. The plot of Applied Load vs. Column Web Transverse Normal Strain also indicates a web buckling which occurs at 10 kips. This is evident in the opposing values of gages CWB, and CWX which are the center strain gages on the web of the column (see Figure C-11). This response represents a bending strain distribution, which can be reasonably associated with buckling. There was significant out of plane displacement in the rafter web, and the center rafter web plunger RPB exhibits a snap through buckling at approximately 15-20 kips (see Figure C-4).

The rafter flanges indicate compression yielding as well as lateral movement, in the differential strains between the C and D gages (see Figure C-6). This lateral movement developed after the web buckling was clearly defined. There appears to be local web crippling at the reentrant corner, however this could be the result of the buckling web interacting with the boundary conditions imposed by the end plate and compression flange (see Figure C-1). In an attempt to verify whether the source of this observed behavior was due to buckling or crippling,

the specimen was unloaded and short transverse stiffeners were installed on the web at the reentrant corner to mitigate crippling. The testing was resumed as test SH-1-4.

2.6.4 Test SH-1-4

The SH-1 specimen was reloaded in negative moment, however short web stiffeners were installed at the reentrant corner, across the crippled portion of the web. This was done in an effort to determine whether the observed localized buckling at the reentrant corner was due to web crippling or overall web buckling. The complete test results are given in Appendix D. The specimen was loaded in 0.5 kip increments to 10 kips to seat the specimen and check the instruments, and was then unloaded. The specimen was reloaded in 0.5 kip increments to 23 kips, at which time a load bang was heard and a load loss occurred. This was attributed to a lateral brace slippage and load release associated with lateral buckling.

Loading was resumed and displacement control was initiated at approximately 19 kips. The load was finally removed when lateral buckling occurred in the rafter compression flange at approximately 20.8 kips and a chord deflection of 3.8 in. At zero load there was a permanent set of 1.0 in. The data points corresponding to the unloading phases of the test were removed from all plots except Figure D-2 for clarity. The maximum applied load was 23 kips, and the controlling limit state was column web buckling. The plot of Applied Load vs Column Web Displacement shows bifurcation buckling behavior in the center of the web at approximately 8 kips (see Figure D-5). This behavior is corroborated by the transverse strain gages on the center of the column web. Gages CWB/CWX exhibit bending strains which cross each other at this point (see Figure D-11) which may also indicates a mild snap through buckling.

2.6.5 Test SH-2-1

The complete results for test SH-2-1 are given in Appendix E. The specimen was incrementally loaded to 9 kips to seat the specimen and check instrumentation, and then unloaded. At approximately 16 kips the Applied Load vs. Chord Deflection curve indicated non linear behavior (see Figure E-4). At 23 kips the specimen was unloaded although not entirely to zero load. The specimen was then reloaded and at approximately 24.5 kips and 2.0 in. chord deflection, displacement control was initiated. At 24.4 kips and 2.4 in, chord deflection, the specimen was again unloaded and reloaded in several increments to 24 kips and displacement

control was resumed. At 25.6 kips and 2.55 in chord deflection yield lines became apparent in the compression flanges and in the web near the reentrant corner. After slight load loss, at 25 kips and a 3.1 in chord deflection, lateral buckling occurred in the rafter compression flange, and the load was removed. At zero load there was a permanent set of 1.00 in.

The data points corresponding to the unloading phases of the test were removed from all plots except for clarity. The maximum applied load was 26.08 kips, and the failure mode was column web buckling at the reentrant corner. At approximately 18 kips the web displacement transducer CPB indicated a snap through buckling (see Figure E-7). This instrument exhibits another reversal in direction when the entire specimen begins to exhibit yield behavior. The magnitude of the rafter web displacement is higher than that of the column, but no apparent buckling is evident. This could be due to initial imperfections producing a "pre-buckled" shape.

2.6.6 Test MH-1-1

The complete results for test MH-1-1 are found in Appendix F. The specimen was initially loaded to 8 kips to test instrumentation, and then unloaded. Testing was resumed in 1 kip increments and non linear behavior became evident in the Applied Load vs. Chord Deflection plot at about 62 kips (see Figure F-4). At approximately 75 kips the specimen was unloaded to 10 kips, and reloaded. At approximately 80 kips compression flange yielding was observed in the rafter. At 85.5 kips and 2.5 in. chord deflection displacement control was initiated. At 86 kips and 2.6 in. chord deflection a lateral brace mechanism on the rafter compression flange at the reentrant corner slipped. The specimen was unloaded to realign the braces. After the load was incrementally removed there was a permanent chord deflection of 0.59 in.

The data points corresponding to the unloading phases of the test were removed from all plots except Figure F-4 for clarity. The maximum applied load was 86.47 kips and the controlling limit state appears to be column web buckling. The plot of Applied Load vs Column Web Displacement shows the snap through buckling of CPB at approximately 55 kips (see Figure F-10). This buckling mode is validated by the shift in transverse normal strains, at the center of the web, to a differential bending stress behavior as indicated in the column web transverse strain gages CWB/CWY (see Figure F-13). Large strains are also evident in the rafter compression flange, which indicate lateral movement.

2.6.7 Test MH-1-2

The complete results for test MH-1-2 are given in Appendix G. The specimen was loaded in 5 kip increments until slight non linear behavior was observed in the Applied Load vs. Chord Deflection plot at approximately 65 kips (see Figure G-2). At approximately 75.5 kips and 2.1 in. chord deflection displacement control was initiated. At approximately 76 kips, yield lines became evident in the column compression flange, and the web of the column near the compression flange about 30 in. form the reentrant corner. These are possibly evidence of a change in the buckling shape of the web as the depth decreases. The specimen was incrementally unloaded when at approximately 76 kips and 2.46 in. chord deflection, lateral buckling occurred in the rafter compression flange.

The data points corresponding to the unloading phase of the test were removed from all plots except Figure G-2 for clarity. The maximum applied load was 77.48 kips, and the controlling limit state was column and rafter web buckling at the connection. Both webs exhibit displacement behavior early in the test in both the web displacement plots (see Figure G-4 and Figure G-5) and in the transverse web strain plots (see Figure G-10 and Figure G-11). The column web displacement transducers CPA and CPB indicate initial nonlinear behavior earliest at approximately 45 kips and the transverse strain gages at the column web center show a coincident differential strain buckling pattern at the same load (see Figure G-10 and Figure G-11). The rafter web displacements are not as pronounced as the column, nor are the bending stresses as non linear, but the rafter is clearly also exhibiting web buckling behavior.

2.6.8 Test LH-1-1

The complete test results for Test LH-1-1 are found in Appendix H. The specimen was loaded to approximately 25 kips to seat and check instrumentation, and was then unloaded. Testing began in 2 kip increments up to approximately 54 kips and was unloaded. At zero load there was no permanent set. The specimen was reloaded and non linear behavior became evident in the Applied Load vs. Chord Deflection plot at approximately 80 kips (see Figure H-4). There was a load loss at approximately 162 kips and flange local buckling was observed in the rafter compression flange. Displacement control was initiated at 155.65 kips and a chord deflection of 2 in. Large web displacements were observed in both column and rafter near the connection, and

the rafter compression flange buckling continued to develop with no more increase in load associated with the increase in displacement. The specimen was finally unloaded at 151 kips and 2.3 in. chord deflection. After the load was incrementally removed, there was a permanent chord deflection of 0.5 in.

The data points corresponding to the unloading phases of the test were removed from all plots except Figure H-4 for clarity. The maximum applied load was 162.3 kips and the controlling limit state was rafter and column web buckling. As seen in the web displacement plots, yielding occurred first at approximately 140 kips in the bottom of the rafter web at transducer RPC (see Figure H-9). This yielding coincides with the transition from compression strain to bending action differential strain in the rafter transverse shear strain gages RWC/RWZ near the inside flange (see Figure H-12).

Both rafter and column webs exhibit large displacements and obvious buckled shapes with negligible differences in their development, so the choice of failure location in the rafter is based only on the coincident behaviors stated above. Both rafter and column compression flanges have a divergent strain from the bottom to the top of the flanges, which indicates weak axis bending of the flanges rather than lateral buckling of the specimen. This is consistent with the large out of plane displacements of the webs as the compression forces caused the web to buckle and the flanges to rotate into the web.

It is important to note that large initial imperfections (out of plane) were observed in the webs, and this could contribute to the fact that no clear bifurcation was observed in the web displacements. In this case the webs contained a pre-buckled shape, and the amount of reserve strength observed is not easily explained.

2.7 Material Properties

Material coupons were milled either from the same bar or sheet stock with which the specimens were fabricated or cut from low stress areas of the tested specimens after testing was complete. The coupons were then tested according to ASTM E8 with a 300 kip capacity Universal Testing Machine. The results of the coupon tests are given in Table 2-4. The designations in the first column indicate the element for which the coupon was representative. W indicates web material and FL indicates flange material in those specimens in which the

flanges were equal. Only specimen MH-1 contained unequal flanges and ISFL indicates inside flange material, and OSFL indicates outside flange material.

Table 2-4 Coupon Results

Small Haunch Specimen									
	Milled dimensions			Results					
bar	width (in)	thickness (in)	Area (in^2)	Yield Load (kips)	Yield Stress (ksi)	Ultimate Load (kips)	Ultimate Stress (ksi)	% Elongation	average yield stress (ksi)
W 1	1.500	0.131	0.196	12.51	63.80	14.46	73.76	NA	
W 2	1.500	0.131	0.197	12.56	63.90	14.54	74.00	NA	63.85
FL 1*	1.499	0.378	0.567	31.33	55.30	46.84	82.67	22.07	
FL 2*	1.499	0.373	0.559	30.70	54.90	46.45	83.07	21.09	55.10

Medium Haunch Specimen									
	Milled dimensions			Results					
bar	width (in)	thickness (in)	Area (in^2)	Yield Load (kips)	Yield Stress (ksi)	Ultimate Load (kips)	Ultimate Stress (ksi)	% Elongation	average yield stress (ksi)
OS FL 1*	1.498	0.501	0.750	43.33	57.73	62.65	83.48	23.24	
OS FL 2	1.498	0.492	0.737	42.42	57.55	61.88	83.96	21.68	57.64
W 1*	1.498	0.247	0.370	20.04	54.15	23.81	64.34	25.78	
W 2	1.494	0.247	0.369	19.47	52.75	23.17	62.80	27.34	53.45
IS FL 1*	1.495	0.748	1.118	62.63	56.01	92.60	82.81	23.44	
IS FL 2	1.496	0.743	1.112	59.92	53.91	90.86	81.74	22.46	54.96

Large Haunch Specimen									
	Milled dimensions			Results					
bar	width (in)	thickness (in)	Area (in^2)	Yield Load (kips)	Yield Stress (ksi)	Ultimate Load (kips)	Ultimate Stress (ksi)	% Elongation	average yield stress (ksi)
W 1	1.499	0.308	0.462	28.35	61.40	37.09	80.34	20.51	
W 2	1.497	0.308	0.461	27.94	60.60	36.89	80.00	21.09	61.00
FL 1	1.496	0.617	0.923	50.17	54.35	75.25	81.53	24.22	
FL 2	1.496	0.614	0.919	48.73	53.05	74.90	81.54	23.05	53.70

* cut from tested specimens, otherwise from fabricator provided plate material

2.8 Initial Imperfections

All four specimens were observed to have initial out-of-plane imperfections in the column and rafter webs. In the interest of quantifying the variations in initial shape, measurements were made of each specimen prior to testing. The measurements were made using a displacement transducer (LVDT) mounted to a carriage that was slid along a straight edge supported by the flange tips. It was assumed that the flanges were straight and parallel, and that the straight edge was perfectly straight. The accuracy of the LVDT used was +/- 0.0005 in., but the actual variation in the flanges and carriage assembly would reduce this accuracy.

A photograph of the assembly used for the small specimens is shown in Figure 2-7. Two 40 in. range wire type potentiometers were mounted at the intersections of the flanges and end-plate and were used with the law of cosines to define the coordinates of the LVDT.

Figure 2-7 SH-1 and SH-2 Web Plane Measurement

The wire potentiometers had insufficient range for the medium and large specimens so a 3 in. grid pattern was plotted on 34 in. by 44 in. paper and overlaid on the specimen. Depth

readings were then recorded individually for each grid point. The coordinate system was defined for all specimens with the intersection of the geometric centerline and the gage line being the origin of the y-axis and x-axes respectively, with the positive y axis oriented away from the end-plate. Depth readings were measured over a roughly square area with sides equal to the web depths at the gage line.

The Metal Building Manufacturers Association (MBMA) gives two tolerance limits for the deviations from a plane allowed in the webs of built-up plate girders (MBMA 2006). One limit refers to deviations from a plane on a transverse cross-section and the associated variables are shown in Figure 2-8. The difference between the maximum and minimum measured values along a 2 in. wide transverse strip which contained the gage line was used to define 'C'.

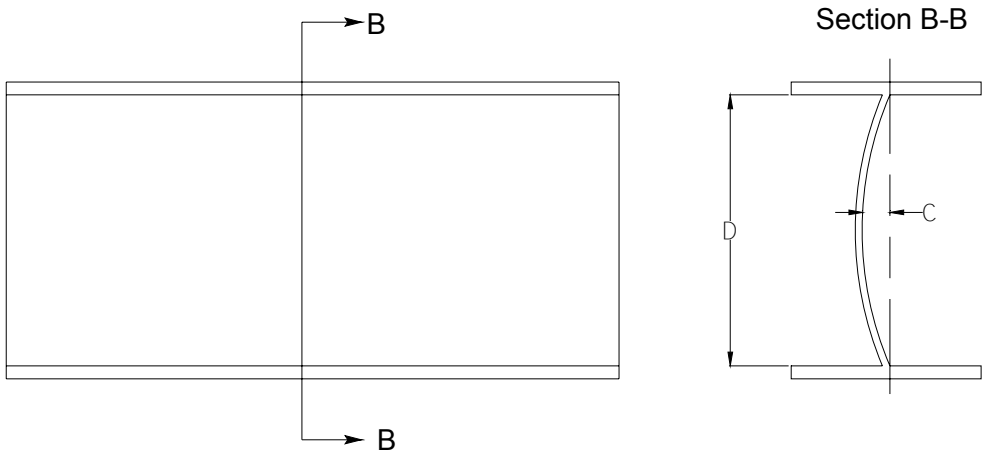

Figure 2-8 Transverse Out of Plane Tolerance

The second limit refers to the deviations in the web along a longitudinal cross-section which is shown in Figure 2-9. According to the author's interpretation of the MBMA definition of deviation along a longitudinal line, the difference between the maximum and minimum measured values along a 2 in. wide longitudinal strip, which contained the geometric centerline, was used to define "f". The tolerance allowed for both of these cases according to MBMA is D/72, where D is the web depth as shown in Figure 2-8. The measured C and f values are listed along with the depth of the web measured along the gage line in Table 2-5. The calculated

MBMA tolerances are also listed. The depth of the member (D) used to define the tolerance for longitudinal deviation is not given by MBMA.

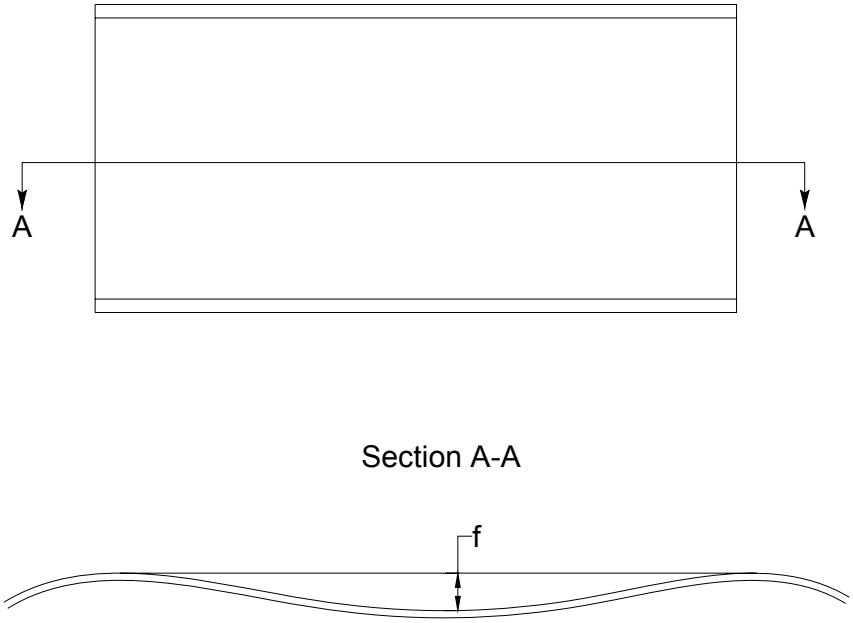

Figure 2-9 Longitudinal Out of Plane Tolerance

The measured web depth at the gage line was also used to define D in this casae. This web depth is measured perpendicular to the neutral axis of the members near the reentrant corner and slightly less than the maximum depth of the members.

Table 2-5 Web Plane Measurements

Specimen		D = measured web depth at gage line (in.)	c = deviation along gage line (in.)	f = deviation along centerline (in.)	MBMA deviation tolerance, D/72 (in)
SH-1	rafter	21.938	0.291	0.326	0.305
	column	21.563	0.157	0.124	0.299
SH-2	rafter	21.938	0.269	0.192	0.305
	column	21.563	0.217	0.278	0.299
MH-1	rafter	35.625	0.091	0.258	0.495
	column	35.625	0.189	0.410	0.495
LH-1	rafter	59.125	0.345	0.744	0.821
	column	59.000	0.238	0.462	0.819

Note: deviation is the difference of the maximum and minimum measured value

Table 2-6 contains ratios of the two deviation measurements to the MBMA tolerance, D/72. Only the SH-1 rafter exceeded one of the MBMA tolerances but the LH-1 rafter and the SH-2 column are within 10 percent of the limit set for deviations from the plane along a longitudinal line. The rows corresponding to the specimens determined to have failed in a shear buckling mode are shaded.

Table 2-6 Comparison of Web Deviations to Tolerance

Specimen		ratio of C to D/72	ratio of f to D/72
SH-1	rafter	0.955	1.070
	column	0.524	0.414
SH-2	rafter	0.883	0.630
	column	0.725	0.928
MH-1	rafter	0.184	0.521
	column	0.382	0.829
LH-1	rafter	0.420	0.906
	column	0.290	0.564

Figure 2-10 is a surface plot of the SH-1 rafter web.

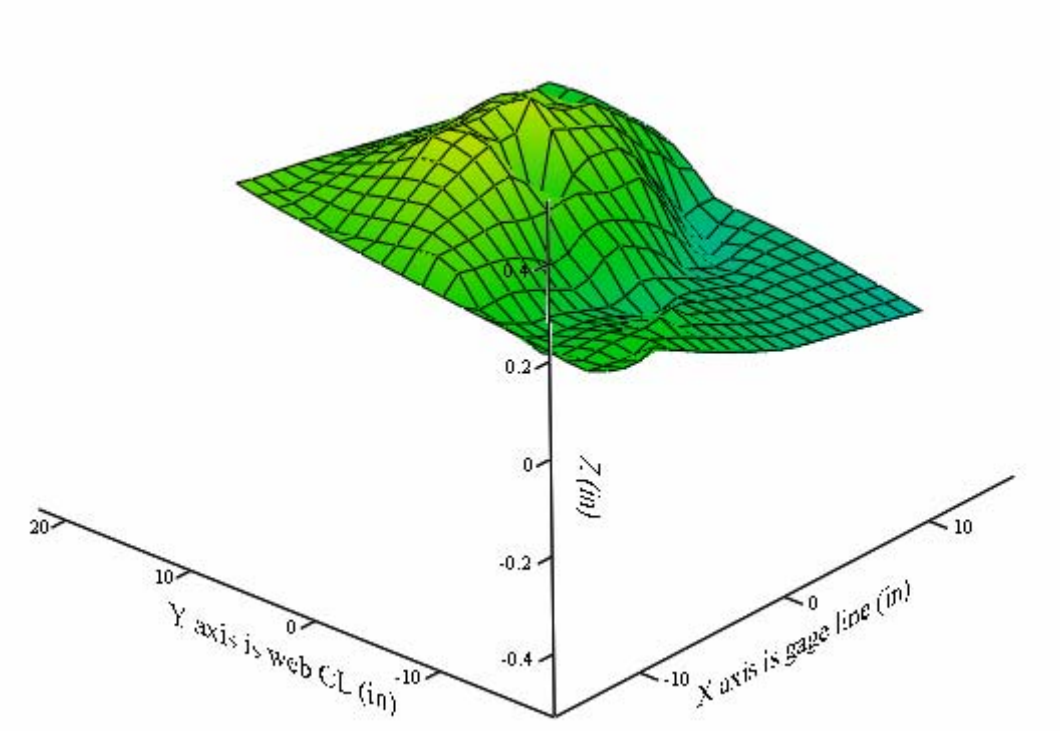

Figure 2-10 SH-1 Rafter Web Surface

Figure 2-11 is a surface plot of the SH-2 column web.

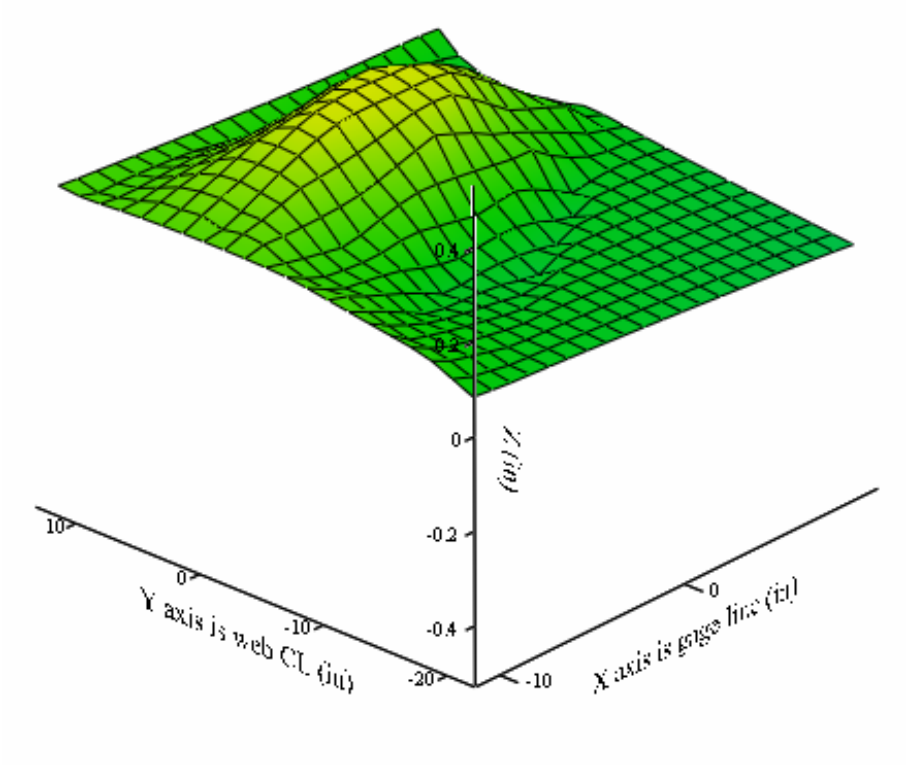

Figure 2-11 SH-2 Column Web Surface

Figure 2-12 is a surface plot of the LH-1 rafter web. The relative smoothness of the LH-1 rafter is possibly due to the fact that fewer readings were taken over a larger area and also the carriage assembly was stationary when the recordings were made.

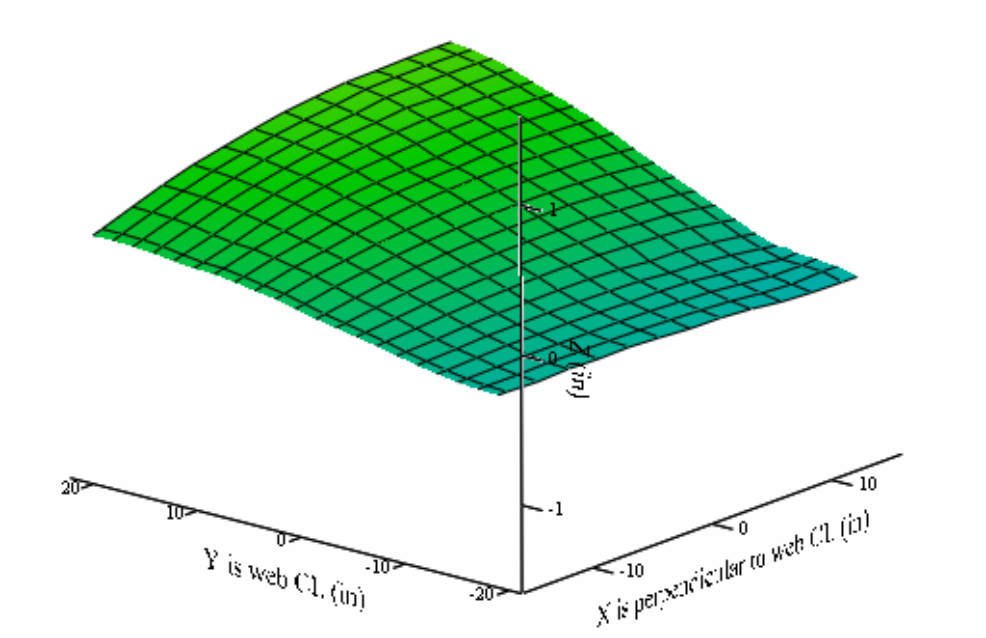

Figure 2-12 LH-1 Rafter Web Surface

2.9 Web Shear Strains

The magnitudes of shearing stresses measured in the web during the tests are of interest in determining the validity of a modified shear approach. The webs were instrumented with rosette strain gages as described in Section 2.4. This strain data permitted the calculation of the magnitude and orientation of the principal stresses, and from these values the shear stresses along the gage line were determined. In an effort to remove the bending stresses associated with out of plane web displacements, the strain gage grids were averaged across the thickness of the web. For example, with reference to Figure 2-5 and Figure 2-6, the average of RWA grid 1 and RWX grid 3 resulted in the average longitudinal normal strain at this location.

Figure 2-13 shows the web shear stresses in the MH-1 specimen rafter. This stress distribution is most typical of the tested specimens, occurring in four out of the six members. Among these four there is an increase in shearing stress near the compression flange which was the bottom flange under test load conditions, and a decrease in the shear stress near the tension flange relative to the shear stress at the mid depth of the web.

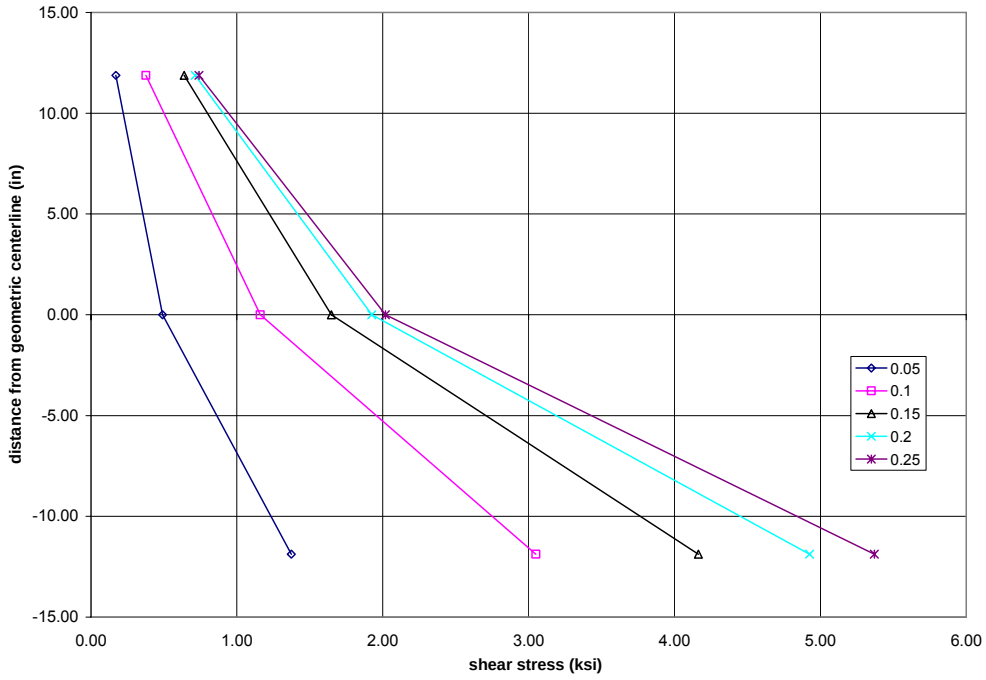

Figure 2-13 MH-1-1 Rafter Shear Stresses at 5% to 25% of Failure Load

These data were further reduced to define a net shear force acting on the web. First it was assumed that the values taken at lower loads would produce more reasonable results and would be less susceptible to the errors induced by high out-of-plane bending strains. 10 percent of the applied failure load was the chosen datum. The area under the shear stress distribution multiplied by the web thickness represents the shear force on the cross-section. This distribution was approximated by assuming the individual values of the measured transverse shear strain to be constant over the adjacent one third of the web height as is depicted in Figure 2-14.

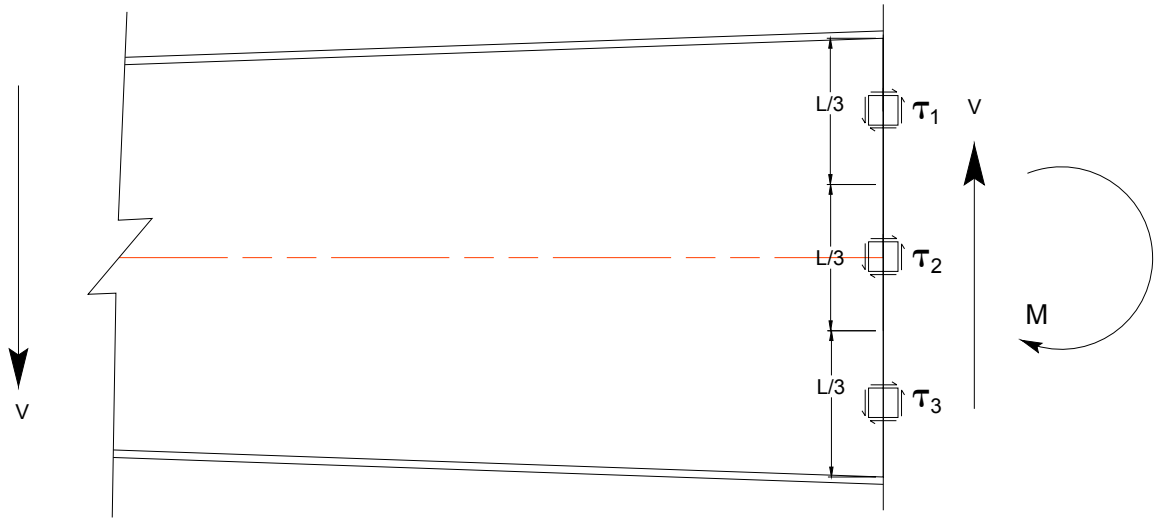

Figure 2-14 Location of Shear Stress Elements from Strain Data

The calculated stresses at the individual gage locations as well as the measured web dimensions and the resulting sum of the corresponding forces are listed in Table 2-7. The shear stresses τ_1 were determined at the strain gage locations located near the tension flange. The shear stresses τ_3 were determined at strain gage locations located near the compression flange. These stresses correspond with the rectangular rosette locations RWA and RWC for the rafters and CWX and CWZ for the columns, as described in Section 2.4. A comparison of these measured values with experimental shear forces is made in Chapter 4.

Table 2-7 Web Shear Forces from Shear Strain Data

Specimen	Member	Shear Stress Locations	Shear Stress (ksi)	L/3 (in)	Web Thickness (in)	Shear Force (kips)	Total Web Shear Force (kips)
SH-1	Rafter	τ_1	0.25	7.31	0.131	0.24	
		τ_2	0.56	7.31	0.131	0.54	
		τ_3	-0.08	7.31	0.131	-0.07	0.70
	Column	τ_1	-0.15	7.19	0.131	-0.14	
		τ_2	1.02	7.19	0.131	0.96	
		τ_3	2.61	7.19	0.131	2.46	3.27
MH-1	Rafter	τ_1	0.38	11.88	0.247	1.10	
		τ_2	1.16	11.88	0.247	3.40	
		τ_3	3.05	11.88	0.247	8.95	13.45
	Column	τ_1	0.57	11.88	0.247	1.66	
		τ_2	1.20	11.88	0.247	3.51	
		τ_3	2.94	11.88	0.247	8.63	13.79
LH-1	Rafter	τ_1	0.34	19.71	0.308	2.04	
		τ_2	0.25	19.71	0.308	1.55	
		τ_3	0.33	19.71	0.308	1.99	5.58
	Column	τ_1	0.39	19.67	0.308	2.36	
		τ_2	0.25	19.67	0.308	1.53	
		τ_3	2.19	19.67	0.308	13.27	17.15

It can be seen from the shear stress column that, except for the SH-1 rafter and LH-1 rafter, the shear stresses increase toward the compression flange as indicated in Figure 2-13. The distributions of shear stress in these two members are shown in Figure 2-15 and Figure 2-16, respectively. These two members also contain high levels of initial web imperfections, with the SH-1 rafter exceeding the tolerance for deviations from a flat plane set by MBMA as discussed in the Section 2.8.

Sample calculations for the determination of web shear stress from strain gage data are given in Appendix I. The reduction of rosette strain gage data to find shear stresses was based on methods presented by Beer et al. (2002) and Holman (1978).

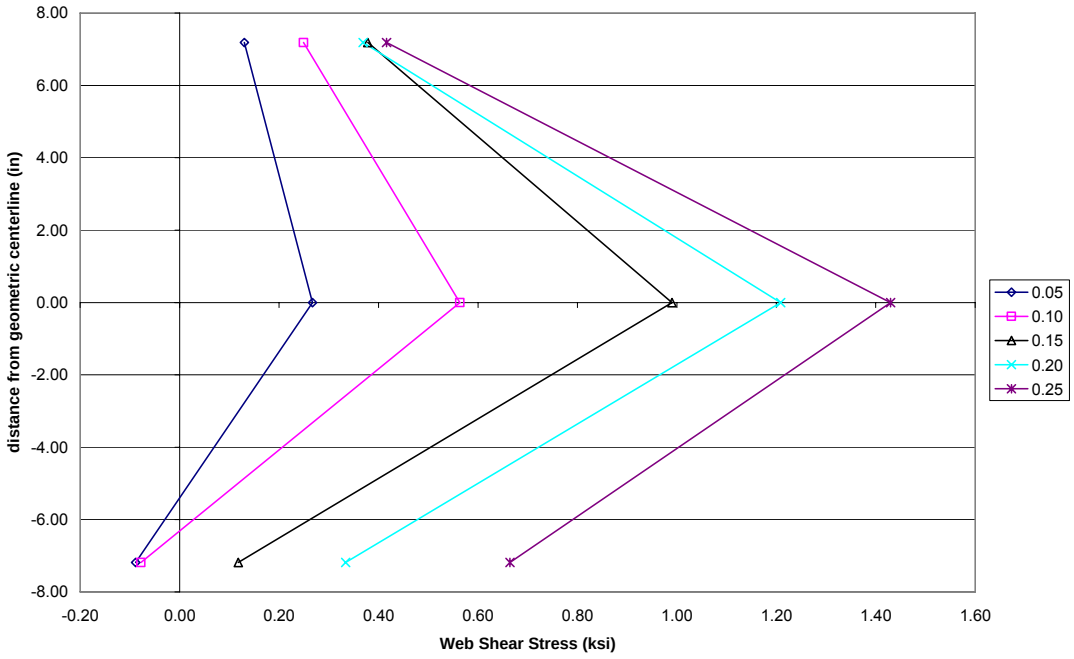

Figure 2-15 SH-1-1 Rafter Stresses at 5% to 25% of Failure Load

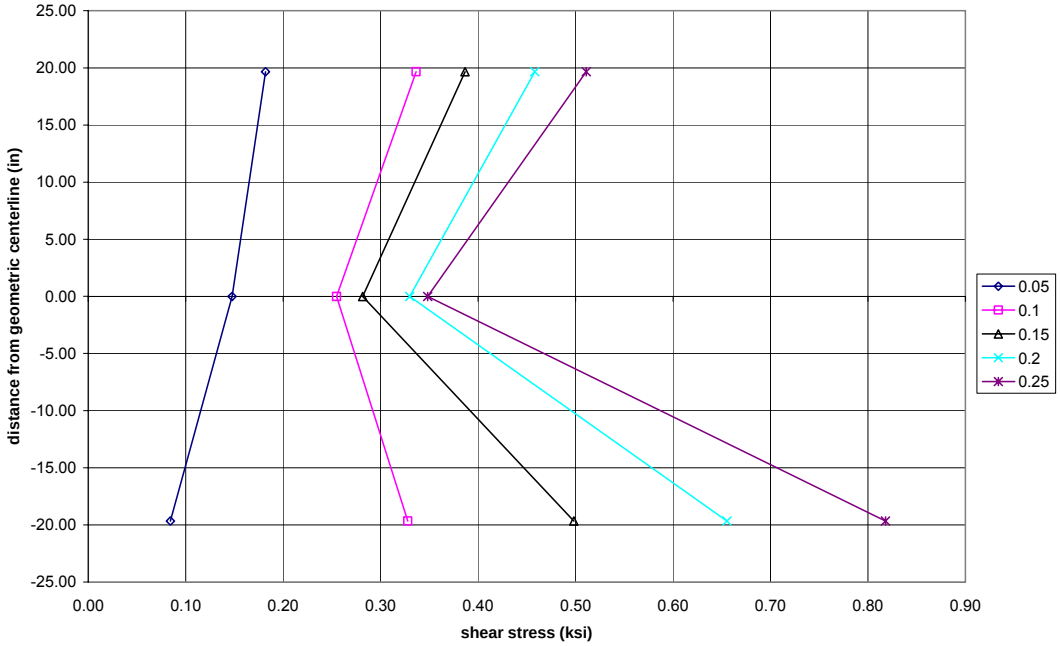

Figure 2-16 LH-1-1 Rafter Web Stresses at 5% to 25% of Failure Load

CHAPTER 3

ANALYTICAL INVESTIGATION

3.1 General

The four experimentally tested knee specimens were analyzed for shear strength according to the AISC provisions for prismatic girders. The following sections present a description of the calculation of modified shear forces, and the details of the shear strength analysis. The calculated shear strengths for tested specimens were compared to both modified and unmodified shear forces. Five specimens from tests by Sumner *et al.* (1995) were also evaluated with modified and unmodified shear forces.

3.2 Geometry

The cross-sections of interest for all of the following analyses are at the sections of greatest web depth, taken perpendicular to the neutral axis and passing through the reentrant corner, as sections B-B in Figure 3-1.

The location of the center of gravity for tapered sections with equal flanges is linear and lies along the geometric centerline. For members with unequal flanges, as was the case with specimen MH-1, the neutral axis varies quadratically along the length. However, this function is very closely approximated by a linear interpolation between the locations of the neutral axis at the ends of the member, corresponding to sections A-A and B-B in Figure 3-1. The deviation in the slope of this line from the geometric centerline was found to be less than 0.15% of the length of the specimen in this case. It was therefore considered reasonable to approximate the orientation of the neutral axis as a straight line parallel to the geometric centerline in the MH specimen.

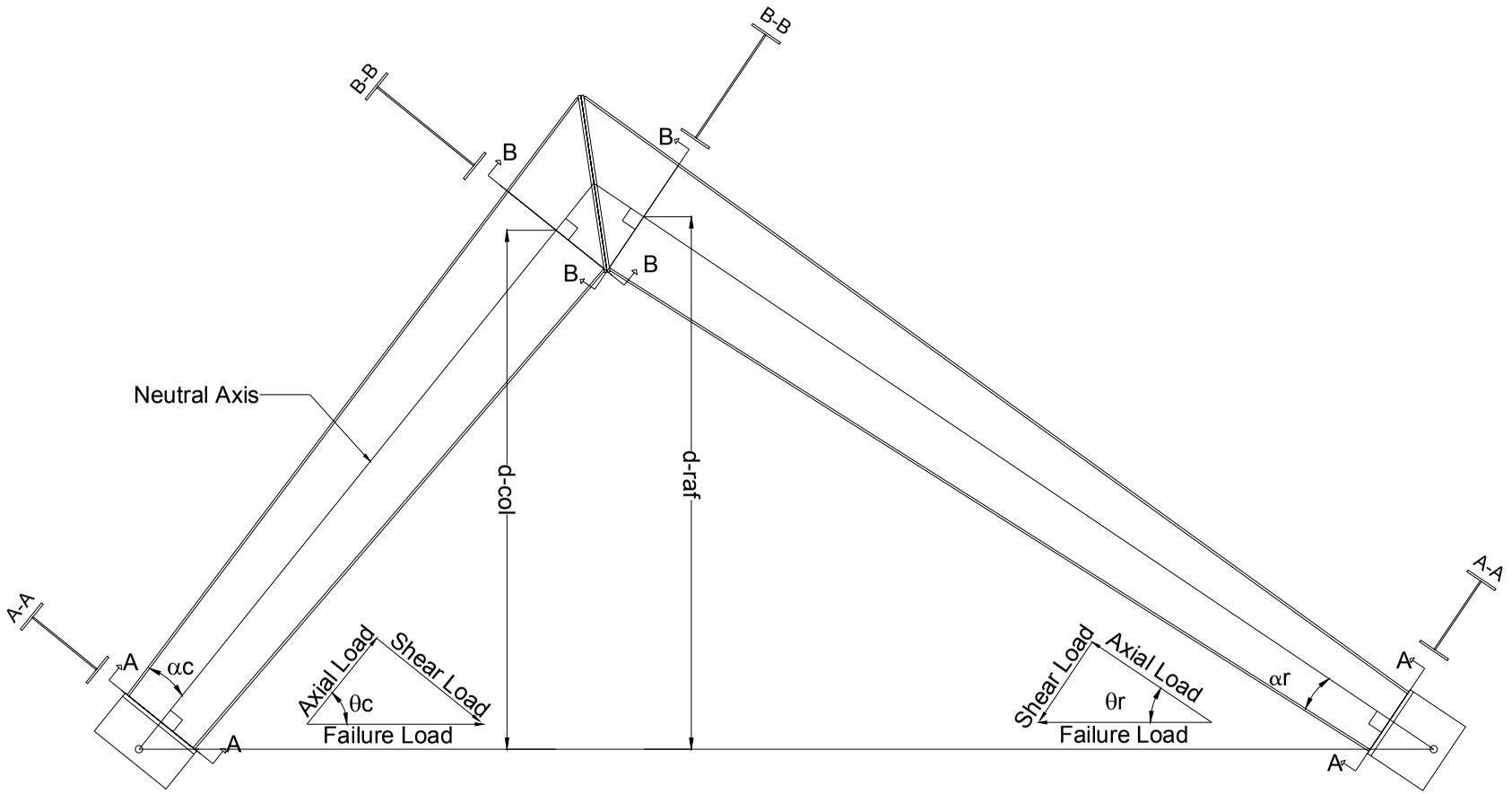

Figure 3-1 Typical Analysis Geometry

The geometry used in the following calculations of shear forces and shear strength is given in Table 3-1.

Table 3-1 Analysis Geometry

Specimen	Member	Angle from applied load to section CG, θ (deg)	Angle of taper, α (deg)	Moment arm to section B-B (in)	Web thickness (in)	Web depth (in)
SH-1	Rafter	33.96	1.80	95.3	0.131	21.99
	Column	51.20	1.80	92.9	0.131	21.95
SH-2	Rafter	33.96	1.80	95.3	0.131	21.99
	Column	51.20	1.80	92.9	0.131	21.95
MH-1	Rafter	33.53	1.60	119.0	0.247	35.94
	Column	48.67	1.40	115.5	0.247	35.96
LH-1	Rafter	31.88	3.50	137.8	0.308	59.99
	Column	44.70	5.30	133.8	0.308	60.06

The moment arm column contains the appropriate values of D-col and D-raf as indicated in Figure 3-1. The geometry used in the calculations of shear forces, and shear strength for the Sumner *et al.* specimens is listed in Table 3-2.

Table 3-2 Analysis Geometry for Sumner *et al.* Specimens

Specimen	Member	Angle from applied load to section CG, θ (deg)	Angle of taper, α (deg)	Moment arm to section B-B (in)	Web thickness (in)	Web depth (in)
Knee 1	Rafter	50.93	1.31	111.8	0.162	23.61
	Column	31.39	1.65	112.5	0.153	24.34
Knee 1A	Rafter	50.93	1.31	111.8	0.162	23.61
	Column	31.39	1.65	112.5	0.153	24.34
Knee 2	Rafter	50.93	1.31	111.8	0.131	23.60
	Column	31.39	1.65	112.5	0.132	24.35
Knee 3	Rafter	50.93	1.31	111.8	0.120	23.60
	Column	31.39	1.65	112.5	0.120	24.35
Knee 7	Rafter	46.53	1.31	174.2	0.242	43.13
	Column	34.39	2.58	176.2	0.249	44.12

3.3 Analysis Details

3.3.1 Determination of Web Shear Forces

Modified and unmodified shear forces were compared to the predicted shear buckling strength of the webs in the following analyses. The unmodified shear force is simply the external applied shear at the cross-section of interest. The modified shear force accounts for the influence of the inclined flanges to effectively decrease the demand placed on the web. The transverse components of the flange forces, used to modify the web shear forces, were calculated in the using an elastic distribution of normal flexural stresses, and assuming the extreme fiber stresses to be constant through the flanges. It is noted that this slightly overestimates the flange forces when compared to an exact value found with the stresses at the center of gravity of the flange.

None of the methods given in Section 1.2.4 accounted for the presence of axial stress in the flanges when finding modified web shear forces. If the flanges are of equal area, an axial compressive stress will decrease the tension flange force identically to the increase in the compression flange force, and there will be no net effect on the modified web shear force. However, when the flanges are not of equal area, as in specimen MH-1, the axial stress will produce a higher force in the thicker flange. The force in the compression flange along its own axis, due to flexural and axial stresses, was defined for this study as follows, with reference to Figure 3-2:

$$P_{cf} = \frac{P_a A_{cf}}{A_g} + \frac{MA_{cf}}{S_{xc}\cos(\alpha)} \qquad (3\text{-}1)$$

Where:
- A_{cf} = area of the compression flange plate, (b_f x t_{cf})
- S_{xc} = elastic section modulus referenced to compression flange, I/y_{fc}
- I = simplified moment of inertia of the cross-section, found with A_{tf}, A_{cf}
- y_{fc} = distance from section center of gravity to compression flange extreme fibers
- α = angle of flange inclination
- P_a = applied axial force
- A_g = cross-section area using the flange plate areas

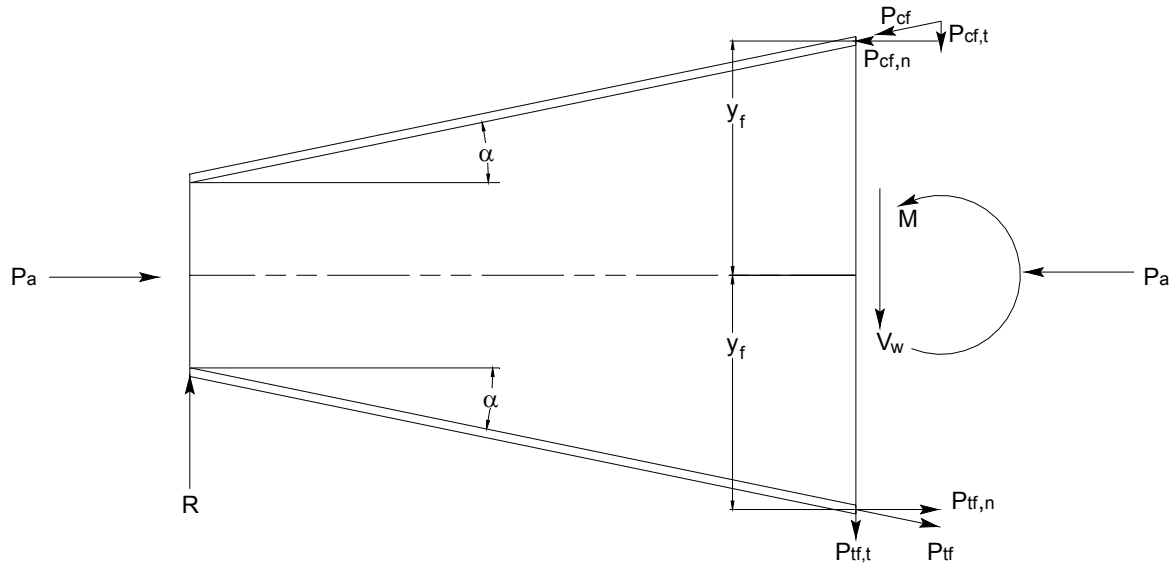

Figure 3-2 Flange Contributions to Modified Web Shear

Likewise the tension flange force along its own axis is:

$$P_{tf} = -\frac{P_a A_{tf}}{A_g} + \frac{MA_{tf}}{S_{xt}\cos(\alpha)} \tag{3-2}$$

Where: A_{tf} = area of the tension flange plate, (b_f x t_{tf})
S_{xt} = elastic section modulus referenced to tension flange, I/y_{ft}
I = simplified moment of inertia of the cross-section, found with A_{tf}, A_{cf}
y_{ft} = distance from section center of gravity to tension flange extreme fibers

The elastic section modulus S_x is calculated with the simplified moment of inertia of the cross-section by using the nominal flange area A_{fl} rather than the slightly larger actual flange area at the cross-section. The use of the elastic section modulus slightly overestimates the flange stresses, by assuming the extreme fiber stresses to be constant through the flange. Finally the sum of the transverse components can be included in the equilibrium of forces in the vertical direction, and the modified web shear force is:

$$V_w = V - \left(P_{cf} + P_{tf}\right)\sin(\alpha) \tag{3-3}$$

3.3.2 AISC Shear Provisions for Prismatic Members

The design of unstiffened tapered steel plate girders for shear resistance has traditionally been accomplished by applying the codified provisions for prismatic members. A recent draft version of the AISC Steel Design Guide Series, "Frame Design Using Web Tapered Members" by Kaehler *et al*. (2007), continues with this practice for the shear design of unstiffened tapered members with only slight amendments to the AISC Specification provisions for the shear design of prismatic members (AISC 2005a). In the Draft Design Guide the limit given by which a tapered member must be considered unstiffened is a panel length greater than $3h_o$. Quite conservatively h_o is the least panel height of the tapered section and is represented by the depth of web at sections A-A in Figure 3-1. The authors recommend that the shear strength be calculated on a cross-section by cross-section basis, with the plate buckling coefficient taken as 5.0. This essentially assumes a panel of infinite length and will produce shear strength predictions approximately 7% more conservative than Bleich's buckling coefficient of 5.34 for infinitely long panels. The panel slenderness is defined by the geometry at the section of interest.

The AISC Specification shear provisions for the nominal shear strength of unstiffened prismatic members are:

$$V_n = 0.6F_y A_w C_v \tag{3-4}$$

$$\text{For } \frac{h}{t_w} \le 1.10\sqrt{\frac{k_v E}{F_y}} \qquad C_v = 1.0 \tag{3-5}$$

$$\text{For } 1.10\sqrt{\frac{k_v E}{F_y}} < \frac{h}{t_w} \le 1.37\sqrt{\frac{k_v E}{F_y}} \qquad C_v = \frac{1.10\sqrt{k_v E/F_y}}{h/t_w} \tag{3-6}$$

$$\text{For } \frac{h}{t_w} > 1.37\sqrt{\frac{k_v E}{F_y}} \qquad C_v = \frac{1.51Ek_v}{(h/t_w)^2 F_y} \tag{3-7}$$

$$k_v = 5 \tag{3-8}$$

Where: k_v = plate buckling coefficient
C_v = web shear coefficient
E = Young's Modulus, 29000 ksi
F_y = nominal yield stress
h = web height at cross-section of interest
t_w = web thickness
A_w = shear area of web (d x t_w)

The two slenderness limits that define the three ranges of C_v in Equation (3-5), Equation (3-6), and Equation (3-7) were developed by Basler (1961a) from experimental data resulting from his work at Lehigh as well as from the results of other tests of unstiffened plate girders with compact webs. It was discovered that there was not a distinct slenderness limit marking the separation of Timoshenko's critical elastic buckling and shear yielding, but that rather a transitional region of inelastic buckling exists between the two behavioral extremes. A curve fitting exercise revealed that the elastic buckling formula does not accurately describe behavior unless the critical shear buckling stress decreases below 80% of the yield stress.

The lower slenderness limit is that which simultaneously satisfies the yield strength Equation (3-4) with C_v defined by elastic buckling in Equation (3-7) and yielding in Equation (3-5). The upper limit is then found by dividing the lower by 0.80 based on the recommendations of Basler. The behavior within these three regions of slenderness is defined by the web shear coefficient. All of the tested specimen webs in the current study were beyond the upper slenderness limit at the cross-section of interest, which is perpendicular to the natural axis at the reentrant corner.

Kaehler *et al.* (2007) also address the issue of determining the applied shear forces at a cross-section. They state that the modified shear approach proposed by Blodgett (1966) lacks research validation, and recommend that the required shear strength at a particular cross-section is that which is necessary to satisfy equilibrium, neglecting the influence of the flanges. The critical section, when the modified shear effects are disregarded, is at the cross-section of greatest web depth if shear is constant. If the shear is not constant, or if the flexural forces in the inclined flanges are included in the analysis, then it is not evident by inspection where the critical cross-section is located, because the resistance to shear varies along the length as well as the shear force to be resisted.

3.4 Analysis Results

3.4.1 Shear Forces at Failure

The modified and unmodified shear forces were calculated at the location of greatest web slenderness for each of the tested specimens, under the applied failure load of the first test performed with each specimen, according to the provisions of Section 3.3.1. The specimen geometries used to determine these shear forces were given previously in Table 3-1 and Table 3-2. The applied failure load and resulting shear and moment on the cross-section, as well as the unmodified and modified web shear forces for the corresponding current study are given in Table 3-3.

Table 3-3 Unmodified and Modified Shear

Specimen	Member	Applied Failure Load, P (kips)	Shear at cross section B-B (kips)	Moment at section B-B (in-kips)	Unmodified Shear $V_{u,exp}$ (kips)	Modified Shear $V_{m,exp}$ (kips)
SH-1	Rafter	26.48	14.79	2523.68	14.79	8.81
	Column	26.48	20.64	2459.86	20.64	14.80
SH-2	Rafter	26.08	14.57	2485.53	14.57	8.68
	Column	26.08	20.32	2422.70	20.32	14.57
MH-1	Rafter	86.47	47.76	10287.51	47.76	35.18
	Column	86.47	64.93	9984.09	64.93	54.27
LH-1	Rafter	162.30	85.71	22361.69	85.71	53.22
	Column	162.30	114.15	21715.90	114.15	66.36

Five additional specimens which were previously tested at the Virginia Tech Structures and Materials Lab were also analyzed. These web tapered steel I-shaped specimens, tested by Sumner *et al.* (1995), were similar in proportion to those of the current study and included unstiffened slender webs. The failure load and resulting forces on the cross-section as well as the unmodified and modified web shear forces are given in Table 3-4.

Table 3-4 Sumner *et al.* Specimens Unmodified and Modified Shear

Specimen	Member	Applied Failure Load, P (kips)	Shear at cross section B-B (kips)	Moment at section B-B (in-kips)	Unmodified Shear $V_{u,exp}$ (kips)	Modified Shear $V_{m,exp}$ (kips)
Knee 1	Rafter	27.00	20.96	3018.33	20.96	16.63
	Column	27.00	14.06	3037.77	14.06	8.48
Knee 1A	Rafter	31.10	24.15	3476.67	24.15	19.15
	Column	31.10	16.20	3499.06	16.20	9.77
Knee 2	Rafter	26.00	20.19	2906.54	20.19	15.79
	Column	26.00	13.54	2925.26	13.54	8.02
Knee 3	Rafter	24.80	19.25	2772.39	19.25	14.98
	Column	24.80	12.92	2790.25	12.92	7.55
Knee 7	Rafter	66.00	47.90	11497.20	47.90	39.38
	Column	66.00	37.28	11630.52	37.28	20.94

3.4.2 Predicted Shear Strength

The predicted shear strengths were determined according to the AISC provisions in Section 3.3.2. It should be noted that the area of web considered in the calculation of the nominal shear strength of prismatic members is the product of the web thickness and the total depth of the member. It was considered inconsistent to include the portion of the web between the flanges in both the web shear area and the flange area when finding the transverse component of the flange force. For this reason, the actual web height, h_w is used in defining the web shear area, A_w for the shear strength calculations rather than the recommended section depth, d. This conservatively underestimates the web strength when applied to the unmodified shear case. The predicted shear strengths are listed in Table 3-5, calculated using measured dimensions and material properties. The relatively small difference between the strength of each specimen's rafter and column member is due to the very small differences in web depth and the same yield stress was used for all web material of the same nominal thickness.

Table 3-5 Predicted Shear Strength

Specimen	Member	Measured yield stress (ksi)	Predicted Shear Strength, V_{pred} (kips)
SH-1	Rafter	63.85	13.43
	Column	63.85	13.46
SH-2	Rafter	63.85	13.43
	Column	63.85	13.46
MH-1	Rafter	53.54	55.08
	Column	53.54	55.05
LH-1	Rafter	61.00	63.99
	Column	61.00	63.90

The shear strengths of Sumner *et al.* test specimens were also determined based on the provisions given in Section 3.3.2. The geometry, measured dimensions and material properties in Table 3-2 were used and the results are listed in Table 3-6.

Table 3-6 Sumner *et al.* Specimens Predicted Shear Strength

Specimen	Member	Measured yield stress (ksi)	Predicted Shear Strength, V_{pred}
Knee 1	Rafter	48.25	23.66
	Column	54.30	19.33
Knee 1A	Rafter	48.25	23.66
	Column	54.30	19.33
Knee 2	Rafter	55.20	12.51
	Column	52.90	12.41
Knee 3	Rafter	56.55	9.62
	Column	56.80	9.32
Knee 7	Rafter	31.60	43.17
	Column	45.00	45.96

CHAPTER 4

COMPARISON OF ANALYTICAL AND EXPERIMENTAL RESULTS

4.1 General

The four specimens tested in the current study were each determined, strain and web displacement data, to have failed in a web shear buckling mode near the reentrant corner. The modified and unmodified shear forces corresponding to the maximum applied load and the predicted shear strengths are given in Table 4-1. The shaded rows indicate locations where the failure mode was determined to be web shear buckling.

Table 4-1 Comparison of Experimental and Predicted Shear Strength

Specimen	Member	Unmodified Shear $V_{u,exp}$ (kips)	Modified Shear $V_{m,exp}$ (kips)	Predicted Shear Strength, V_{pred}	$V_{u,exp}/V_{pred}$	$V_{m,exp}/V_{pred}$
	Rafter	***14.79***	***8.81***	***13.43***	***1.10***	***0.66***
SH-1	Column	20.64	14.80	13.46	1.53	1.10
	Rafter	14.57	8.68	13.43	1.08	0.65
SH-2	***Column***	***20.32***	***14.57***	***13.46***	***1.51***	***1.08***
	Rafter	47.76	35.18	55.08	0.87	0.64
MH-1	***Column***	***64.93***	***54.27***	***55.05***	***1.18***	***0.99***
	Rafter	***85.71***	***53.22***	***63.99***	***1.34***	***0.83***
LH-1	***Column***	***114.15***	***66.36***	***63.90***	***1.79***	***1.04***

In the shaded rows, the ratios in the last two columns which are greater than unity indicate the degree to which the tested strength was greater than the predicted shear strength. Values less than unity indicate the degree to which the analysis method is unconservative. In members which did not fail in shear, the computed ratios are conservative when greater than unity, but inconclusive when less than unity because the full shear capacity of the webs were not reached.

Of the Sumner *et al*. knee specimens, only one failed in a shear buckling mode. Those that did not fail in shear offer only indirect comparisons of experimental and predicted results. The results of the five negative moment tests are given in Table 4-2.

Table 4-2 Sumner *et al.* Experimental and Predicted Shear Strength

Specimen	Member	Unmodified Shear $V_{u,exp}$ (kips)	Modified Shear $V_{m,exp}$ (kips)	Predicted Shear Strength, V_{pred}	$V_{u,exp}/V_{pred}$	$V_{m,exp}/V_{pred}$
	Rafter	***20.96***	***16.63***	***23.66***	***0.89***	***0.70***
Knee 1	Column	14.06	8.48	19.33	0.73	0.44
	Rafter	24.15	19.15	23.66	1.02	0.81
Knee 1A	Column	16.20	9.77	19.33	0.84	0.51
	Rafter	20.19	15.79	12.51	1.61	1.26
Knee 2	Column	13.54	8.02	12.41	1.09	0.65
	Rafter	19.25	14.98	9.62	2.00	1.56
Knee 3	Column	12.92	7.55	9.32	1.39	0.81
	Rafter	47.90	39.38	43.17	1.11	0.91
Knee 7	Column	37.28	20.94	45.96	0.81	0.46

It should be noted that web shear buckling was the observed failure mode only in the Knee 1 rafter of the Sumner *et al*. tests. In this case both the modified and unmodified shears produce unconservative results, achieving only 70 percent and 89 percent of the predicted strength, respectively. In all other cases ratios less than unity do not necessarily indicate unconservative analysis because the full capacities of the webs were not realized.

4.2 Measured Web Strain

The web strain measurements provided no evidence in support of a modified shear theory. The shear forces were calculated from strain data taken at 10 percent of the maximum applied load, as described in Section 2.9. These values as well as the experimental modified and unmodified shear forces at the gage line are given in Table 4-3.

Table 4-3 Shear Forces from Strain Data

Specimen	Member	Applied Load at 10% of max (kips)	Shear from Strain Data V_{strain}(kips)	Unmodified Shear $V_{u,exp}$ (kips)	Modified Shear $V_{m,exp}$ (kips)	$V_{u,exp}/V_{strain}$	$V_{m,exp}/V_{strain}$
	Rafter	2.6	0.70	1.45	0.82	2.07	1.17
SH-1	Column	2.6	3.27	2.02	1.42	0.62	0.43
	Rafter	8.6	13.45	4.75	3.54	0.35	0.26
MH-1	Column	8.6	13.79	6.46	5.51	0.47	0.40
	Rafter	16.1	5.58	8.56	3.96	1.53	0.71
LH-1	Column	16.1	17.15	11.39	6.79	0.66	0.40

The last two columns contain ratios of the unmodified experimental shear-to-the shear from strain data and modified experimental shear-to-the shear from strain data. Values less than

unity indicate a web shear force derived from shear strain data to be larger than the experimental shear. In most cases the shear forces in the web determined from measured strain data are substantially higher than both of the experimental forces calculated from the applied load and specimen geometry. Only in the LH-1 rafter and SH-1 rafter have web shear stresses, determined from strain data, which are lower than the experimental shear forces. These members were also shown to have high levels of initial web imperfections, which may have led to instability of the web even at loads as low as 10 percent of the maximum sustained load. It can be seen that the stresses calculated from the strain data do not show any obvious trend in support of the modified shear theory, but they do indicate an interaction between the distribution of shear stresses in the web and the forces in the inclined flanges.

It was shown in Section 2.9 that much larger shear strains were typically present near the compression flange. The cause of larger measured shear strains in the compression region of the web is not immediately evident. In some cases in which out-of-plane bending strains were measured across the thickness of the web, the tension strain and compression strain were disproportionate. When averaging these values, the net differential bending strain can produce larger calculated shear strains than were actually present. If much larger differential strains typically exist in the lower portion of the web, they could be reasonably attributed to several phenomena other than the shear buckling mode. Two possibilities include localized web crippling resulting from the adjacent concentrated force applied by the connected specimen (ie rafter compression flange bearing on the column), or out-of-plane bending due to flexural compressive stresses. Either of these sources could be responsible for a destabilization of the web in the lower portion of the knee area rendering it more susceptible to buckling, and high differential bending strains.

It has been claimed by Basler (1961b) that stiffened slender web elements of prismatic plate girders can, subsequent to small lateral displacements, transfer their compressive bending stresses to the adjacent flange and still carry their full portion of shear stresses. This maintenance of shear strength was attributed to the contribution of a tension field, and it was with stiffened plate girder test data that Balser's proposed shear and flexure interaction equations were validated. It can be reasonably assumed that out of plane web displacement in the compression region of a tapered member will cause a redistribution of the web bending stress to

the compression flange. It is however not clear how the forces in the inclined compression flange will in influence the web.

Basler also claimed that the bending moment will not inhibit the web's ability to carry shear before plastic yielding of the flange takes place. As has already been discussed, the assumption of a plastic stress distribution is not compatible with tapered member design so the effects of flange stresses beyond yield need not be considered. However, there is clearly some interaction between the inclined compression flange and the shear stresses present in the web even at loads much lower than yielding. The modified shear theories discussed in Chapter 3 make no provision for the observed demand placed on the web by the compression flange. The assumption that a transverse component of the compressive flange force, acting in the direction of the web shear force, would diminish the shear force in the web without adverse interaction is perhaps overly simplistic.

4.3 Discussion

The test results from the current study, in which web shear buckling was observed to initiate instability, do not show consistent support for a modified shear. The use of an unmodified shear force produces a conservative design in all of the specimens in the current study. It can be seen that the prediction equations are overly conservative in some cases. The LH-1 rafter ultimately sustained a load 80 percent higher than predicted, and the SH-2 Column was conservative by 57 percent. These two examples are the most extreme cases, however and the ratio of predicted shear strength to unmodified experimental load is 1.38 on average. The results obtained from Sumner *et al*. test data also do not indicate a consistent prediction of web shear strength using a modified shear force. The use of both modified and unmodified shear forces produced unconservative results in the Knee 1 rafter of the Sumner *et al.* study.

The nominal shear strengths of the columns and rafters are negligibly different, as shown in Table 4-1. Due to the orientation of the tested specimens, the unmodified and modified shear forces in the rafters are an average of 73 percent and 66 percent of the shear in the columns, respectively. Thus, column web buckling should occur prior to rafter web buckling. However web buckling occurred first in the specimen SH-1 rafter, and in the LH-1 specimen, both rafter and column web buckling occurred.

The rafters in specimens LH-1 and SH-1, which exhibited shear buckling failures at lower than predicted values, also contained higher initial imperfections than the associated columns. The ratios of deviations to the MBMA tolerance criteria along both a transverse (c) and longitudinal (f) line were given in Table 2-6, with the shaded rows indicating the failure location due to web shear buckling. The deviations in the SH-1 rafter exceeded the D/72 limit along the centerline and the longitudinal deviation of the LH-1 rafter was more than 90 percent of the D/72 limit.

Failure consistently occurred in the member with a higher imperfection ratio along the centerline. The LH-1 specimen failed in both the rafter and column. If the observed early failures in the rafters are in fact a result of these web imperfections, then some interesting observations can be made. As has already been stated, the column webs were the more likely location of web shear buckling failure. If the LH-1 and SH-1 rafters are removed from the study for the sake of argument, it can be seen in Table 4-1 that the modified shear produces highly favorable results.

CHAPTER 5

CONCLUSIONS AND RECOMMENDATIONS

5.1 Summary and Conclusions

This study involved simulated gravity load tests of four slender, unstiffened web tapered gable frame knee specimens. Initial imperfections in the web plane were measured and compared to tolerance limits set by The Metal Building Manufacturers Association (MBMA). Theoretical shear forces in the webs near the column and rafter connection were determined by a modified shear approach, which accounts for the transverse component of force in the inclined flanges, and by an unmodified approach which is determined directly from the externally applied shear. The web plate shear strengths were calculated according to the AISC provisions for prismatic members. Several observations can be made when comparing the experimental and analytical results.

The measured initial deviations in the webs from a flat plane may be reasonably correlated with earlier than predicted failures in the rafters of specimen SH-1 and LH-1. If these imperfections did influence early buckling, the modified shear forces appear to produce very accurate results. However it is not certain that these failures were the result of web imperfections, and the web shear stresses determined from strain data do not support a modified shear method as presented in Section 3.3.1. The shear strains indicate higher shear stresses near the compression flange and lower shear stresses near the tension flange. This suggests that there is some interaction between the flexural forces in the inclined flanges and the shear forces in the web. The presence of higher shear stresses near the compression flange indicate that the transverse component of the flange force may have a negative influence on the web shear, rather than acting to reduce the shear demand on the web.

The presence of a variable shear stress distribution is also not addressed by the AISC provisions for prismatic members that were used in the strength analysis. It has been shown that the use of unmodified shear forces and the AISC shear design provisions produce conservative results but it is acknowledged that these approaches do not accurately address the stresses present in slender unstiffened tapered steel members.

The current study has shown that the shear forces which the unstiffened web plate must be designed to resist can only be consistently determined using unmodified shear forces. For this reason, it is recommended that the rafter and column web plates of slender, unstiffened tapered members similar to those shown in Figure 2-1, be designed using unmodified shear forces. When unmodified shear forces are used, the calculation of a web plate's shear capacity appears to be adequately managed by the provisions for prismatic girders, according to the AISC strength equations presented in Section 3.3.2.

5.2 Recommendations for Future Research

The current study has raised several questions about the performance of slender webs in tapered members. Similar tests, with measured imperfections of members with stockier web elements, would be useful to determine the relative interaction of web plate slenderness and deviations from a flat plane. Such tests may also present more conclusive evidence for a modified shear force. While it was shown that the current AISC shear design method for prismatic members is adequate for design, it does not account for the observed variation in shear stress distributions across the web depth. The cause of variation in shear stress distribution was not obvious. Tests of tapered members with stockier webs would be very helpful in establishing the shear strain distribution across the web in the absence of differential bending strains, which may be useful in defining the influence of inclined flange forces on shear and flexure interaction.

Another issue that could not be addressed in the current study is the effect of concentrated forces introduced at the reentrant corner by the adjacent member compression flange. The code provisions used to determine the adequacy of a web element to resist crippling and local yielding due to concentrated forces were developed using yield line models and test data from prismatic members (Roberts 1981). These provisions cannot be reasonably applied to the geometry and load paths at the reentrant corner of a diagonal knee connection.

REFERENCES

AISC. (1974). *Supplement No. 3 to The Specification for the Design, Fabrication and Erection of Structural Steel for Buildings (1969)*, American Institute of Steel Construction, NY.

AISC. (1994). *Manual of Steel Construction – Load and Resistance Factor Design*, American Institute of Steel Construction, Inc., Chicago, IL.

AISC. (2005a). *Specification for Structural Steel Buildings*, American Institute of Steel Construction, Inc., Chicago, IL.

AISC. (2005b). *Steel Construction Manual, 13th ed.*, American Institute of Steel Construction, Inc., Chicago, IL.

Amirikian, A. (1951). "Wedge-beam framing." *Proceedings - American Society of Civil Engineers*, 77(Separate 53).

Basler, K. (1961a). "Strength of Plate Girders in Shear." *ASCE Journal of the Structural Division,* 87(ST7 Part 1), 151-180.

Basler, K. (1961b). "Strength of Plate Girders Under Combined Bending and Shear." *ASCE Journal of The Structural Division,* 87(ST7 Part 2), 181-197.

Basler, K., and Thurlimann, B. (1961). "Strength of Plate Girders in Bending." *ASCE Journal of the Structural Division*, 87(ST6), 153-181.

Beer, F. P., Johnston, Jr., E. R., DeWolf, J.T. (2002). *Mechanics of Materials.* McGraw Hill, Boston.

Bleich, F. (1952). *Buckling Strength of Metal Structures*, McGraw-Hill Book Co., NY.

Blodgett, O. W. (1966). *Design of Welded Structures*, The James F. Lincoln Arc Welding Foundation, Cleveland, OH.

Bresler, B., Lin, T. Y., and Scalzi, J. B. (1968). *Design of Steel Structures*, John Wiley and Sons, Inc., New York.

Computers and Structures, Inc. (2006). *SAP2000 v10 - Integrated Structural Analysis & Design Software*, Computers and Structures, Inc., Berkeley, California.

Holman, J.P. (1978). *Experimental Methods for Engineers.* McGraw Hill, New York.

Kaehler, R. C., White, D., and Kim, Y. D. (2007). *Frame Design Using Web Tapered Members, Steel Design Guide Series (Draft-Jul. 10, 2007)*, American Institute of Steel Construction, Chicago, IL.

Lee, G. C., Ketter, R. L., and Hsu, T. L. (1981). *Design of Single Story Rigid Frames*, Metal Building Manufacturers Association, Cleveland, OH.

Lee, G. C., Morrell, M. L., and Ketter, R. L. (1972). "Design of Tapered Members." *Welding Research Council Bulletin*, 173, 1-32.

MBMA. (2006). *Metal Building Systems Manual*, Metal Building Manufacturers Association, Inc., Cleveland, OH.

Mirambell, E., and Zarate, A. V. (2000). "Web Buckling of Tapered Plate Girders." *Proceedings of the Institution of Civil Engineers, Structures and Buildings*, 140(1), 51-60.

Mirambell, E., and Zarate, A. V. (2004). "Shear Strength of Tapered Steel Plate Girders." *Proceedings of the Institution of Civil Engineers, Structures and Buildings*, 157(5B5), 343-354.

Murray, T. M., and Shoemaker, W. L. (2003). *Flush and Extended Multiple Row Moment End Plate Connections*, American Institute of Steel Construction, Chicago, IL.

Roberts, T. M. (1981). "Slender Plate Girders with Edge Loading." *Proceedings of the Institution of Civil Engineers*, *Part 2*, 71(Sept.), 805-819.

Shah, P. (2007). "Linear and Nonlinear Stability Analysis of Steel Frames with Web-Tapered Members," MS Thesis, Virginia Polytechnic Institute and State University, Blacksburg, VA.

Sullivan, S., and Charney, F. A. (2006). "Performance of Diagonal Knee Connections With and Without Stiffeners." Research Report No. CEE/VPI-ST06/02, Department of Civil and

Environmental Engineering, Virginia Polytechnic Institute and State University, Blacksburg, VA.

Sumner, E. A. (1995). "Experimental and Analytical Investigation of the LRFD Strength of Tapered Members," MS Thesis, Virginia Polytechnic Institute and State University, Blacksburg, VA.

Sumner, E. A., Borgsmiller, J. T., and Murray, T. M. (1995). "Experimental Investigation of Rigid Knee Joints." Research Report No. CE/VPI-ST-95/12, Department of Civil and Environmental Engineering, Virginia Polytechnic Institute and State University, Blacksburg, VA.

Tall, L. (1974). *Structural Steel Design*, John Wiley and Sons, New York.

Williams, C. D., and Harris, E. C. (1957). *Structural Design in Metals*, The Ronald Press Company, New York.

APPENDIX A. TEST SH-1-1 RESULTS

PROJECT: American Buildings Company
TEST NAME: ABC-SH-1-1 (knee test 1)
TEST DATE: October 25, 2006
PURPOSE: Negative Bending Moment Test for Web Buckling w/o Stiffeners

CONNECTION DESCRIPTION:

NOMINAL YIELD STRESS: ……	55 ksi
GAGE: ……..	3 in
END PLATE WIDTH: …….	6 in
END PLATE THICKNESS: ……	1/2 in

BOLT DATA:

BOLT DIAMETER: ……	3/4 in
BOLT TYPE: ……...	A490
BOLT PRETENSION: ……	14 kips

COLUMN DATA: (MEASURED)

OUTSIDE FLANGE WIDTH: …….	6 in
OUTSIDE FLANGE THICKNESS: ……	0.375 in
INSIDE FLANGE WIDTH: ……..	6 in
INSIDE FLANGE THICKNESS: …….	0.377
WEB DEPTH AT BASE(PERP. TO OS FLANGE): ……..	14.81 in
WEB DEPTH AT REENTRANT CORNER(PERP. TO OS FLANGE): ……	22.0 in
WEB THICKNESS: …….	0.131 in
FLANGE YIELD STRESS: ……	55.1 ksi
WEB YIELD STRESS: ……	63.8 ksi

RAFTER DATA: (MEASURED)

OUTSIDE FLANGE WIDTH: …….	6 in
OUTSIDE FLANGE THICKNESS: …….	0.376 in
INSIDE FLANGE WIDTH: ……..	6 in
INSIDE FLANGE THICKNESS: …….	0.378 in
WEB DEPTH AT BASE(PERP. TO OS FLANGE): ……...	11.81 in
WEB DEPTH AT REENTRANT CORNER(PERP. TO OS FLANGE): ……	22.13 in
WEB THICKNESS: …….	0.131 in

EXPERIMENTAL:

MAXIMUM LOAD: ……...	26.5 kips
FAILURE LOCATION:	Rafter Web at Reentrant Corner
FAILURE MODE:	Web Buckling

DISCUSSION

- Some opening of the end plates was observed at the tension flanges however no obvious yield lines were apparent.

PROJECT: American Buildings Company
TEST NAME: ABC-SH-1-1 (knee test 1)
TEST DATE: October 25, 2006
PURPOSE: Negative Bending Moment Test for Web Buckling w/o Stiffeners

DISCUSSION (CONTINUED)

- The specimen was unloaded before the failure mode became visibly apparent, so that positive moment loading response could be investigated.

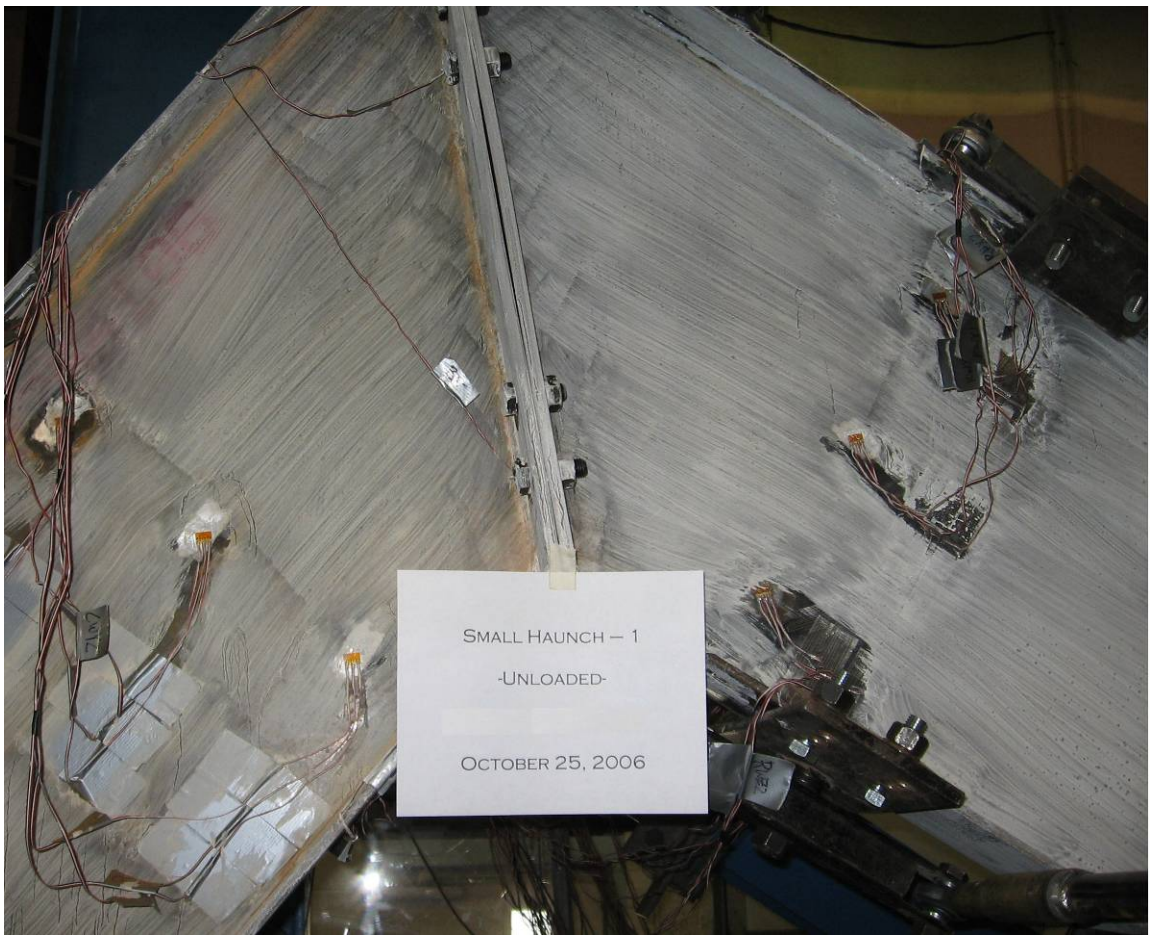

Figure A-1 SH-1-1 After Testing

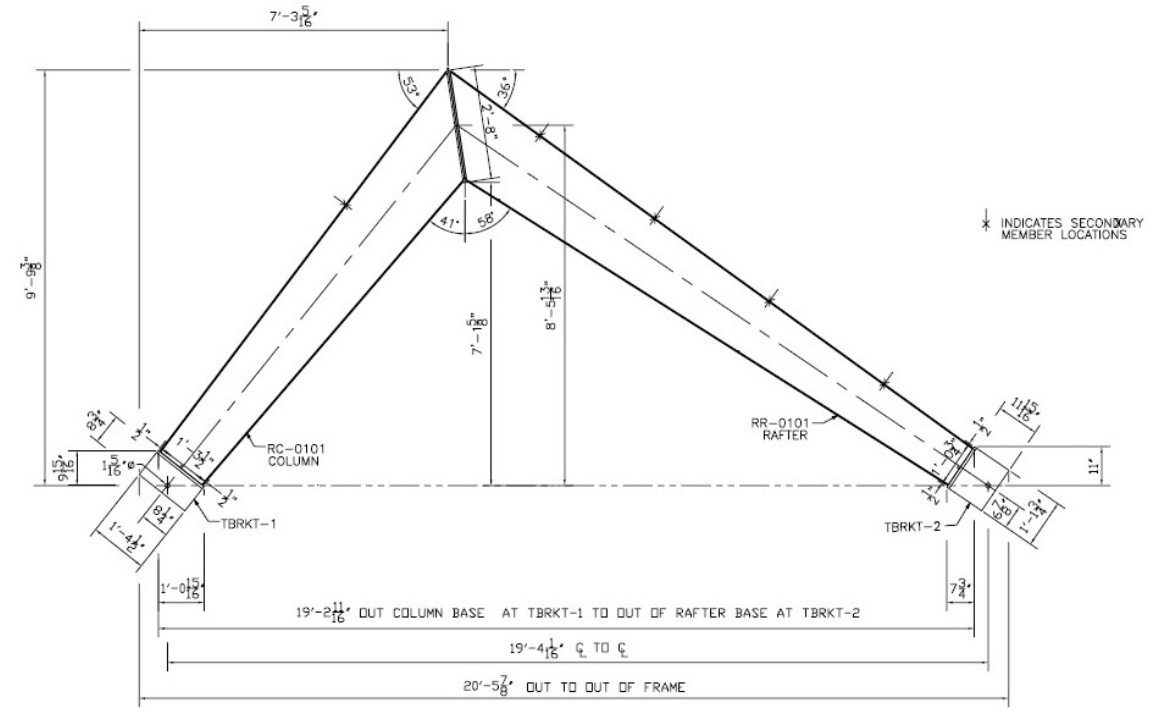

Figure A-2 SH-1 Specimen Dimensions

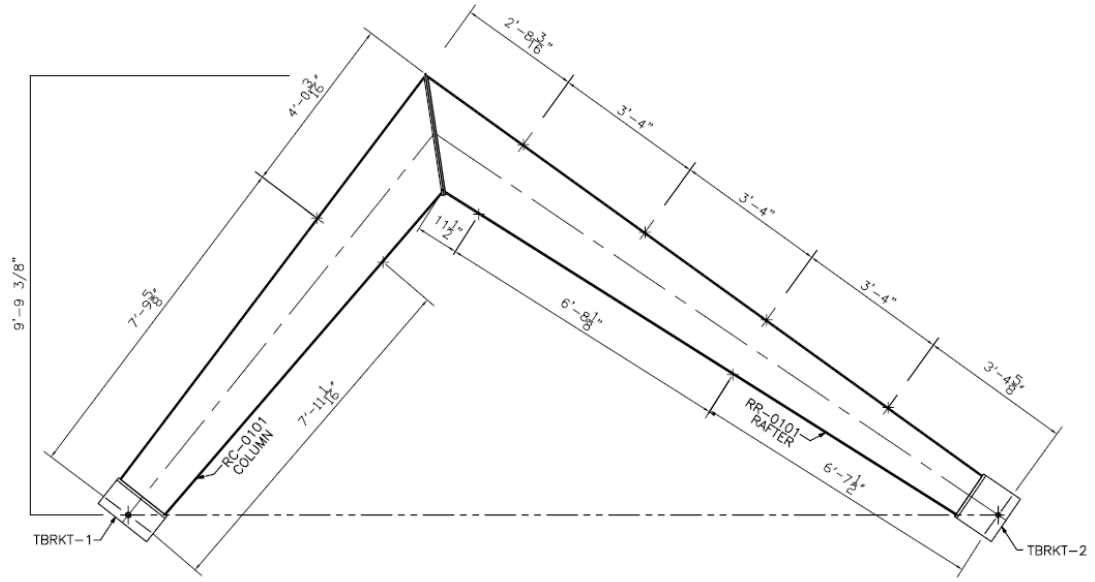

Figure A-3 SH-1 Lateral Brace Locations

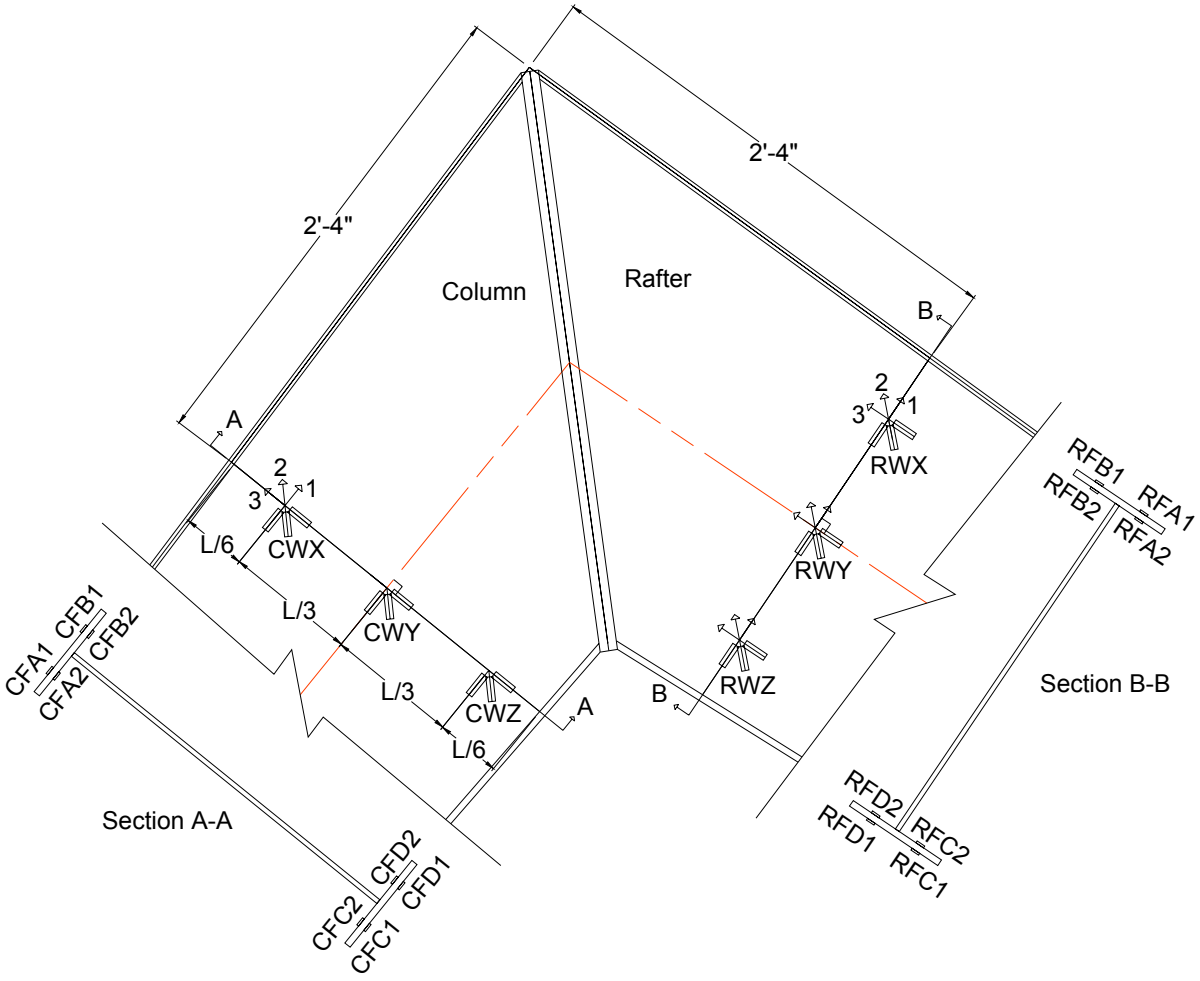

Figure A-4 Web and Flange Strain Gages As Viewed From the South

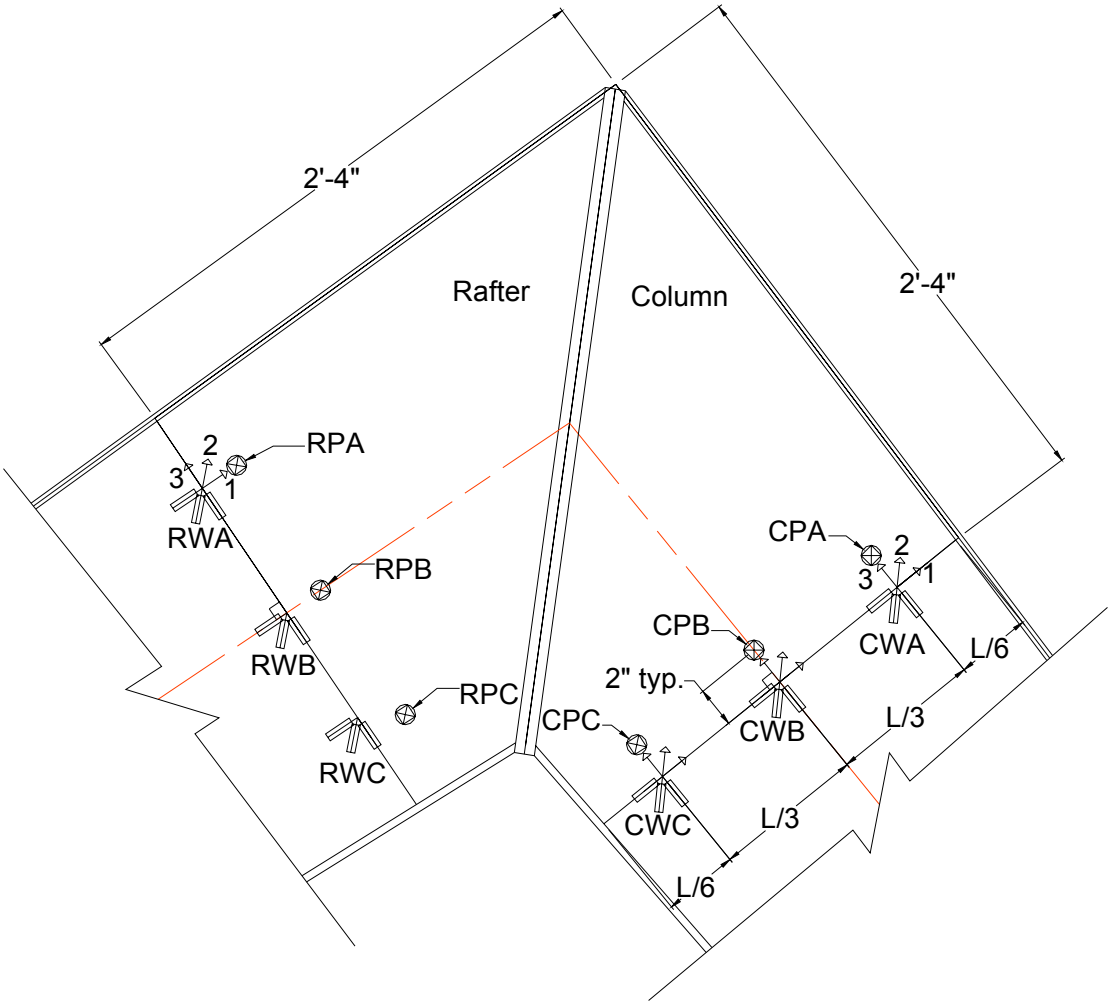

Figure A-5 SH-1 Web Strain Gages and LVDT's As Viewed from the North.

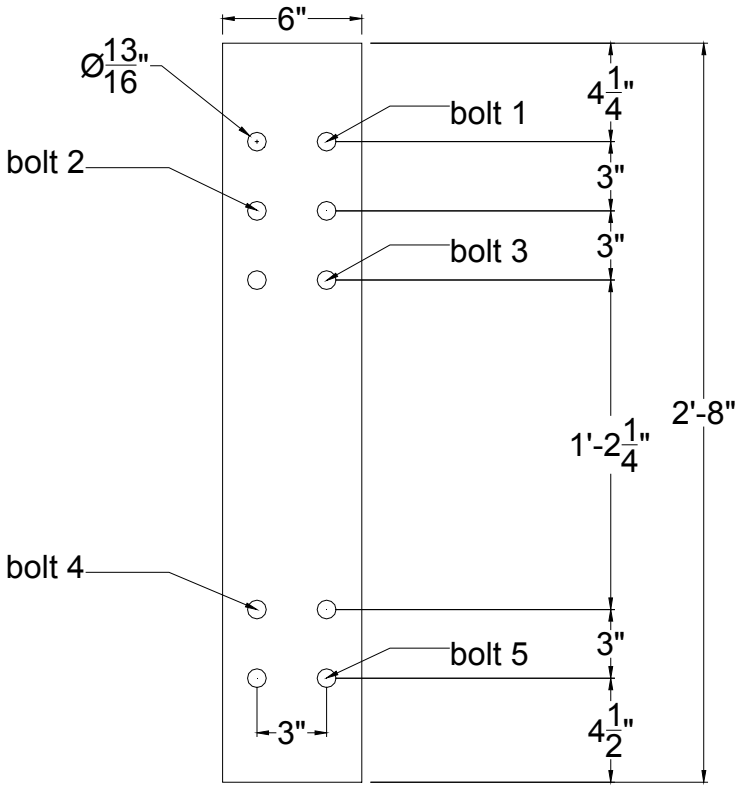

Figure A-6 SH-1 Gaged Bolt Orientation Viewed From the West

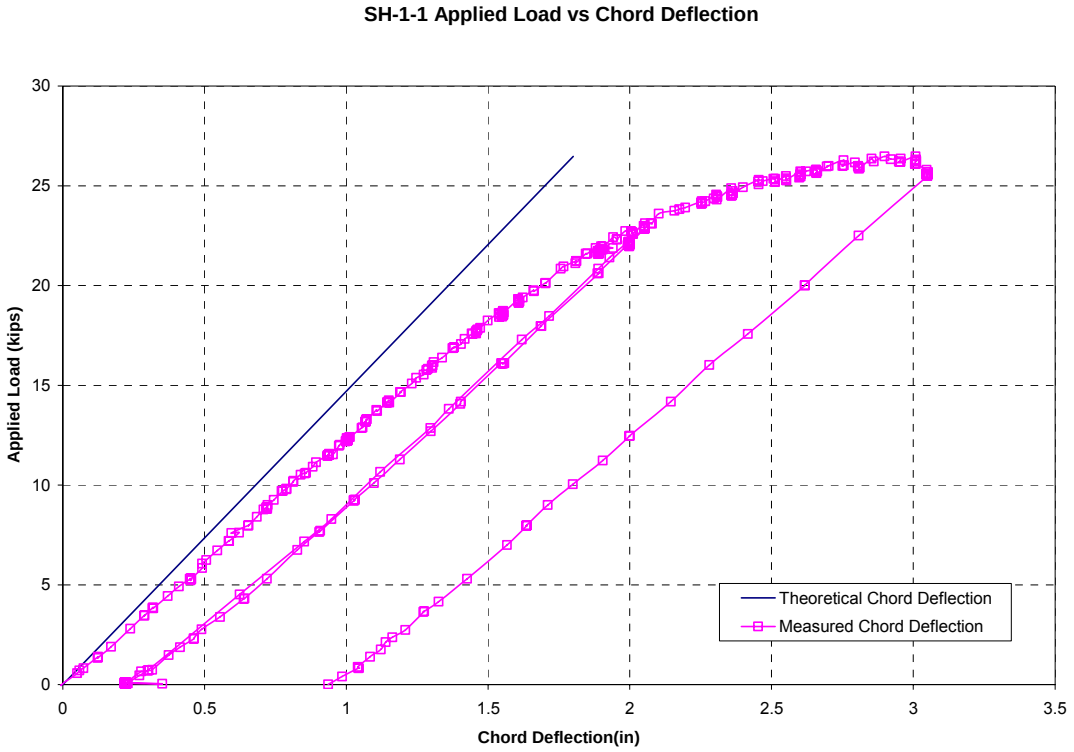

Figure A-7

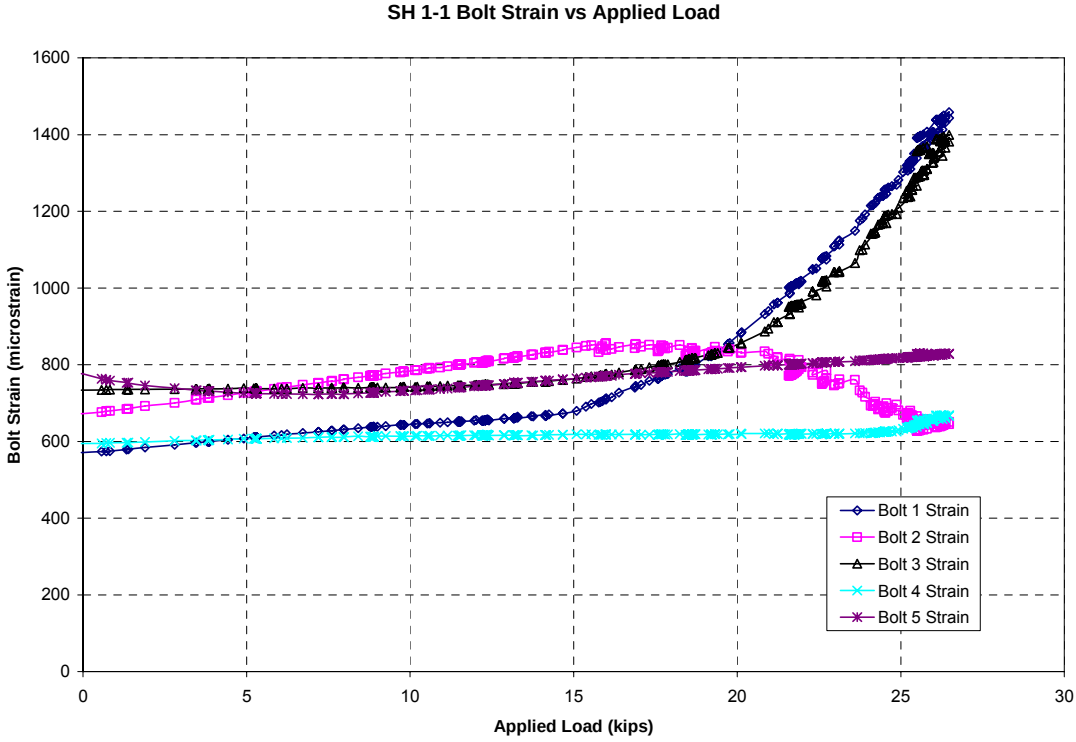

Figure A-8

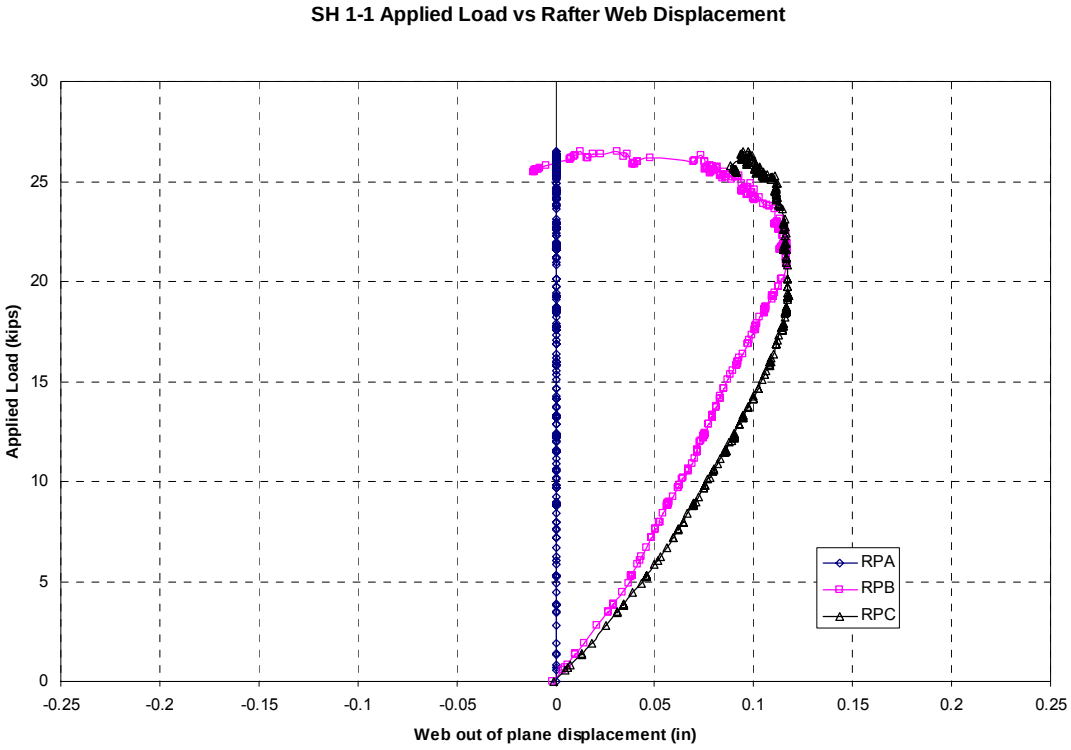

Figure A-9

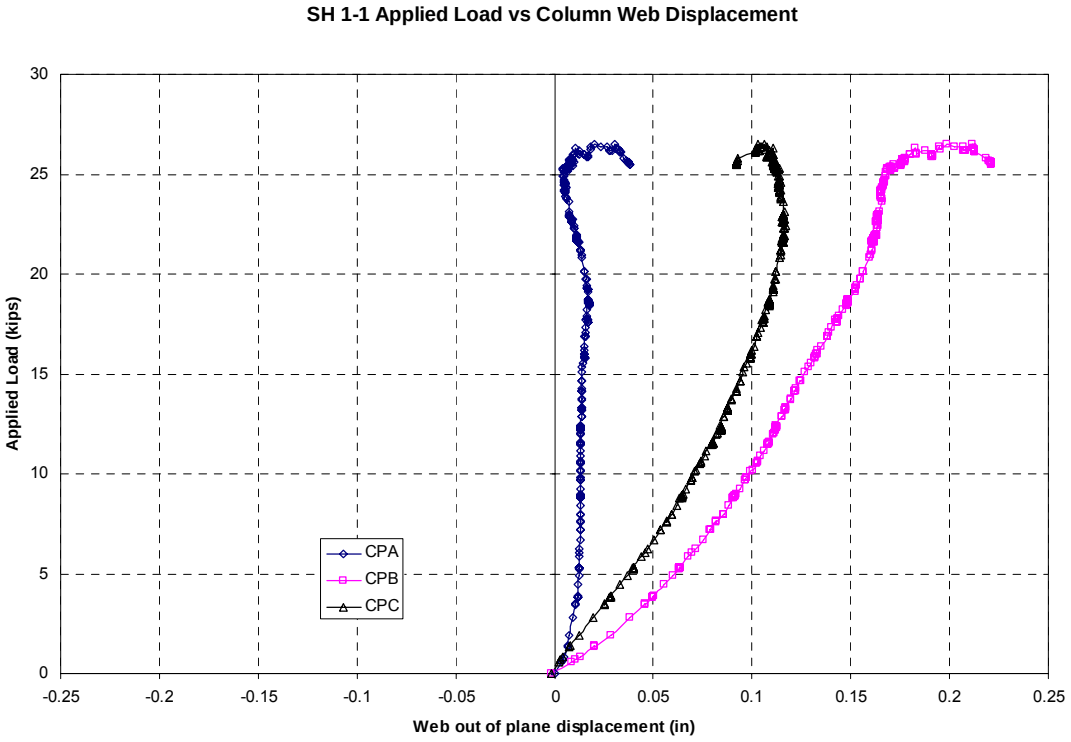

Figure A-10

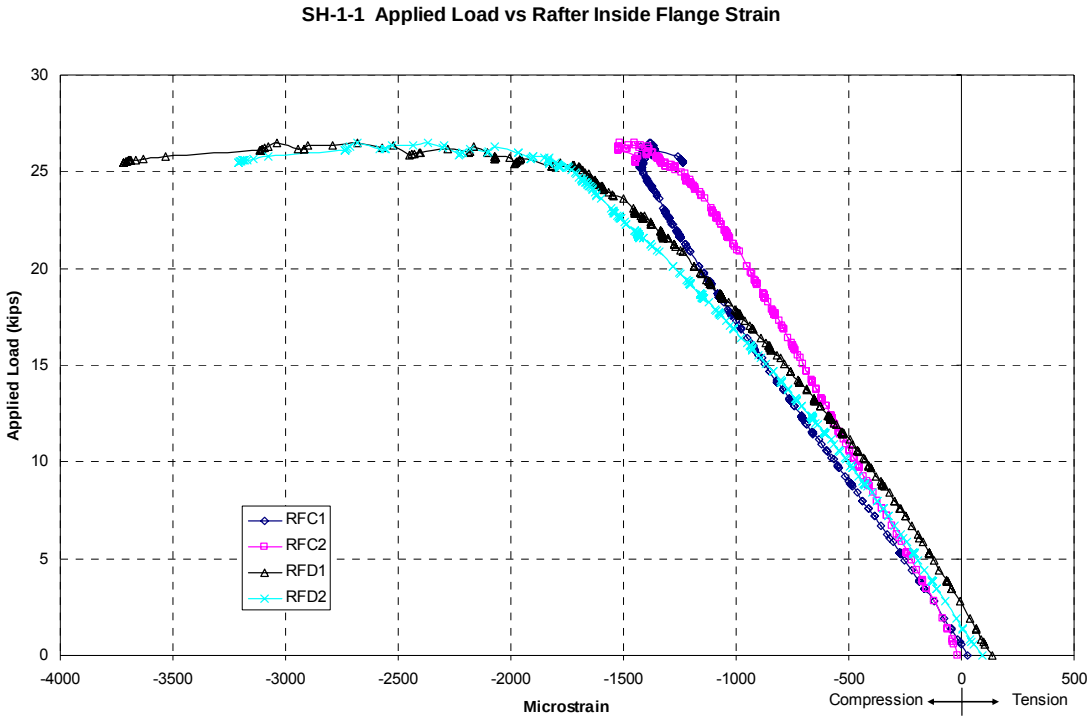

Figure A-11

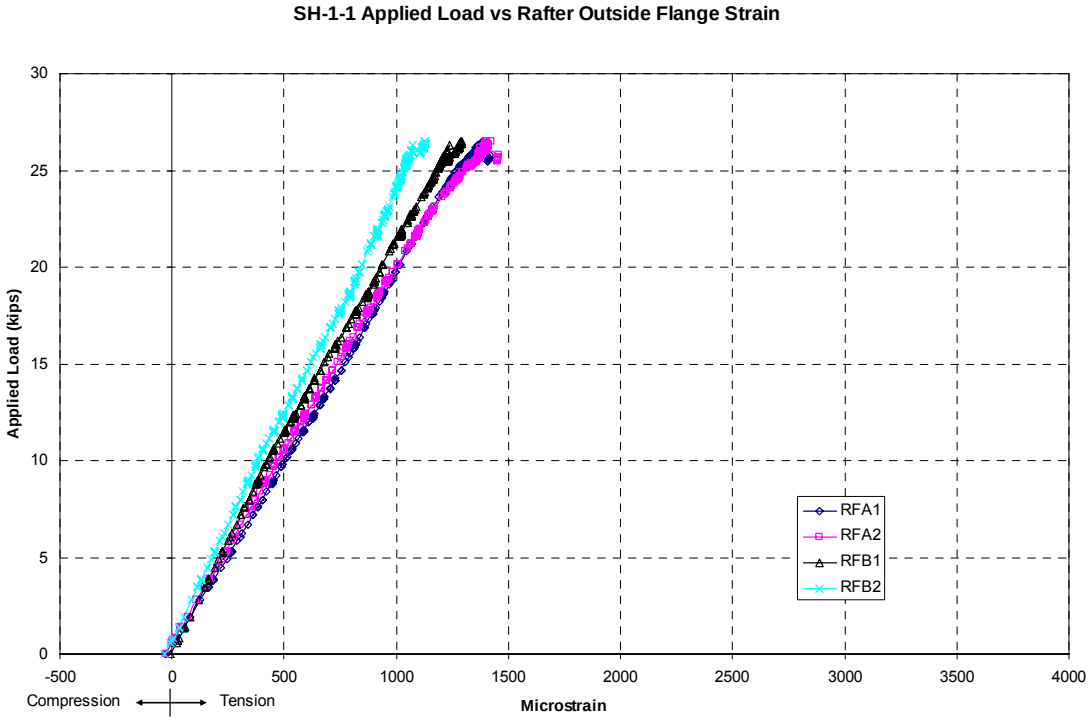

Figure A-12

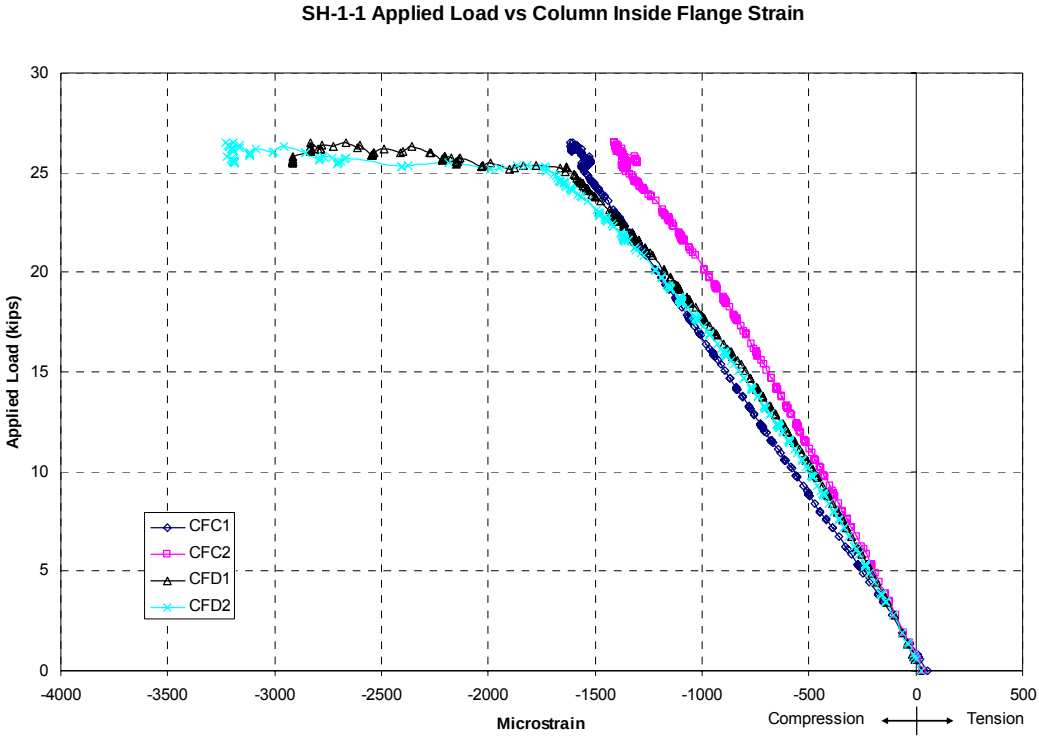

Figure A-13

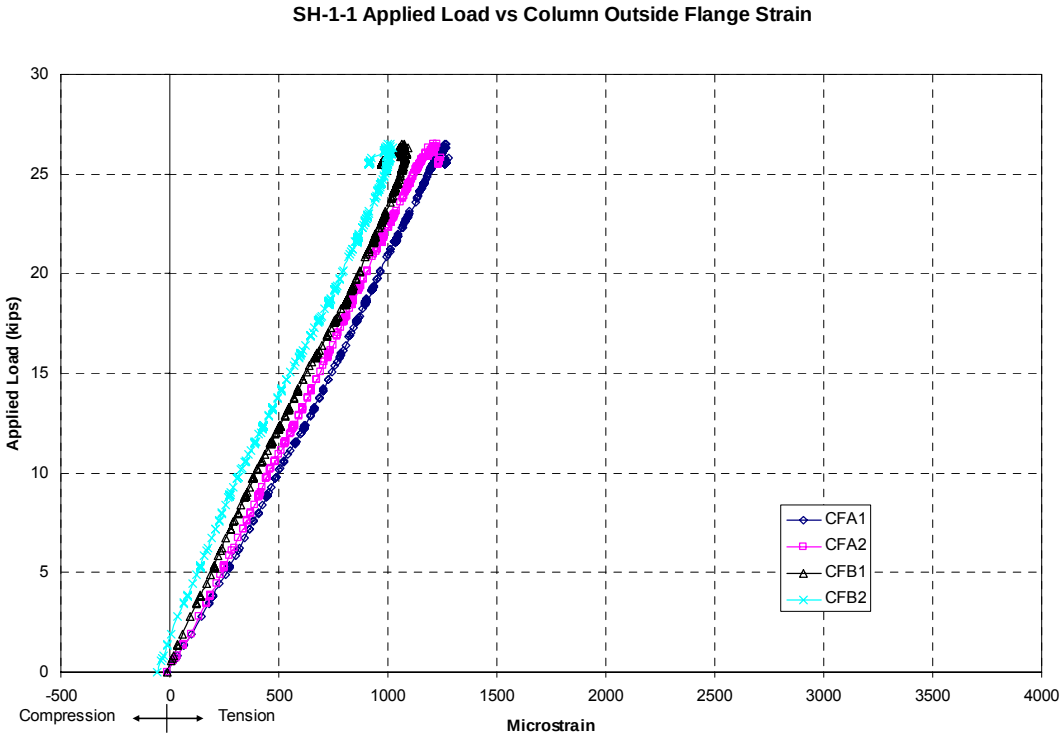

Figure A-14

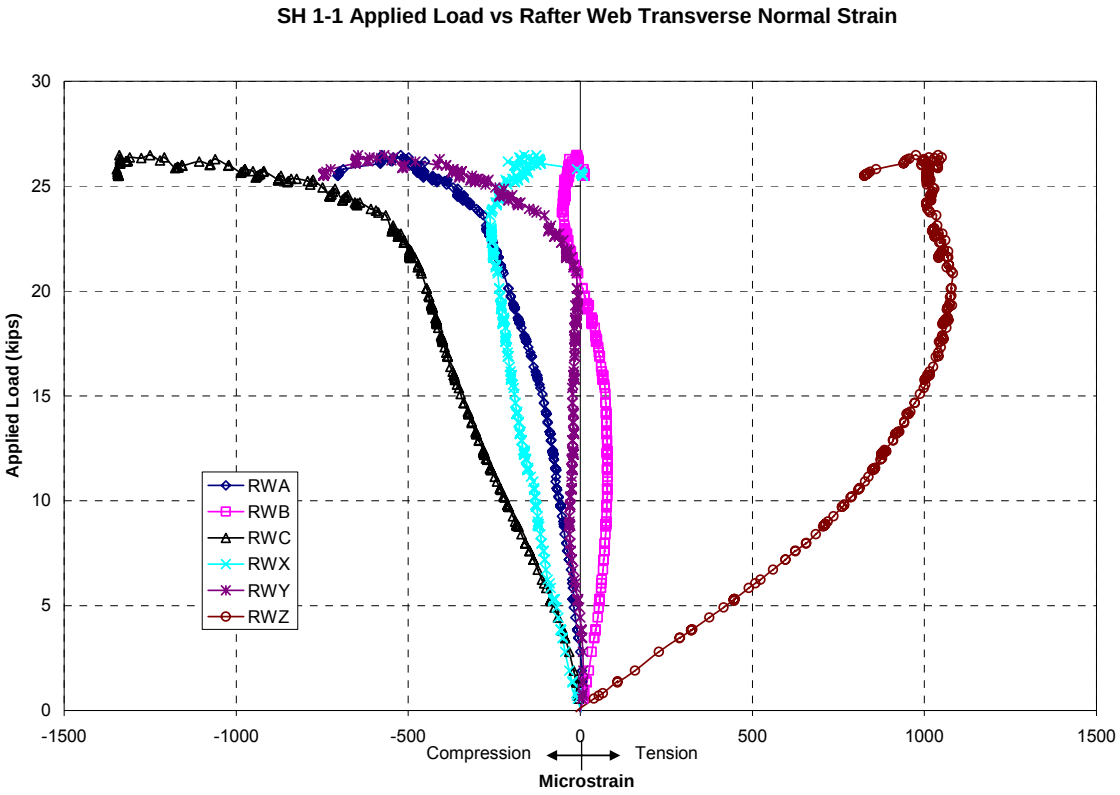

Figure A-15

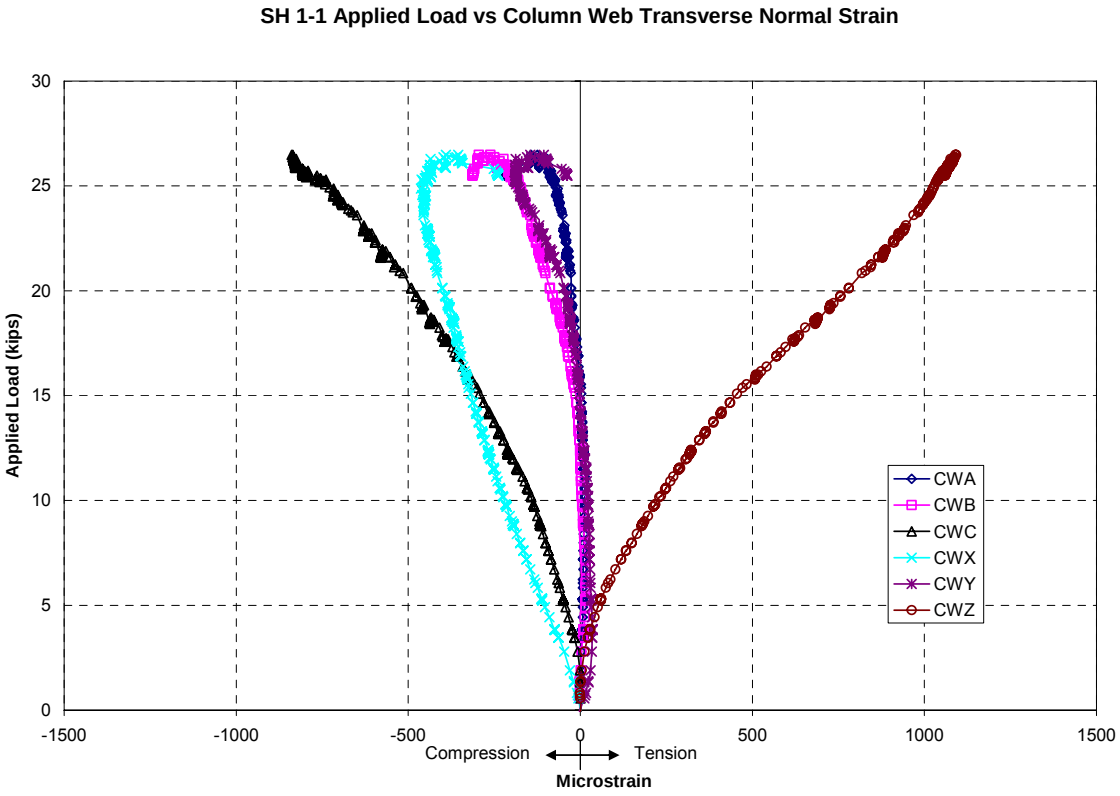

Figure A-16

APPENDIX B. TEST SH-1-2 RESULTS
(POSITIVE MOMENT)

PROJECT: American Buildings Company
TEST NAME: ABC-SH-1-2 (knee test 2)
TEST DATE: October 27, 2006
PURPOSE: Positive Bending Moment Test for Web Buckling w/o Stiffeners

CONNECTION DESCRIPTION:

NOMINAL YIELD STRESS: ……	55 ksi
GAGE: ……..	3 in
END PLATE WIDTH: …….	6 in
END PLATE THICKNESS: ……	1/2 in

BOLT DATA:

BOLT DIAMETER: ……	3/4 in
BOLT TYPE: ……...	A490
BOLT PRETENSION: ……	14 kips

COLUMN DATA: (MEASURED)

OUTSIDE FLANGE WIDTH: …….	6 in
OUTSIDE FLANGE THICKNESS: ……	0.375 in
INSIDE FLANGE WIDTH: ……...	6 in
INSIDE FLANGE THICKNESS: …….	0.377
WEB DEPTH AT BASE(PERP. TO OS FLANGE): ……..	14.81 in
WEB DEPTH AT REENTRANT CORNER(PERP. TO OS FLANGE): ……	22.0 in
WEB THICKNESS: …….	0.131 in

RAFTER DATA: (MEASURED)

OUTSIDE FLANGE WIDTH: …….	6 in
OUTSIDE FLANGE THICKNESS: …….	0.376 in
INSIDE FLANGE WIDTH: ……...	6 in
INSIDE FLANGE THICKNESS: …….	0.378 in
WEB DEPTH AT BASE(PERP. TO OS FLANGE): ……...	11.81 in
WEB DEPTH AT REENTRANT CORNER(PERP. TO OS FLANGE): ……	22.13 in
WEB THICKNESS: ……..	0.131 in

EXPERIMENTAL:

MAXIMUM LOAD: ……...	20.15 kips
FAILURE LOCATION:	N/A
FAILURE MODE:	N/A

DISCUSSION

- The test showed a marked difference in stiffness from the negative moment test, and this was attributed to the greater potential for end plate separation at the inside flanges.

PROJECT: American Buildings Company
TEST NAME: ABC-SH-1-2 (knee test 2)
TEST DATE: October 27, 2006
PURPOSE: Positive Bending Moment Test for Web Buckling w/o Stiffeners

DISCUSSION (CONTINUED)

- At 10.25 kips the specimen was unloaded through zero to negative 8.95 kips (negative moment) to verify the change in stiffness due to direction of loading.
- The specimen was then reloaded in positive moment up to 20.15 kips
- Test aborted when Bolt 5 approached design strength.

Figure B-1 SH-1-2 After Testing

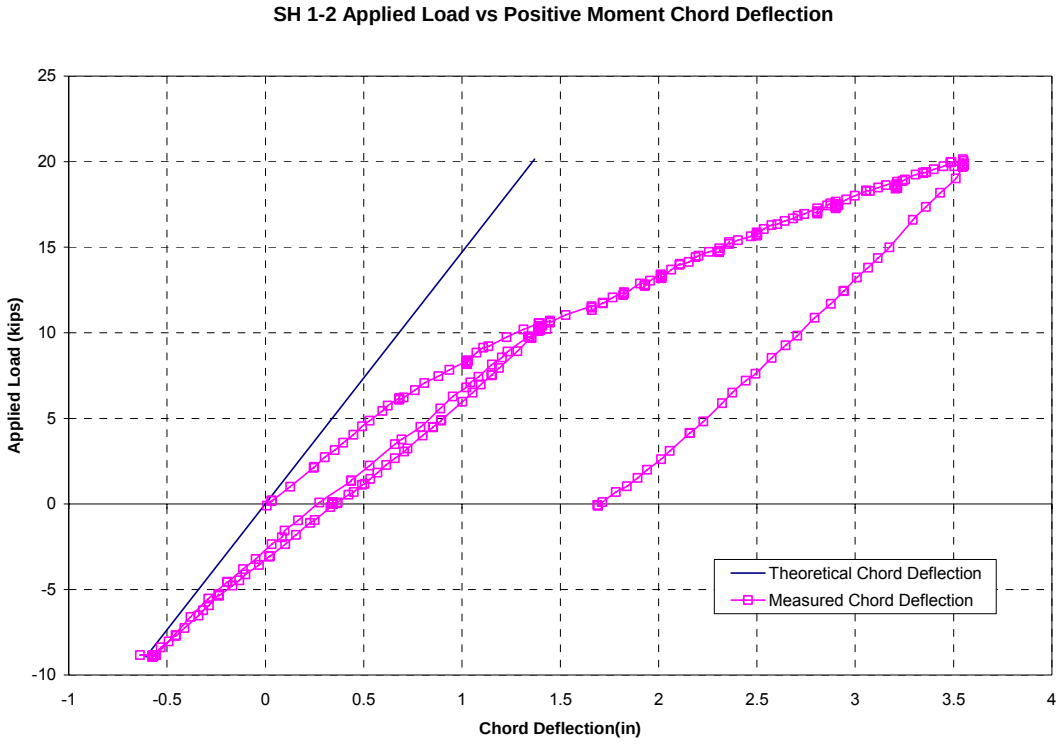

Figure B-2

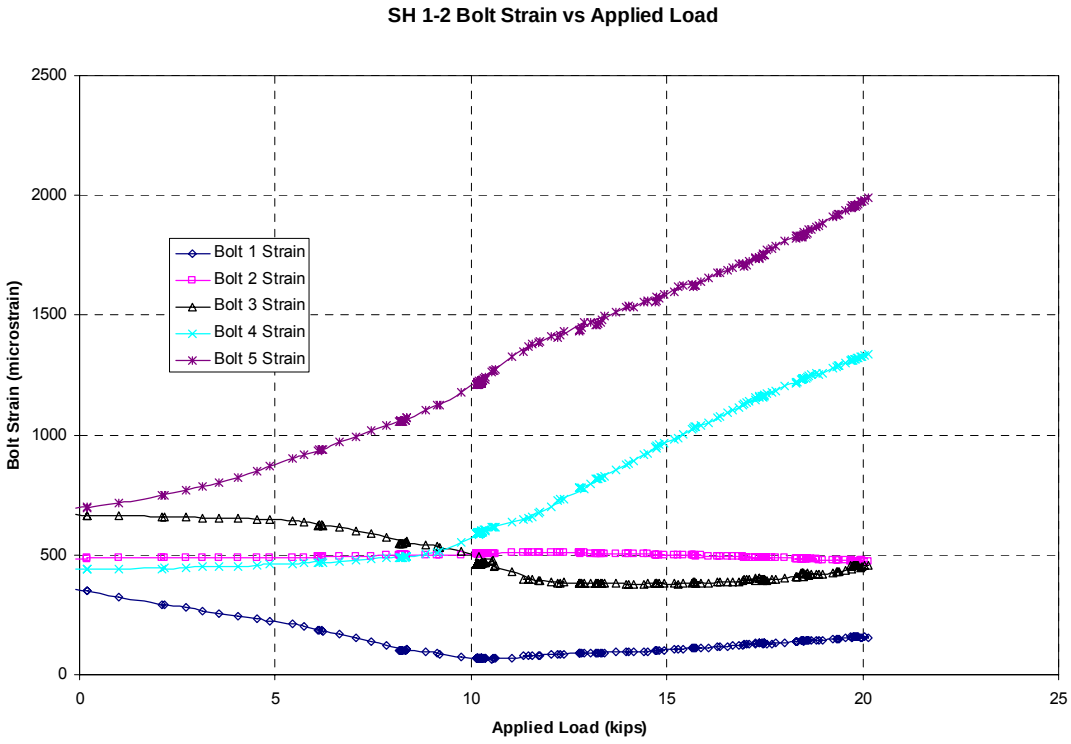

Figure B-3

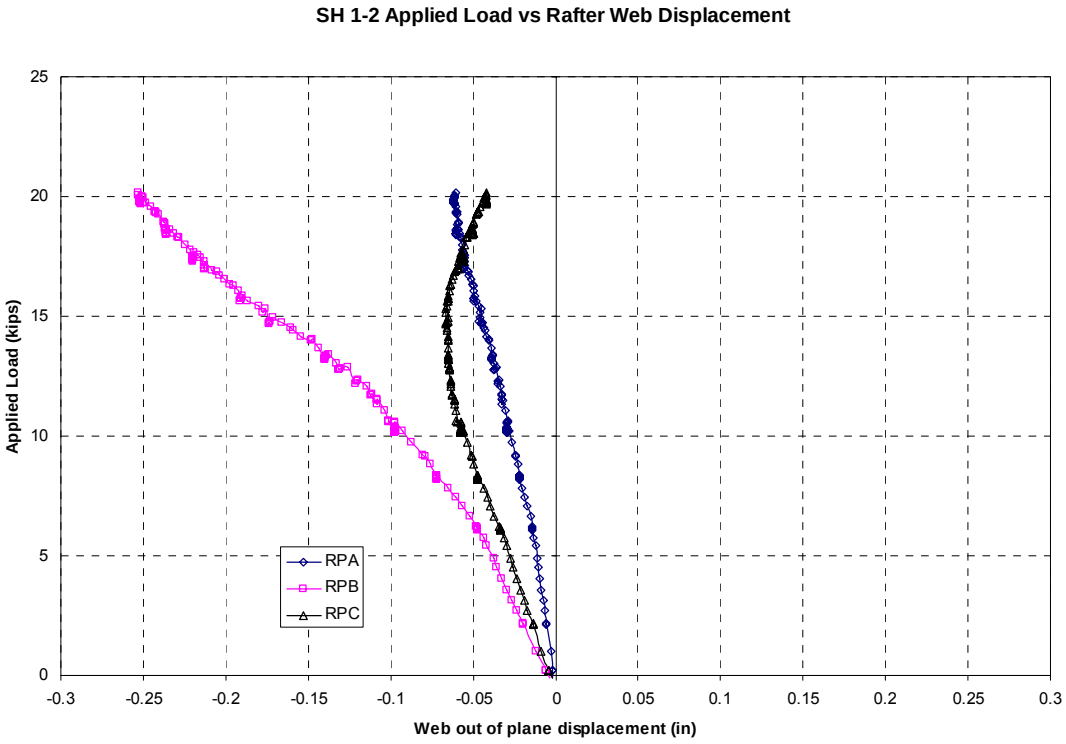

Figure B-4

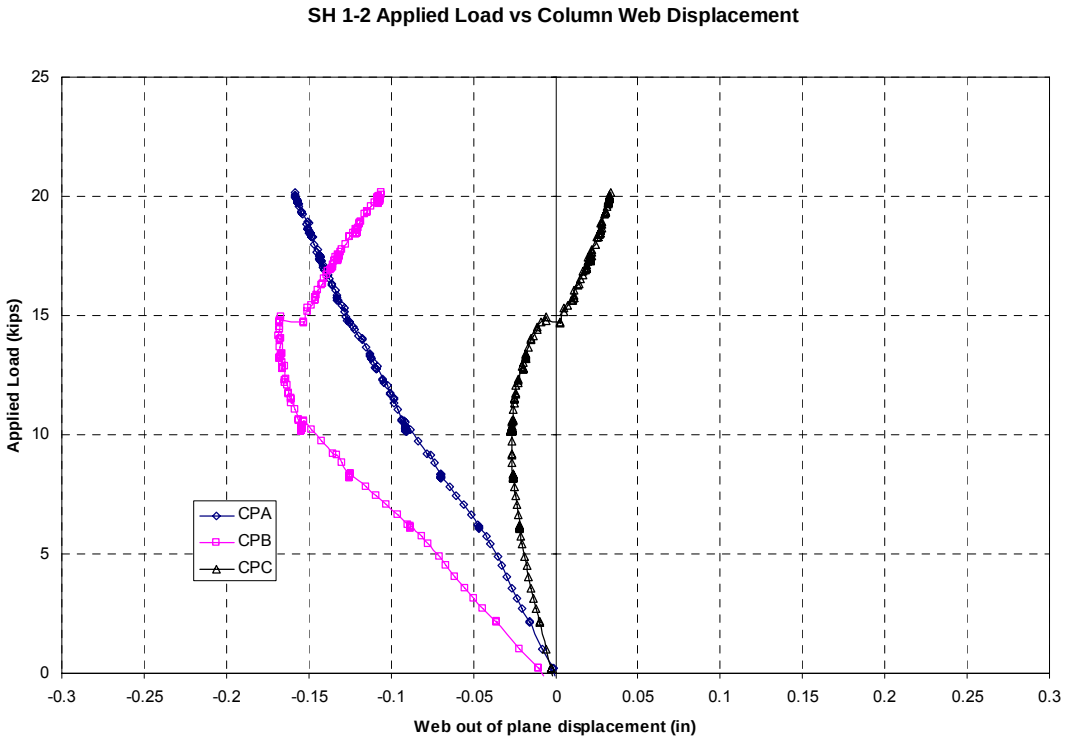

Figure B-5

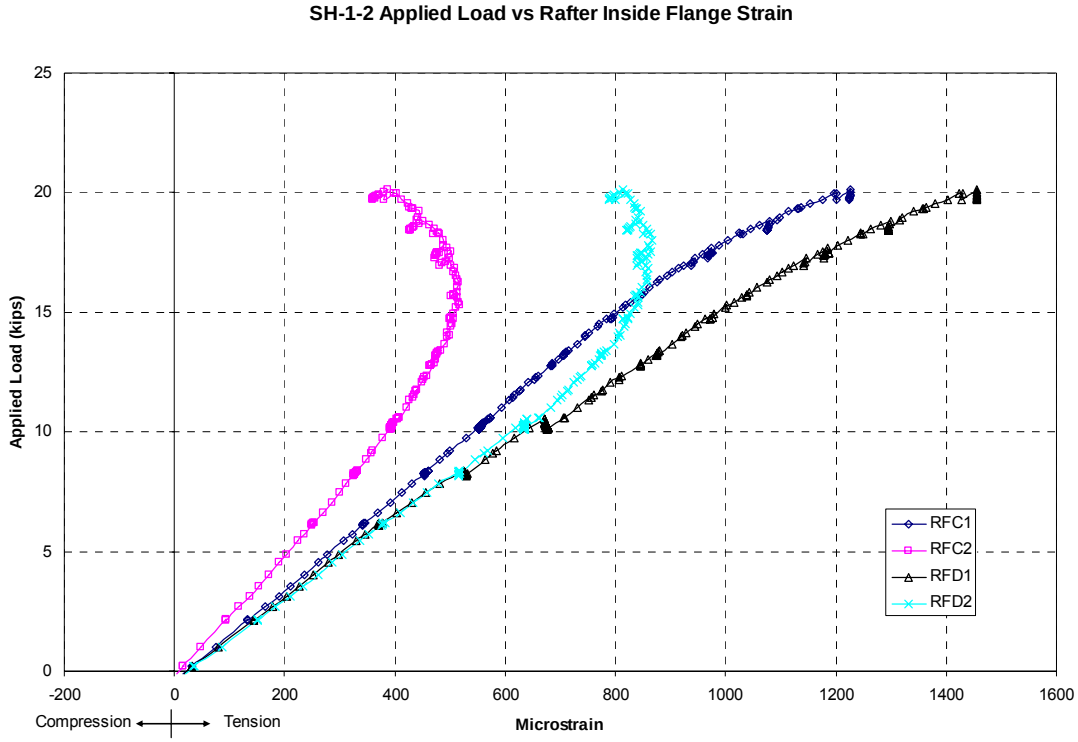

Figure B-6

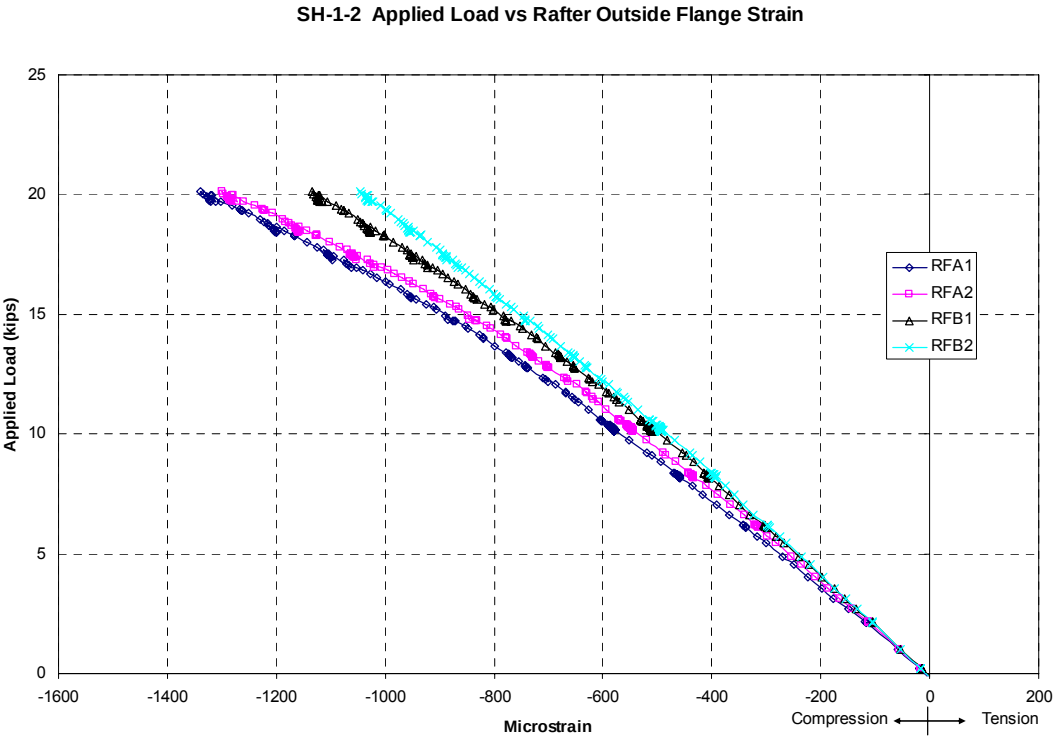

Figure B-7

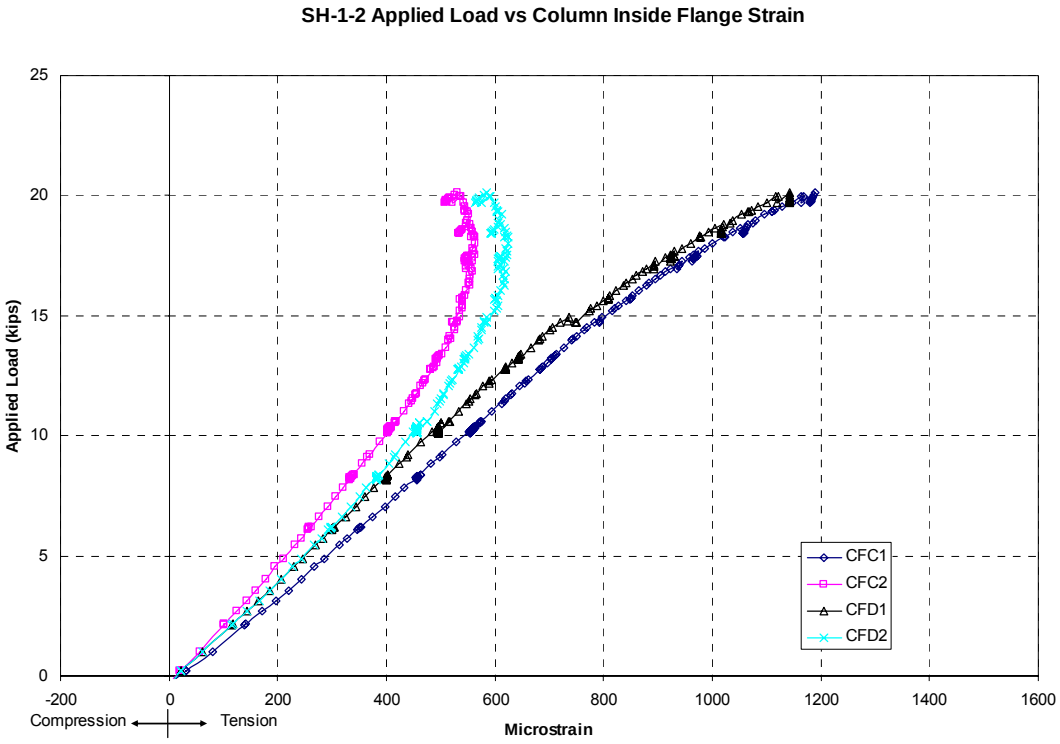

Figure B-8

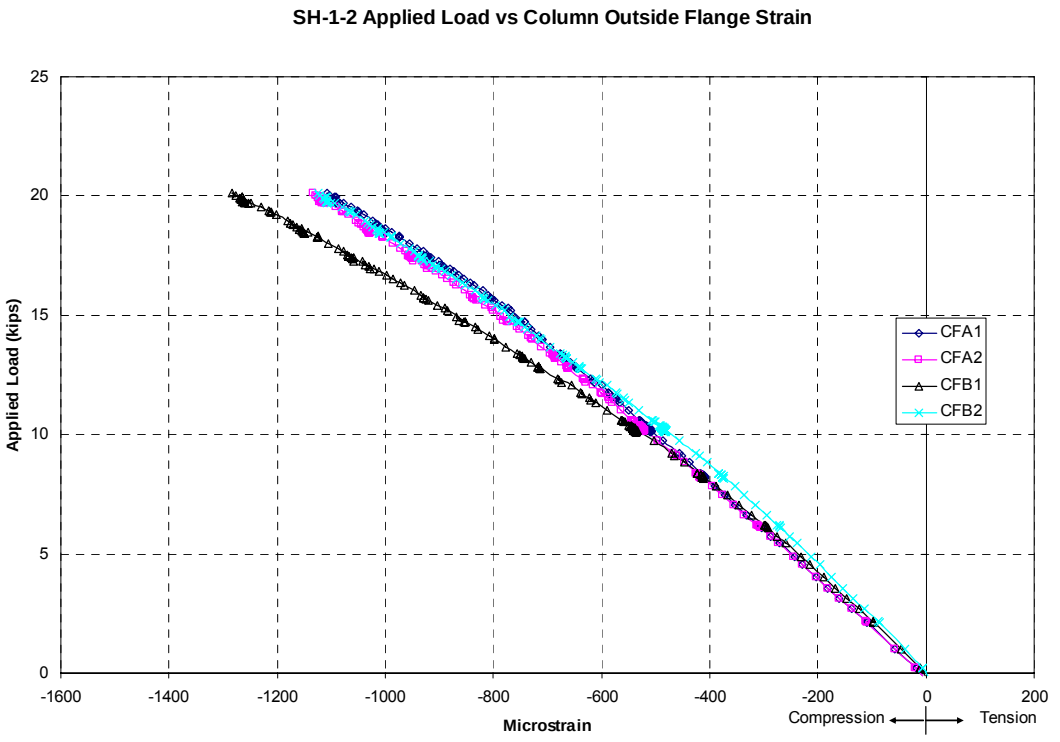

Figure B-9

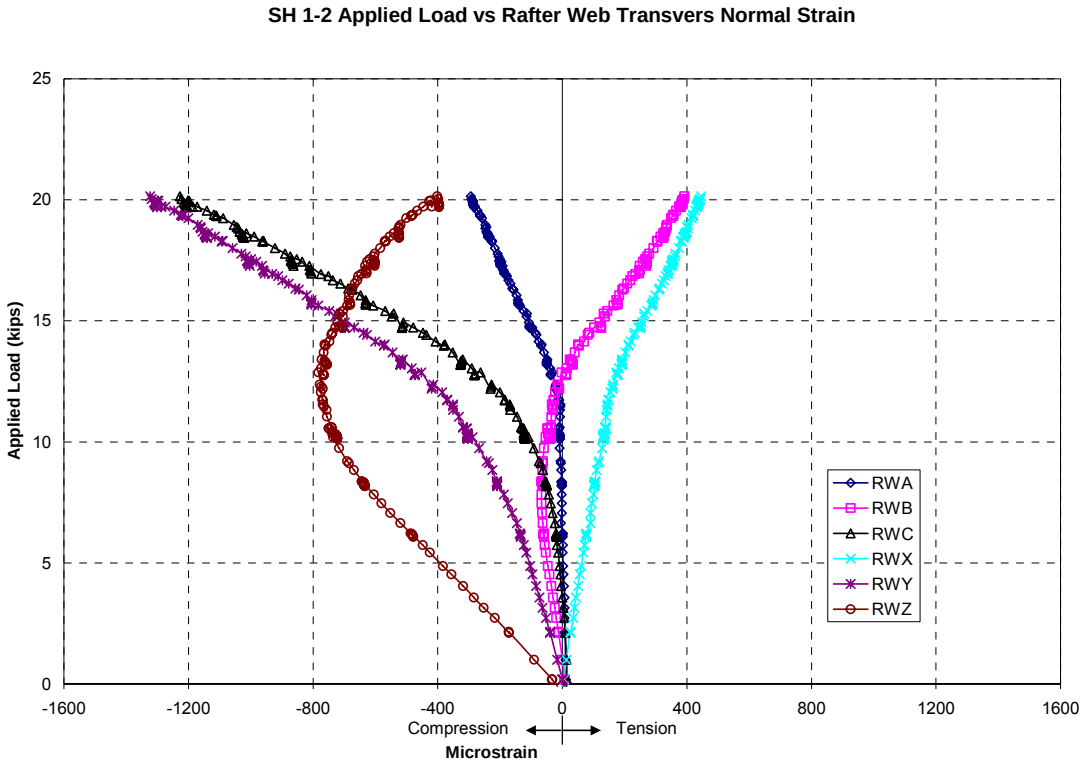

Figure B-10

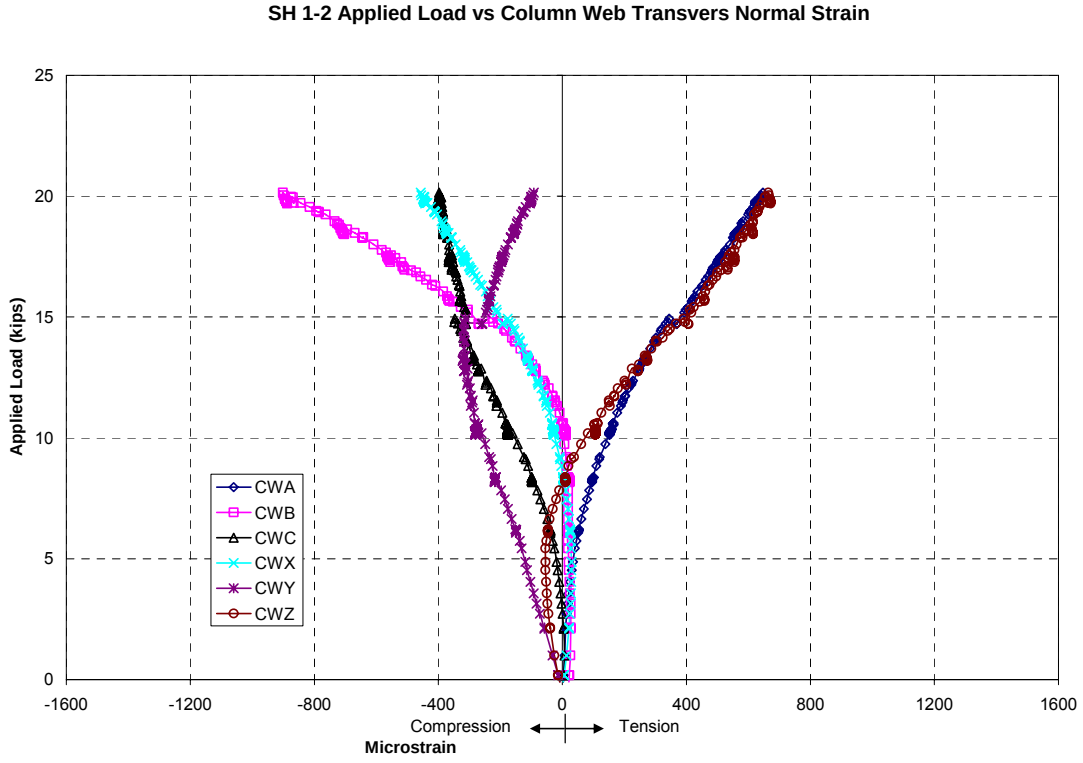

Figure B-11

APPENDIX C. TEST SH-1-3 RESULTS

PROJECT: American Buildings Company
TEST NAME: ABC-SH-1-3 (knee test 3)
TEST DATE: November 6, 2006
PURPOSE: Negative Bending Moment Test for Web Buckling w/o Stiffeners

CONNECTION DESCRIPTION:

NOMINAL YIELD STRESS: ……	55 ksi
GAGE: ……..	3 in
END PLATE WIDTH: …….	6 in
END PLATE THICKNESS: ……	1/2 in

BOLT DATA:

BOLT DIAMETER: ……	3/4 in
BOLT TYPE: ……...	A490
BOLT PRETENSION: ……	14 kips

COLUMN DATA: (MEASURED)

OUTSIDE FLANGE WIDTH: …….	6 in
OUTSIDE FLANGE THICKNESS: ……	0.375 in
INSIDE FLANGE WIDTH: ……...	6 in
INSIDE FLANGE THICKNESS: …….	0.377
WEB DEPTH AT BASE(PERP. TO OS FLANGE): ……..	14.81 in
WEB DEPTH AT REENTRANT CORNER(PERP. TO OS FLANGE): ……	22.0 in
WEB THICKNESS: …….	0.131 in

RAFTER DATA: (MEASURED)

OUTSIDE FLANGE WIDTH: …….	6 in
OUTSIDE FLANGE THICKNESS: …….	0.376 in
INSIDE FLANGE WIDTH: ……...	6 in
INSIDE FLANGE THICKNESS: …….	0.378 in
WEB DEPTH AT BASE(PERP. TO OS FLANGE): ……...	11.81 in
WEB DEPTH AT REENTRANT CORNER(PERP. TO OS FLANGE): ……	22.13 in
WEB THICKNESS: ……..	0.131 in

EXPERIMENTAL:

MAXIMUM LOAD: ……...	25.0 kips
FAILURE LOCATION:	Column Web at Reentrant Corner
FAILURE MODE:	Web Buckling

DISCUSSION

- The structure showed significantly less stiffness up to about 12 kips, which is attributed to the closing of the end plates after yielding induced from Knee Test 2.
- Once linear behavior consistent with the prediction curve was exhibited, the specimen was unloaded and the test resumed.

PROJECT: American Buildings Company
TEST NAME: ABC-SH-1-3 (knee test 3)
TEST DATE: November 6, 2006
PURPOSE: Negative Bending Moment Test for Web Buckling w/o Stiffeners

DISCUSSION (CONTINUED)

- At 23.76 kips column and rafter web buckling or crippling became evident at the intersection of the compression flanges and end plates.
- The load was removed so that short stiffener plates could be installed at these locations, to validate web buckling.
- A positive moment load of approximately 8.25 kips was imposed in an attempt to reverse the web crippling and allow for easier stiffener plate installation.

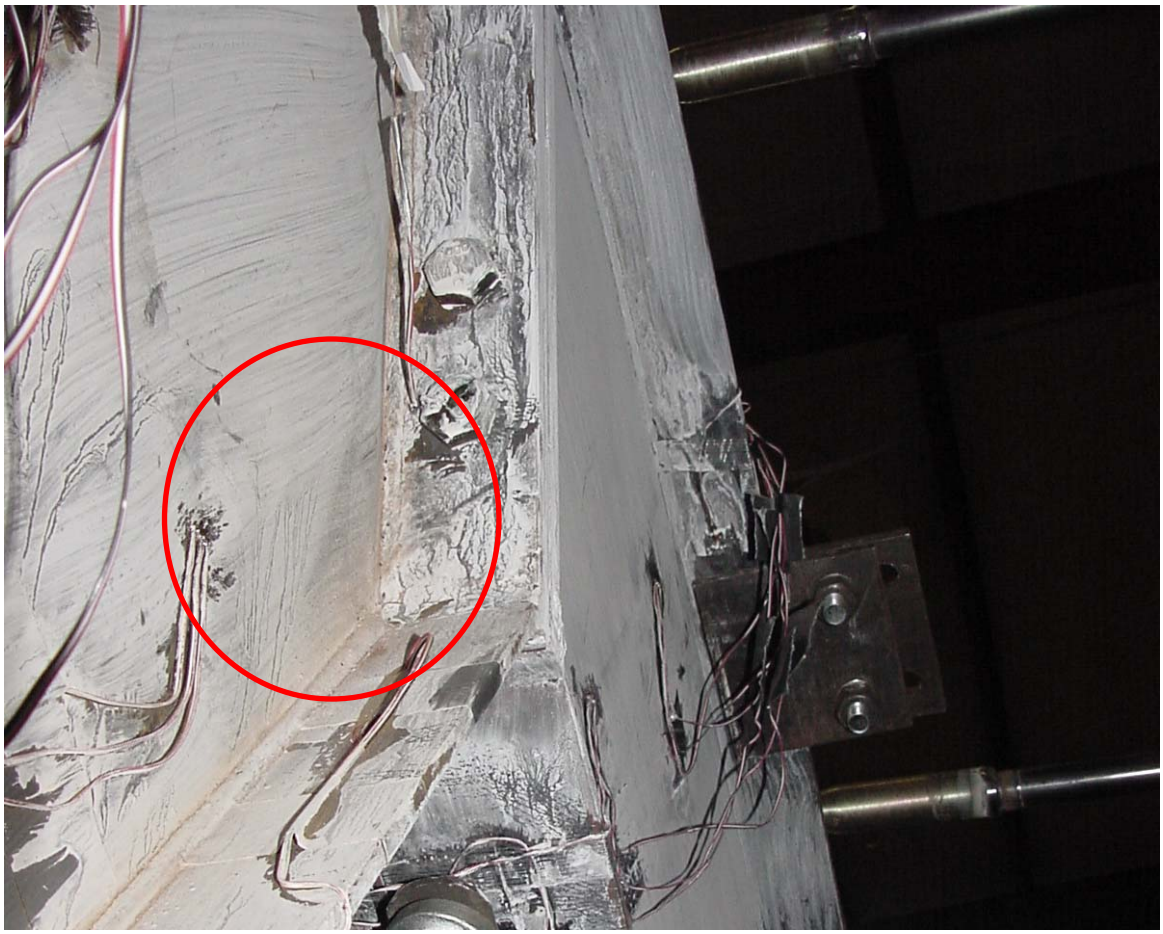

Figure C-1 SH-1-3 Possible Web Crippling At Reentrant Corner

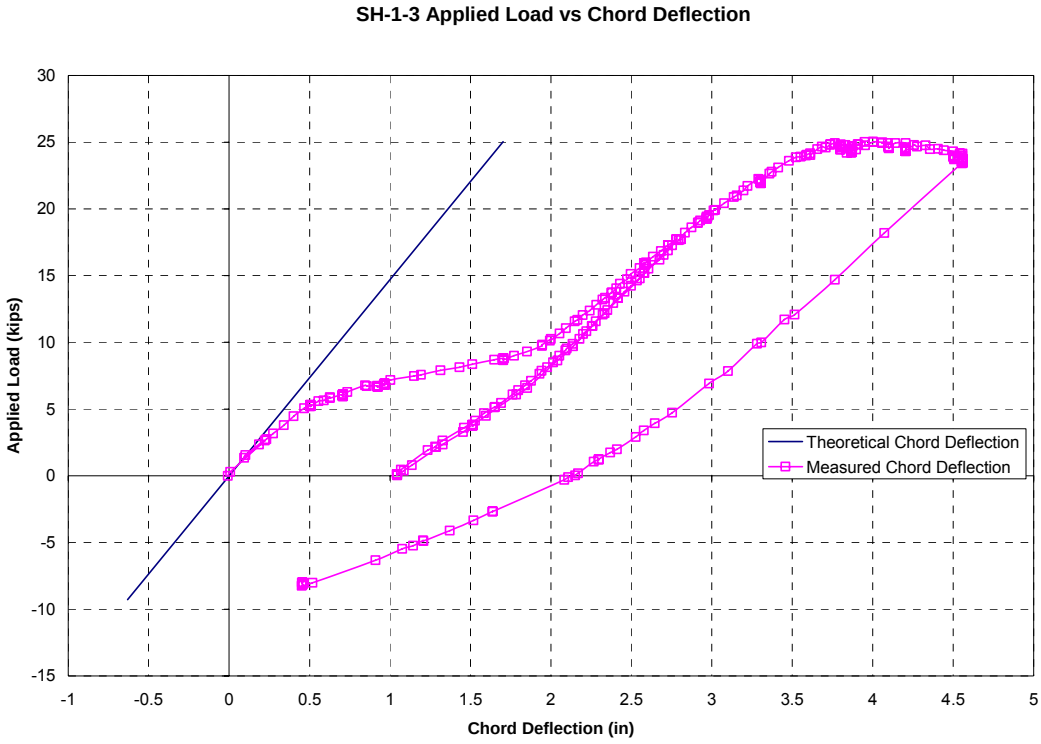

Figure C-2

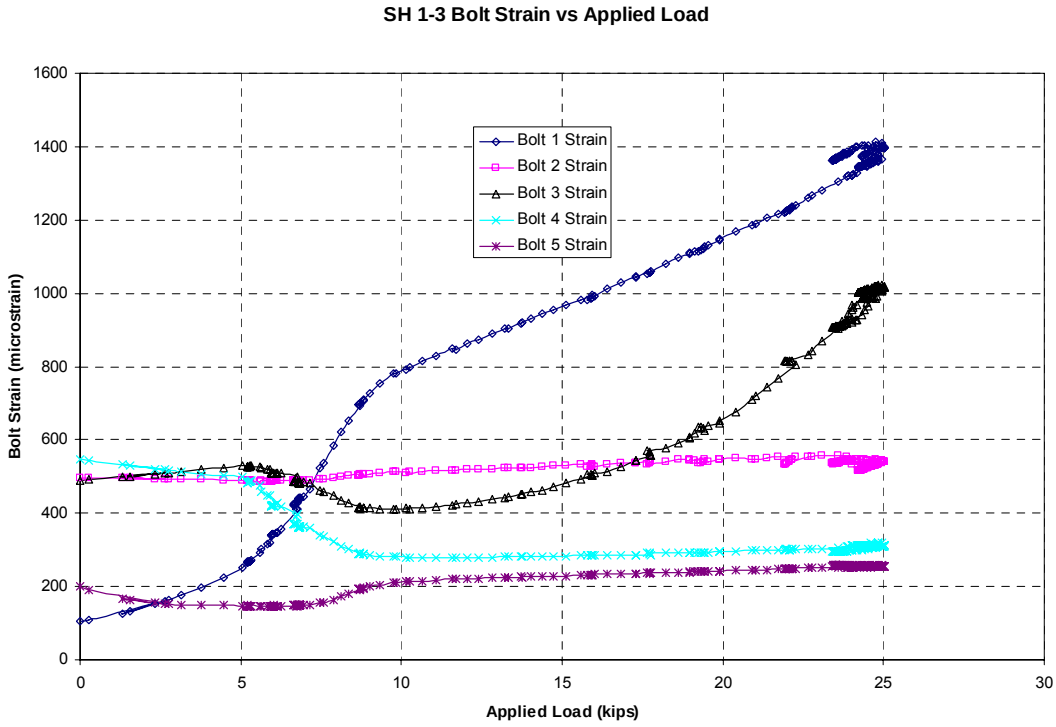

Figure C-3

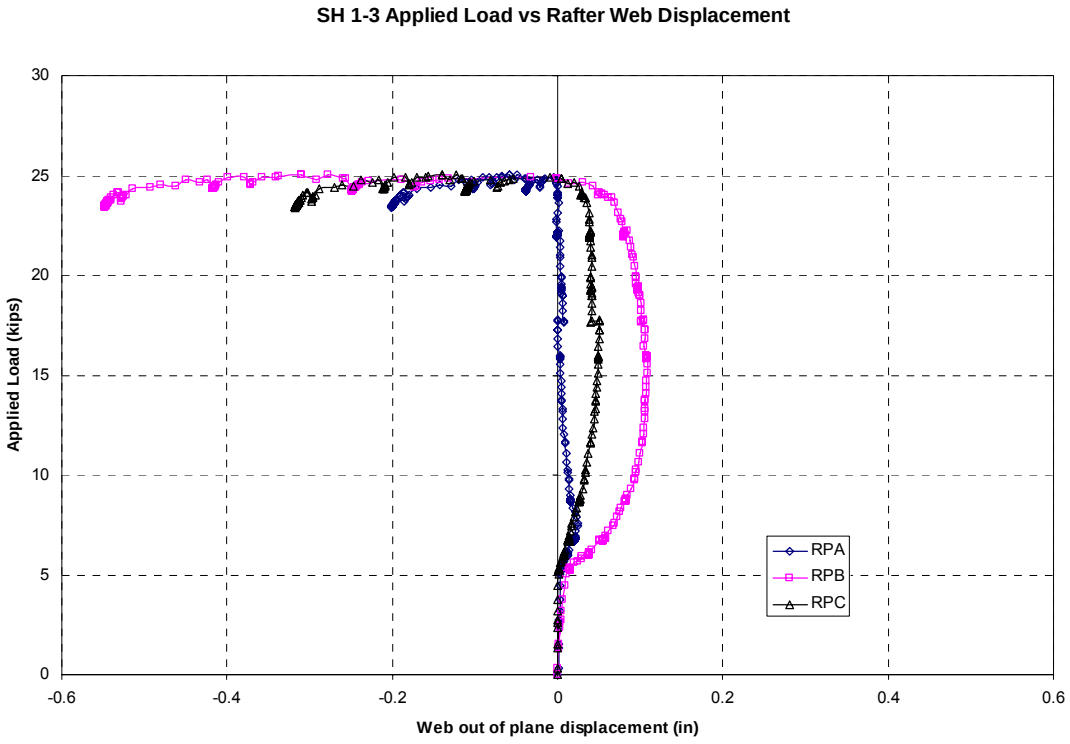

Figure C-4

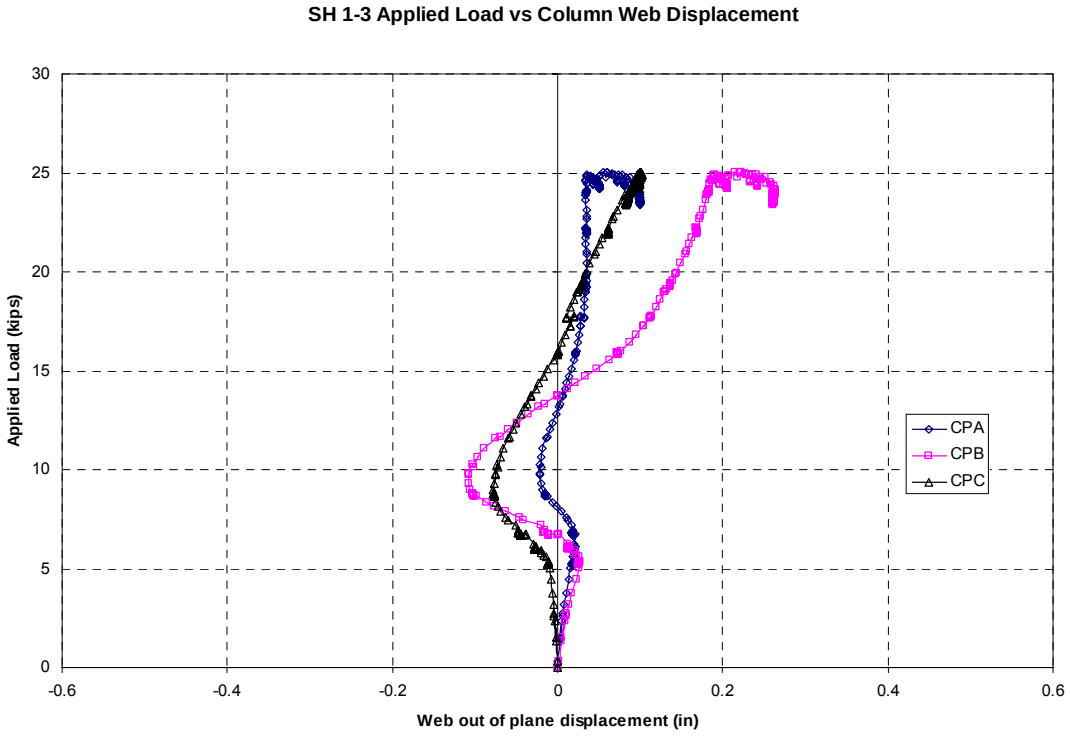

Figure C-5

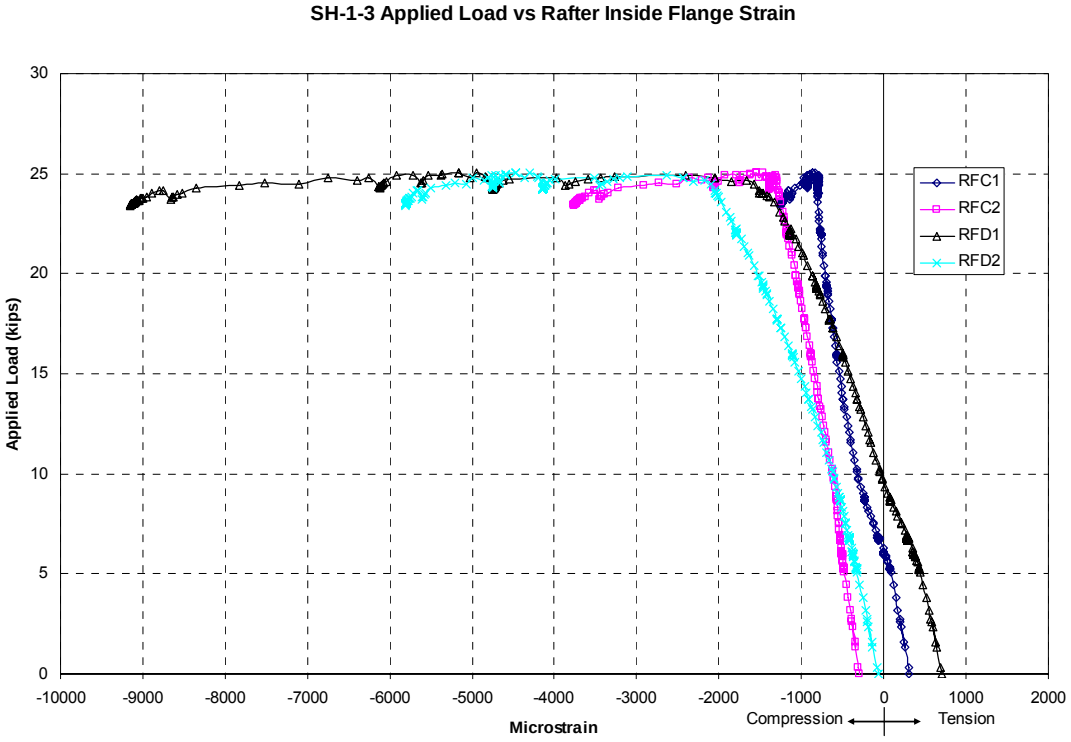

Figure C-6

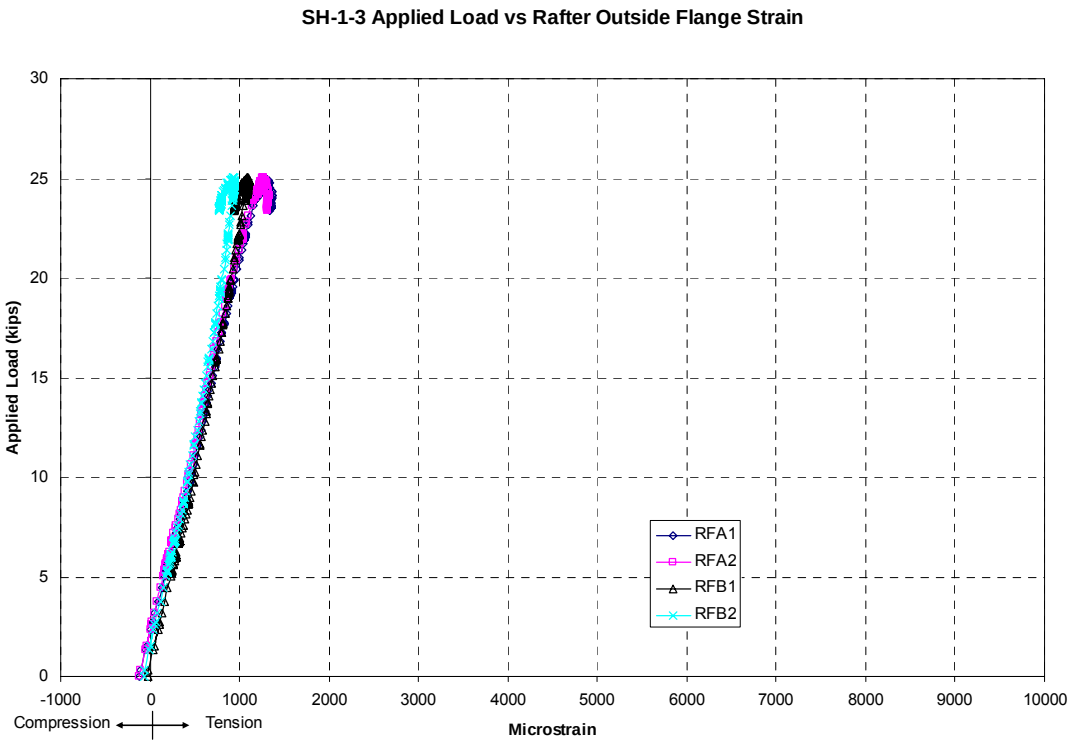

Figure C-7

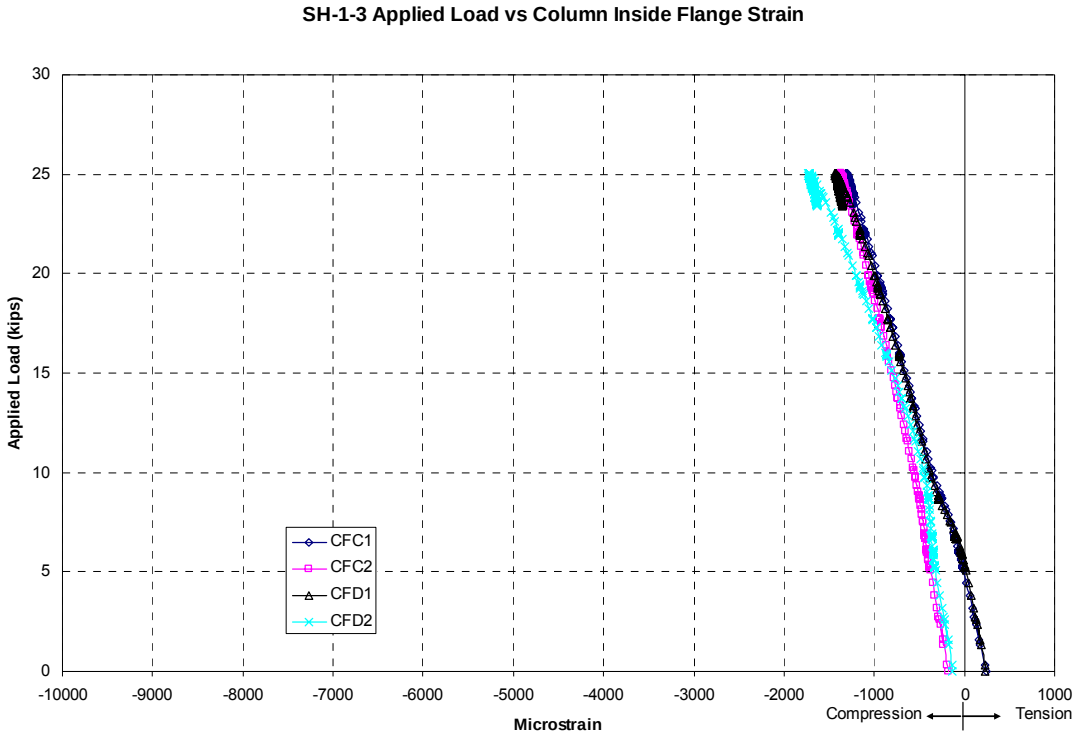

Figure C-8

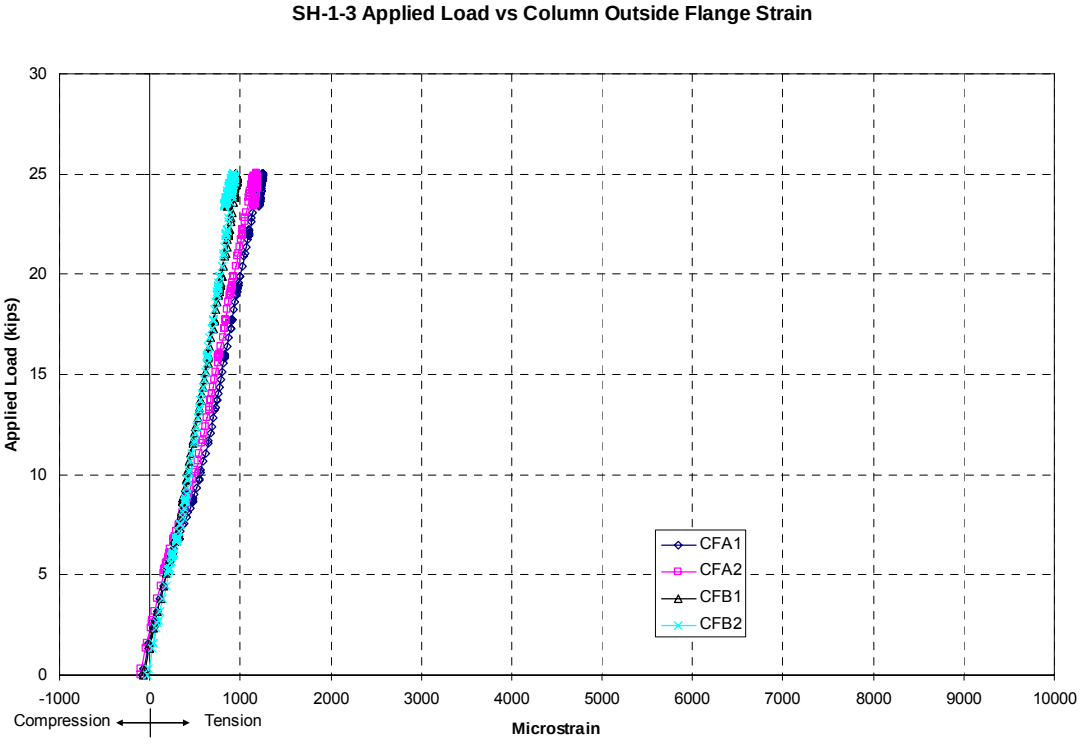

Figure C-9

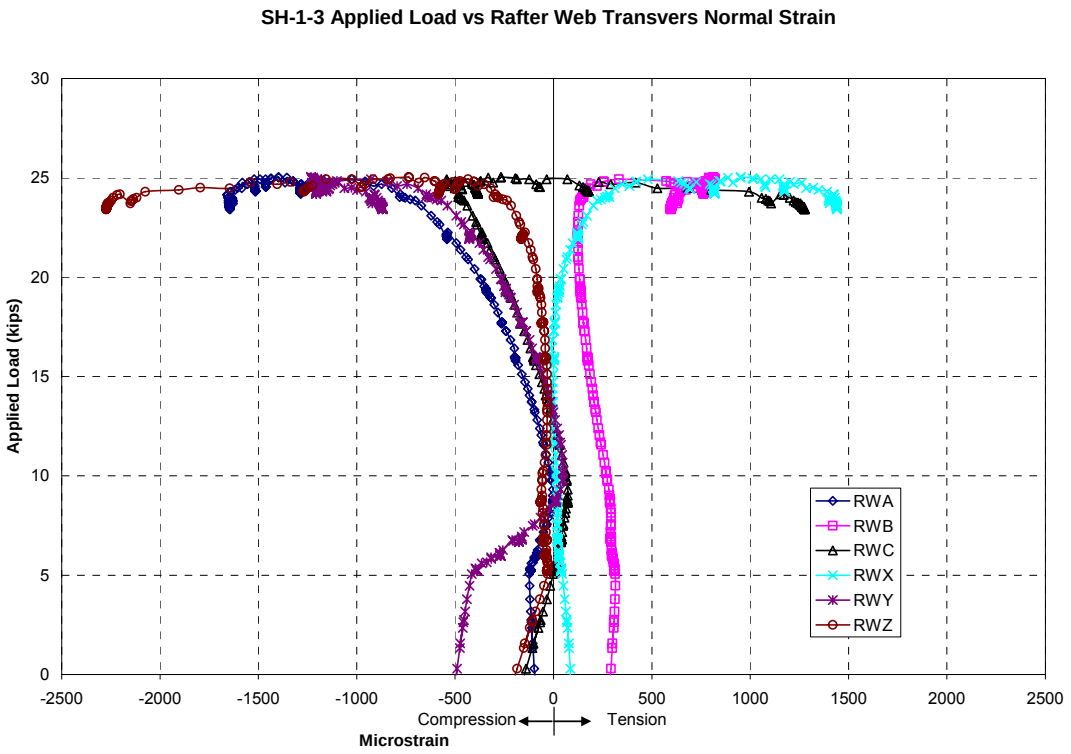

Figure C-10

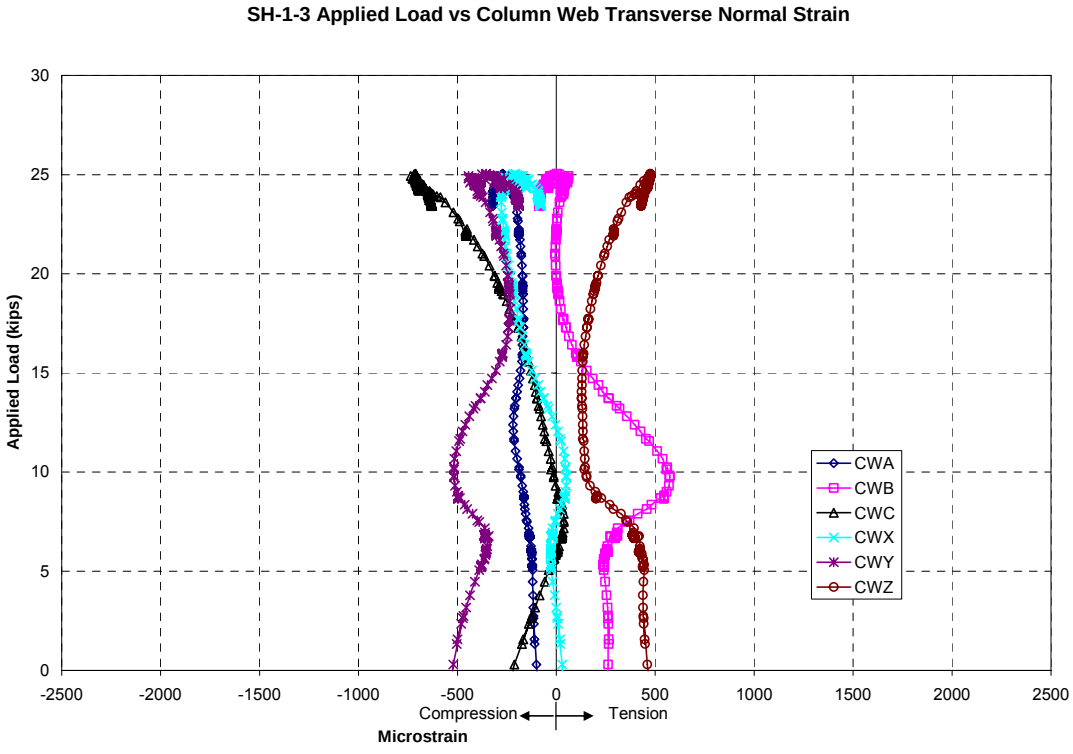

Figure C-11

APPENDIX D. TEST SH-1-4 RESULTS

PROJECT: American Buildings Company
TEST NAME: ABC-SH-1-4 (knee test 4)
TEST DATE: November 10, 2006
PURPOSE: Negative Bending Moment Test for Web Buckling w/o Stiffeners

CONNECTION DESCRIPTION:

NOMINAL YIELD STRESS: ……	55 ksi
GAGE: ……..	3 in
END PLATE WIDTH: …….	6 in
END PLATE THICKNESS: ……	1/2 in

BOLT DATA:

BOLT DIAMETER: ……	3/4 in
BOLT TYPE: ……...	A490
BOLT PRETENSION: ……	14 kips

COLUMN DATA: (MEASURED)

OUTSIDE FLANGE WIDTH: …….	6 in
OUTSIDE FLANGE THICKNESS: ……	0.375 in
INSIDE FLANGE WIDTH: ……...	6 in
INSIDE FLANGE THICKNESS: …….	0.377
WEB DEPTH AT BASE(PERP. TO OS FLANGE): ……..	14.81 in
WEB DEPTH AT REENTRANT CORNER(PERP. TO OS FLANGE): ……	22.0 in
WEB THICKNESS: …….	0.131 in

RAFTER DATA: (MEASURED)

OUTSIDE FLANGE WIDTH: …….	6 in
OUTSIDE FLANGE THICKNESS: …….	0.376 in
INSIDE FLANGE WIDTH: ……...	6 in
INSIDE FLANGE THICKNESS: …….	0.378 in
WEB DEPTH AT BASE(PERP. TO OS FLANGE): ……...	11.81 in
WEB DEPTH AT REENTRANT CORNER(PERP. TO OS FLANGE): ……	22.13 in
WEB THICKNESS: ……..	0.131 in

EXPERIMENTAL:

MAXIMUM LOAD: ……...	22.96 kips
FAILURE LOCATION:	Column Web at Reentrant Corner
FAILURE MODE:	Web Buckling

DISCUSSION

- Short stiffener plates were welded to the web at the end plate and compression flange intersection, to control web crippling.
- At approximately 22.88 kips a loud noise and load loss occurred. Some slipping of lateral brace supports was apparent at top of rafter outside flange.

PROJECT: American Buildings Company
TEST NAME: ABC-SH-1-4 (knee test 4)
TEST DATE: November 10, 2006
PURPOSE: Negative Bending Moment Test for Web Buckling w/o Stiffeners

DISCUSSION (CONTINUED)

- At 21.12 kips, lateral torsional buckling occurred in the bottom flange of the rafter between brace points.

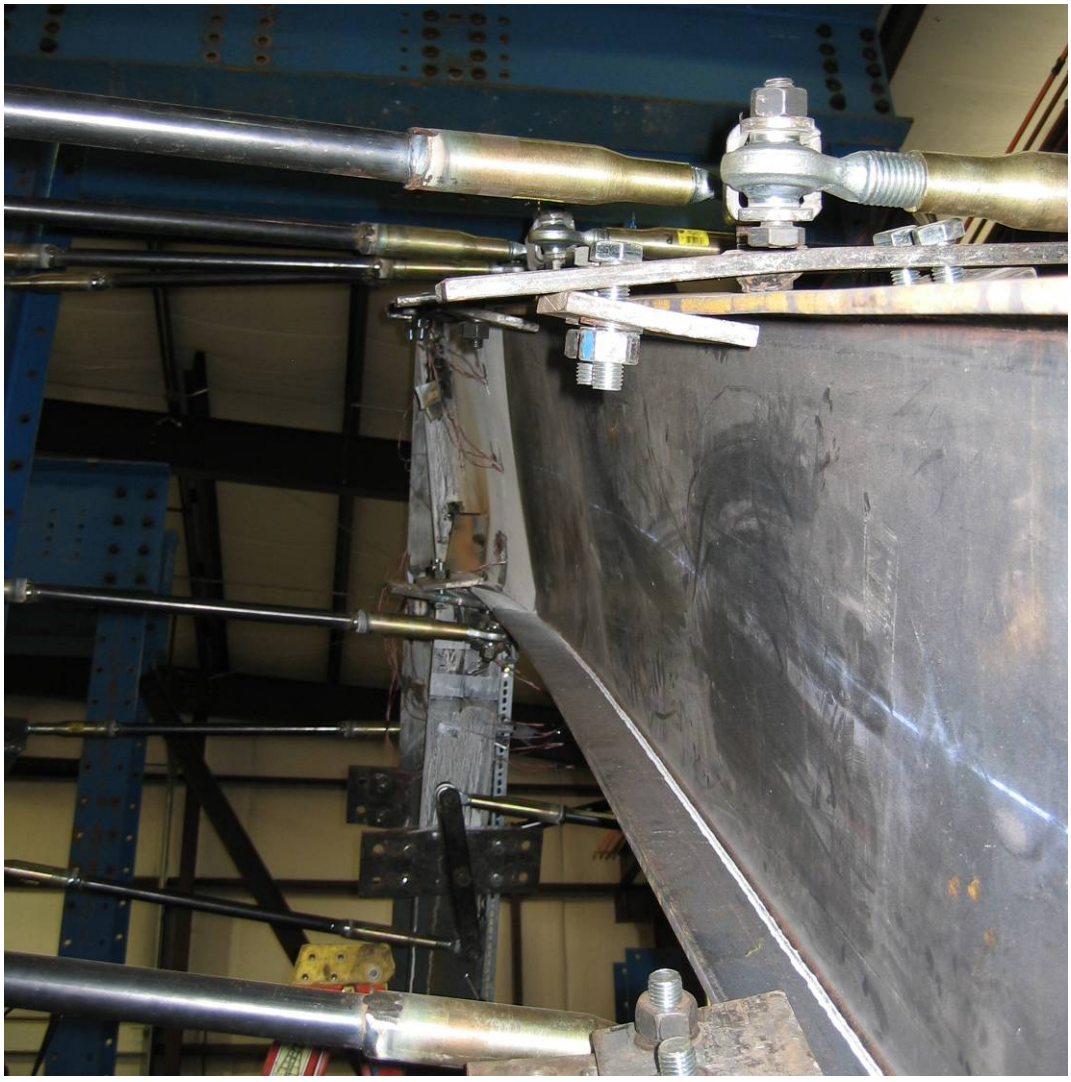

Figure D-1 SH-1-4 Lateral Torsional Buckling

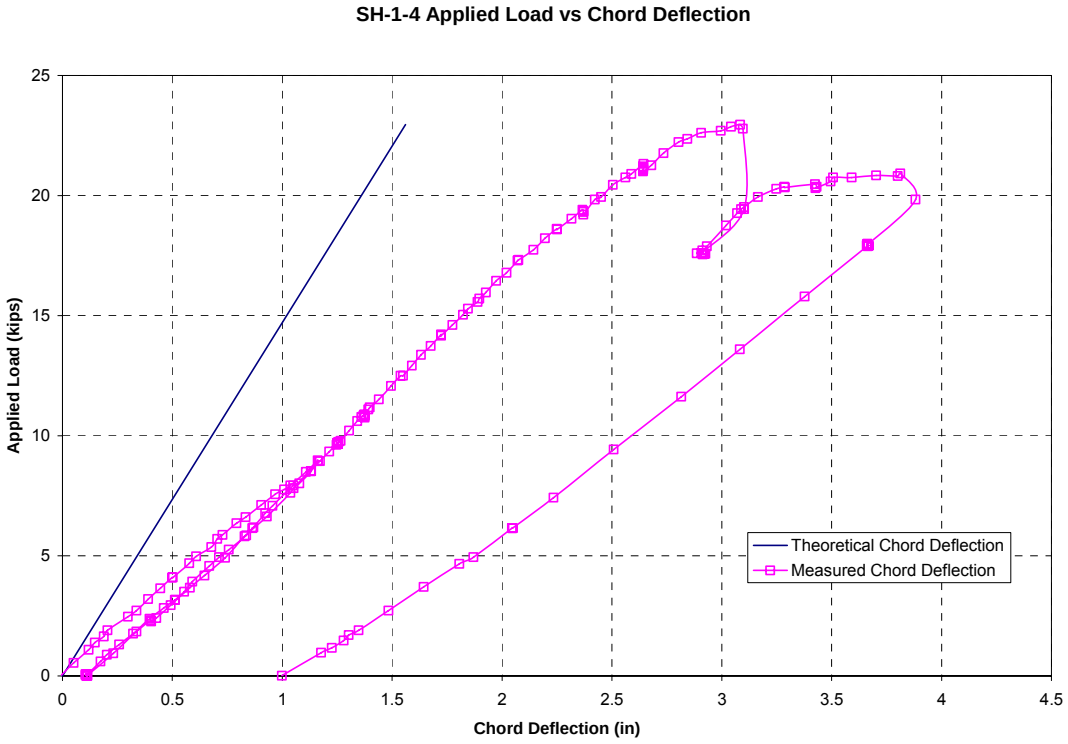

Figure D-2

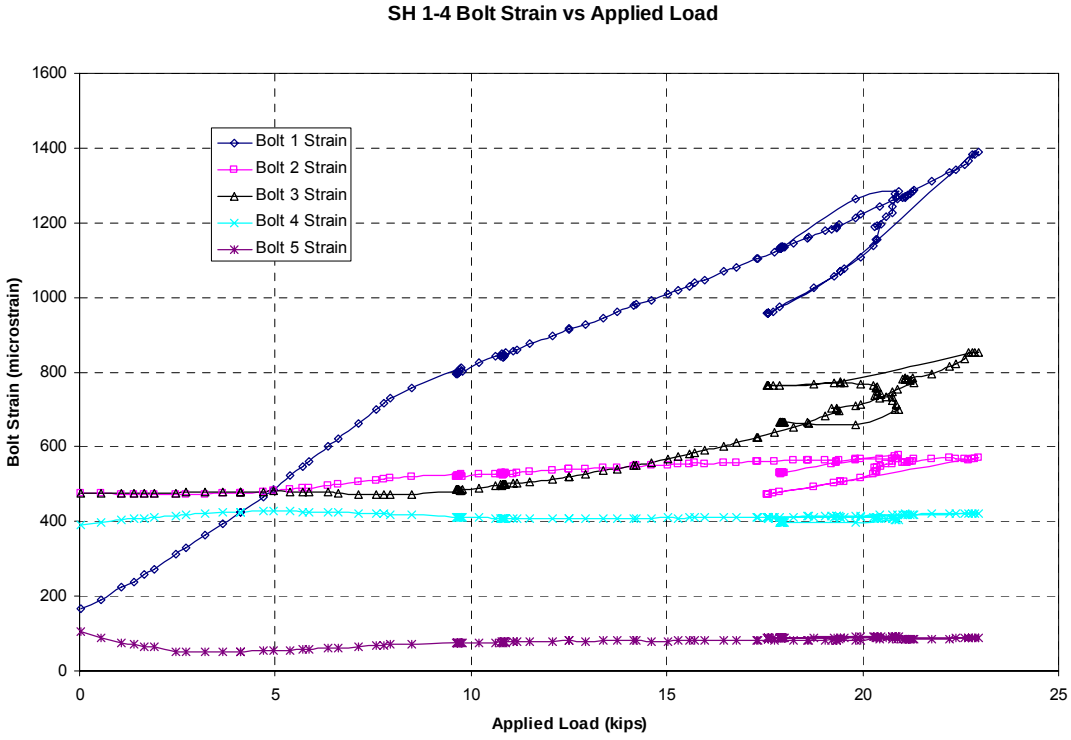

Figure D-3

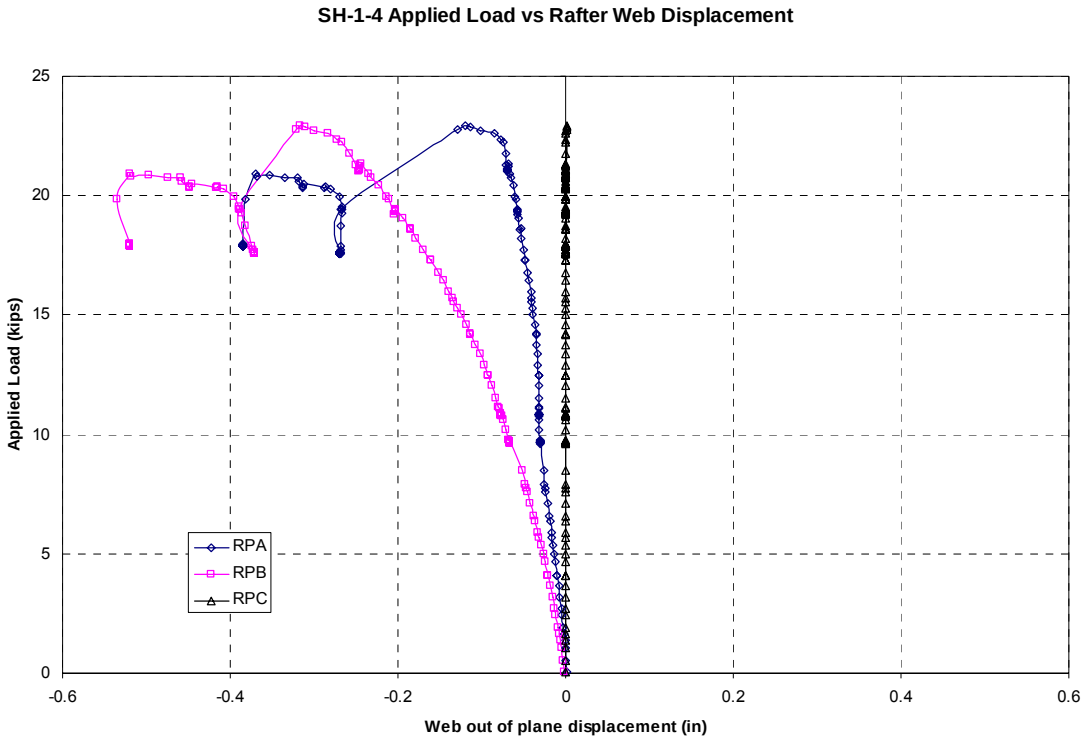

Figure D-4

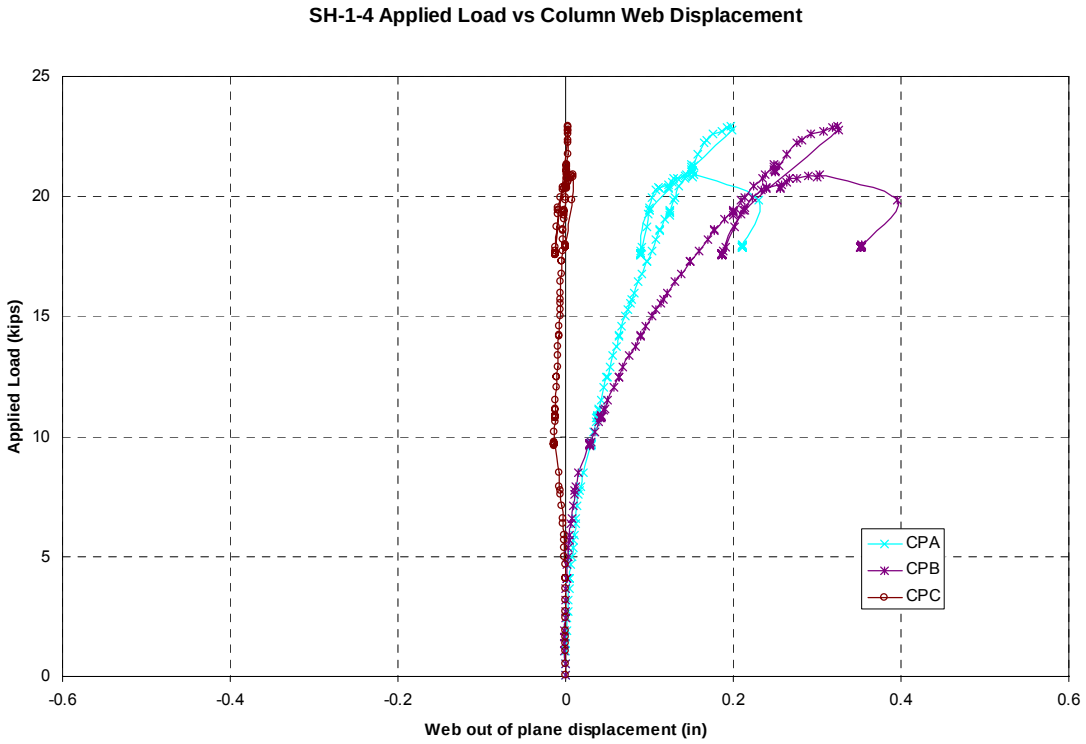

Figure D-5

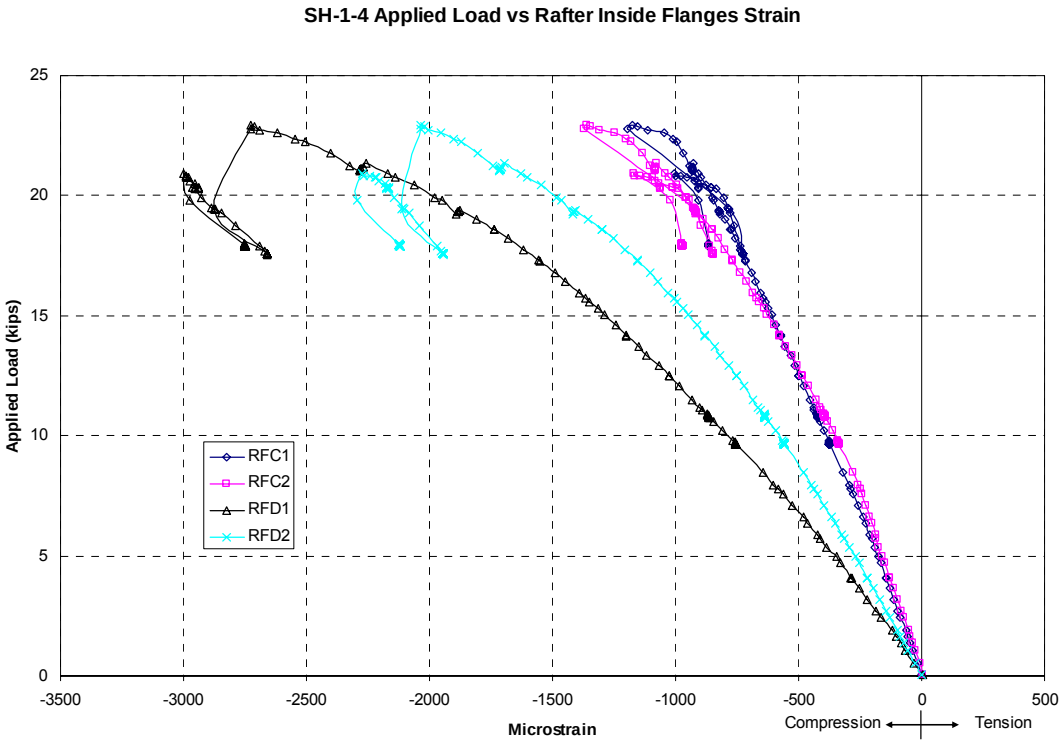

Figure D-6

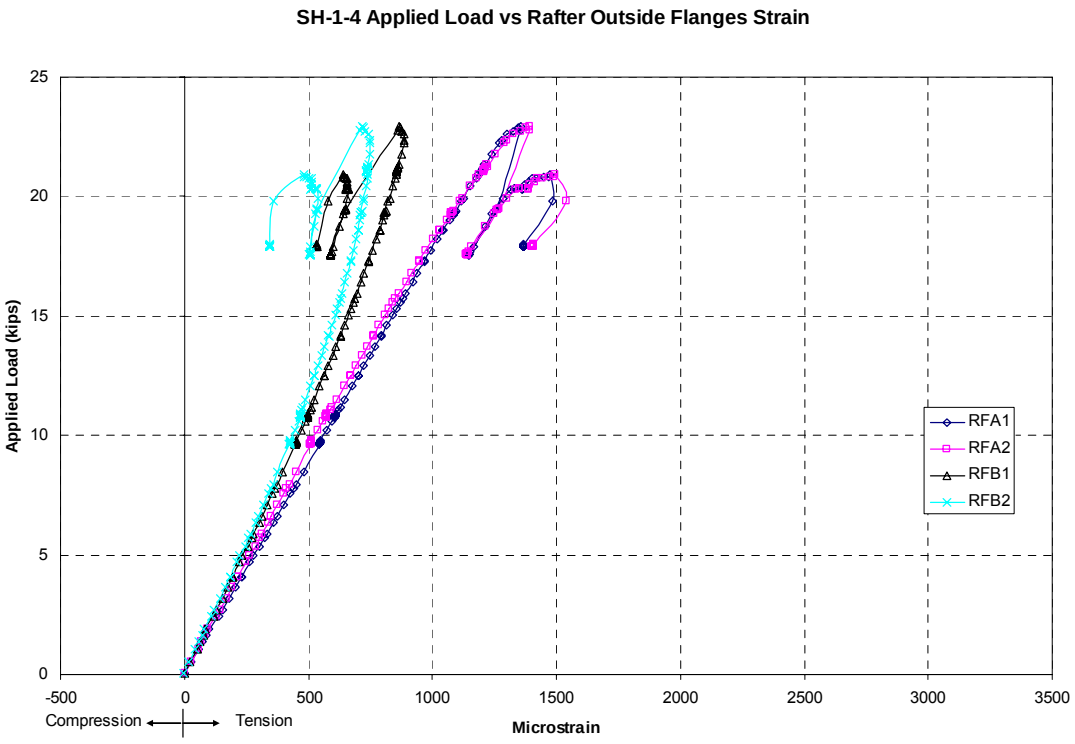

Figure D-7

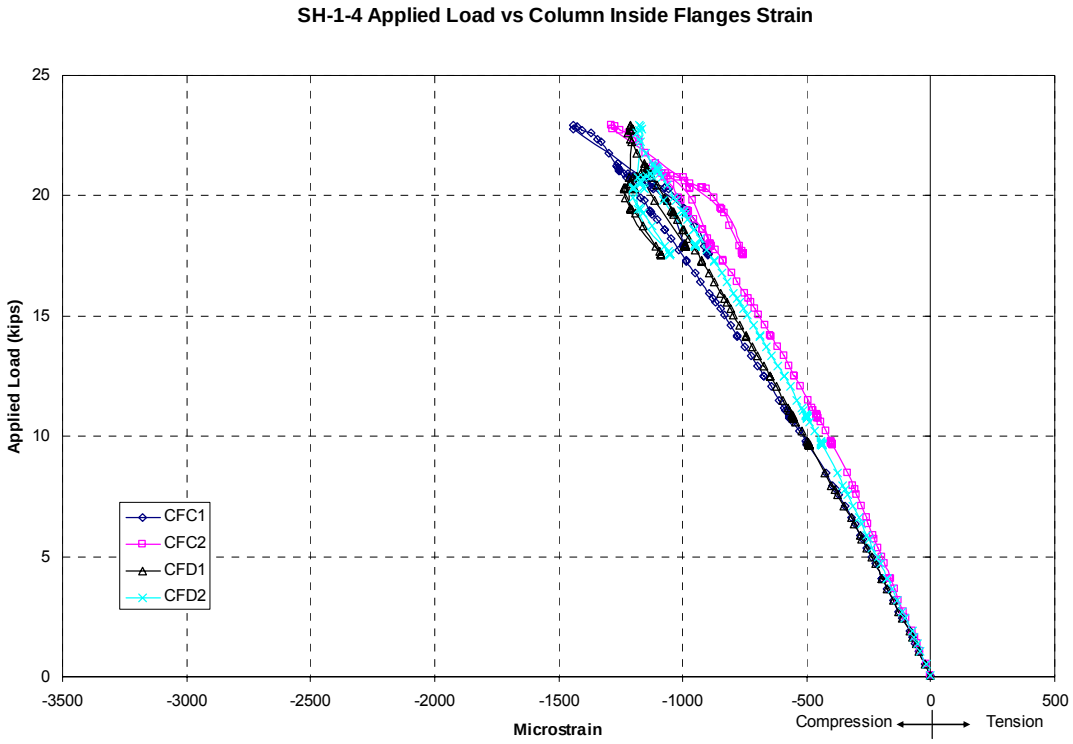

Figure D-8

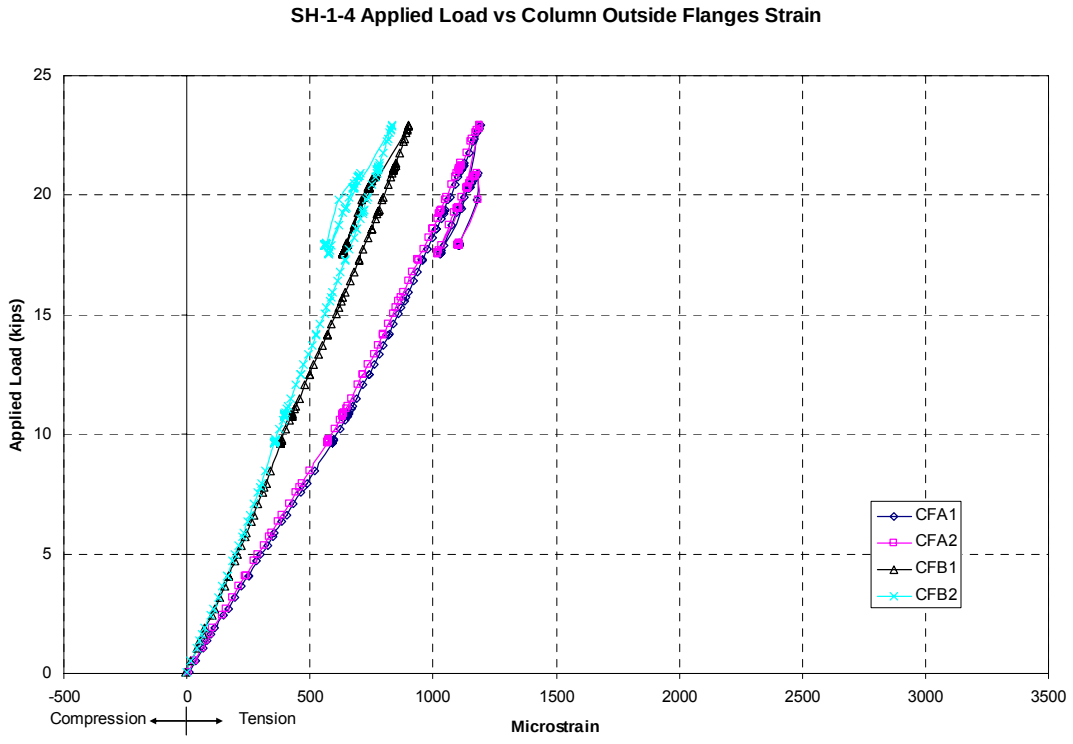

Figure D-9

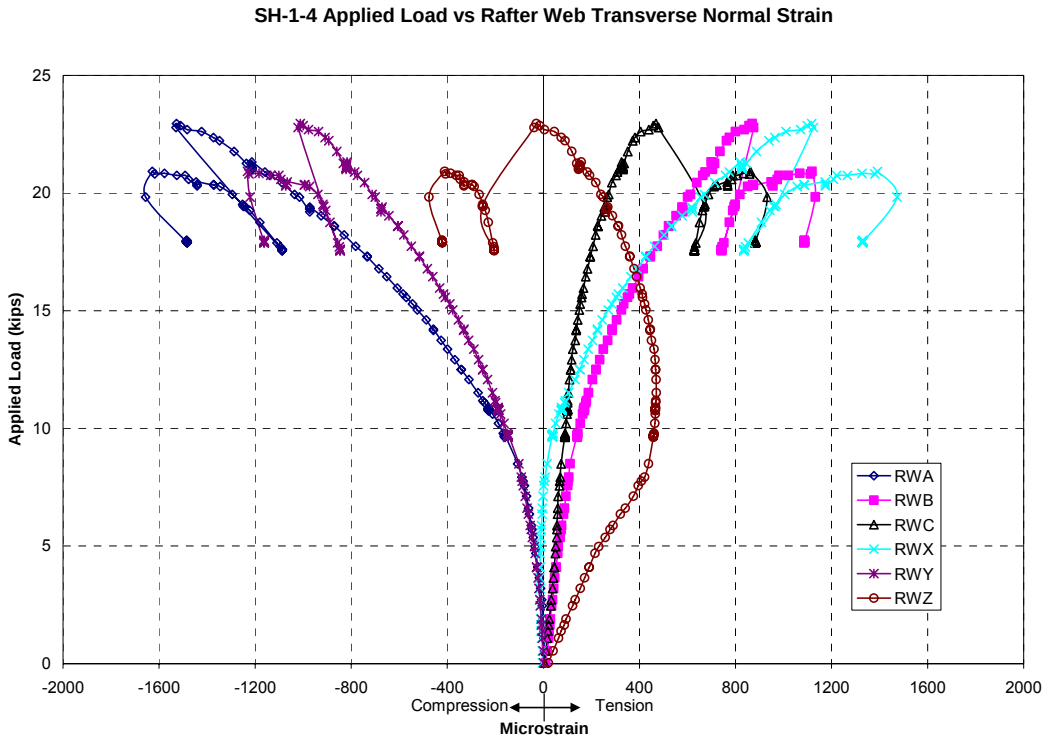

Figure D-10

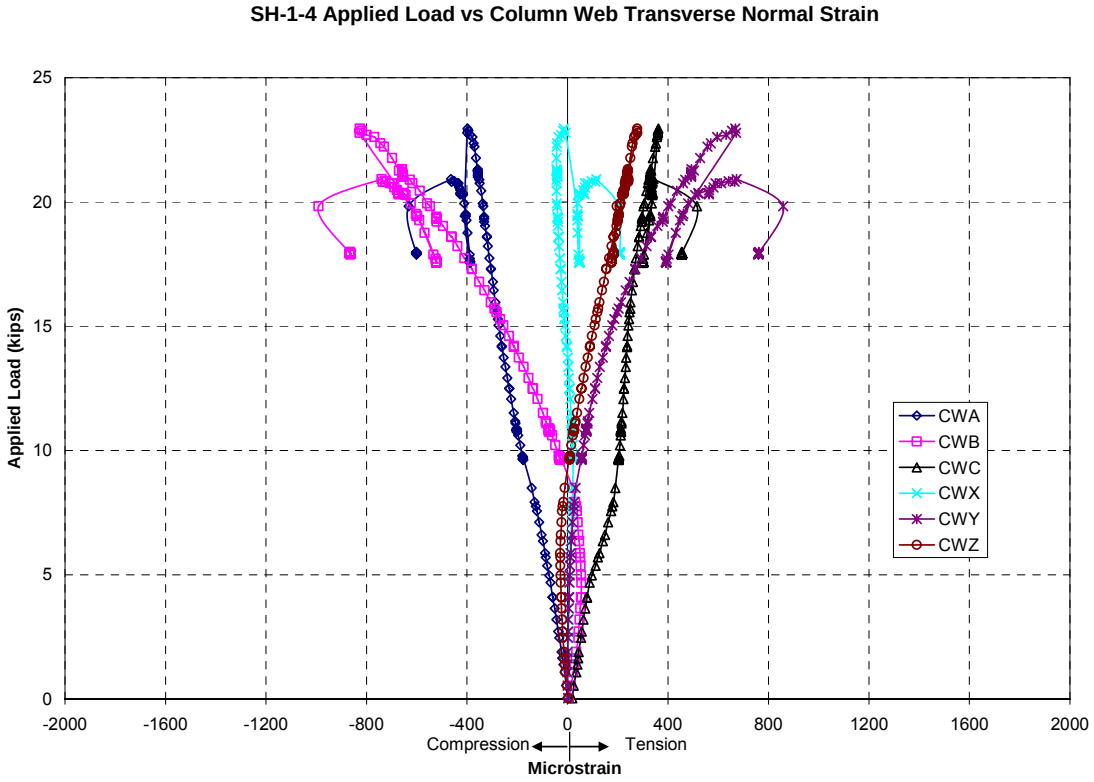

Figure D-11

APPENDIX E. TEST SH-2-1 RESULTS

PROJECT: American Buildings Company
TEST NAME: ABC-SH-2-1 (knee test 5)
TEST DATE: November 27, 2006
PURPOSE: Negative Bending Moment Test for Web Buckling w/o Stiffeners

CONNECTION DESCRIPTION:

NOMINAL YIELD STRESS: ……	55 ksi
GAGE: ……..	3 in
END PLATE WIDTH: ……	6 in
END PLATE THICKNESS: ……	1/2 in

BOLT DATA:

BOLT DIAMETER: ……	3/4 in
BOLT TYPE: ……...	A490
BOLT PRETENSION: ……	14 kips

COLUMN DATA: (MEASURED)

OUTSIDE FLANGE WIDTH: ……	6 in
OUTSIDE FLANGE THICKNESS: ……	0.375 in
INSIDE FLANGE WIDTH: ……..	6 in
INSIDE FLANGE THICKNESS: …….	0.377
WEB DEPTH AT BASE(PERP. TO OS FLANGE): ……..	14.81 in
WEB DEPTH AT REENTRANT CORNER(PERP. TO OS FLANGE): ……	22.0 in
WEB THICKNESS: …….	0.131 in

RAFTER DATA: (MEASURED)

OUTSIDE FLANGE WIDTH: ……	6 in
OUTSIDE FLANGE THICKNESS: …….	0.376 in
INSIDE FLANGE WIDTH: ……..	6 in
INSIDE FLANGE THICKNESS: …….	0.378 in
WEB DEPTH AT BASE(PERP. TO OS FLANGE): ……...	11.81 in
WEB DEPTH AT REENTRANT CORNER(PERP. TO OS FLANGE): ……	22.13 in
WEB THICKNESS: ……..	0.131 in

EXPERIMENTAL:

MAXIMUM LOAD: ……...	26.08 kips
FAILURE LOCATION:	Column Web at Reentrant Corner
FAILURE MODE:	Web Buckling

DISCUSSION:

- At approximately 7 kips large web deflections were observed in the plunger readings, and a loud popping sound was heard. The specimen was unloaded and web displacement transducers were realigned.
- Loading resumed to 8.8 kips and unloaded.

PROJECT: American Buildings Company
TEST NAME: ABC-SH-2-1 (knee test 5)
TEST DATE: November 27, 2006
PURPOSE: Negative Bending Moment Test for Web Buckling w/o Stiffeners

DISCUSSION (CONTINUED)

- After resuming loading, at approximately 18.5 kips, the column web transducers indicate a reversal in direction.
- Specimen unloaded again at 22.2 kips, and reloaded.
- At 23.8 kips yield lines were observed in the web at reentrant corner.
- At 24.6 kips and 2.55 inches chord deflection, yield lines were apparent in the webs at the intersection of tension flanges and end plates. Crippling in the web at the reentrant corner was also visible, as was yielding in the compression flanges.
- At 25 kips and 3.1 inches chord deflection, lateral torsional buckling occurred between braced points on the rafter inside flange.

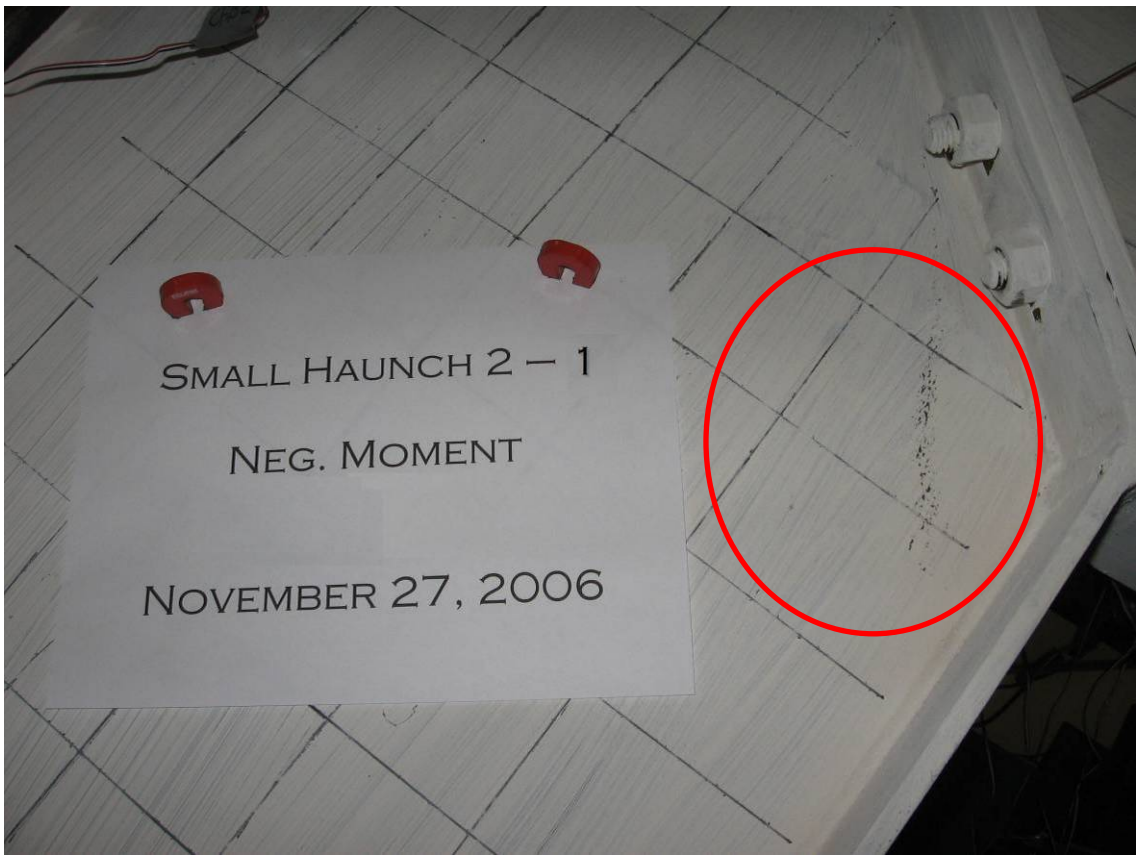

Figure E-1 SH-2-1 Possible Web Crippling at Reentrant Corner

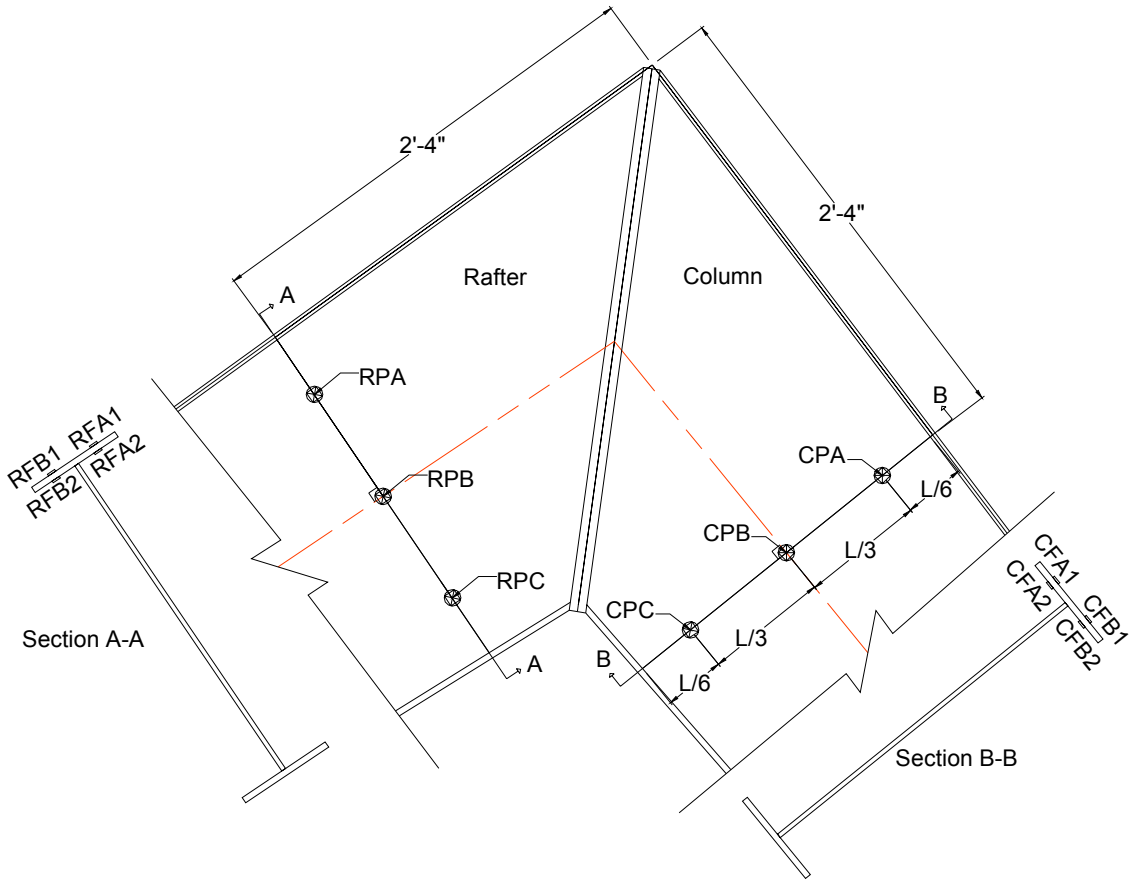

Figure E-2 SH-2 Flange Gages and Web LVDT's As Viewed from the North.

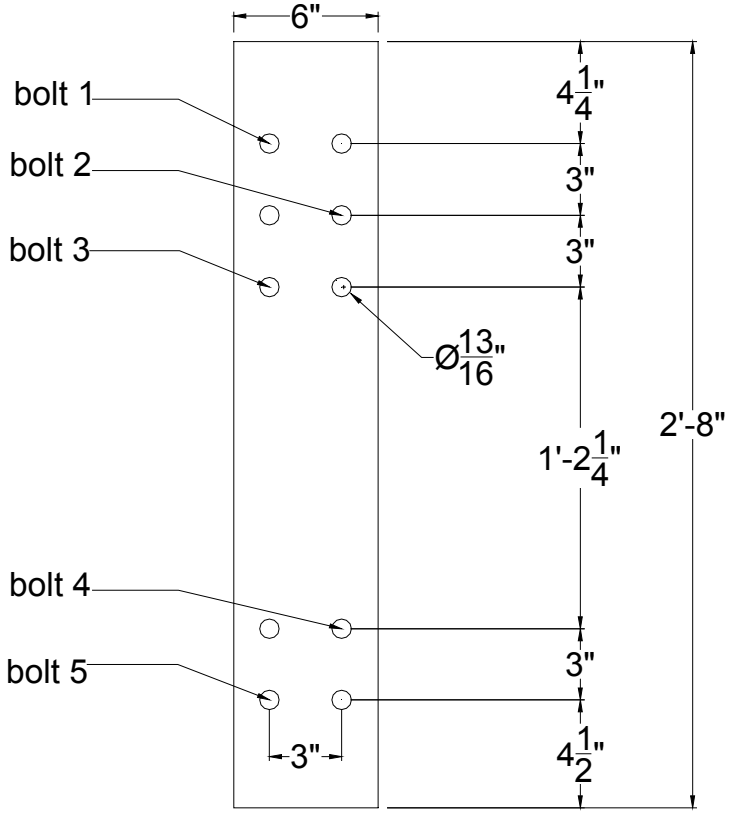

Figure E-3 SH-2 Bolt Gages as Viewed from the West.

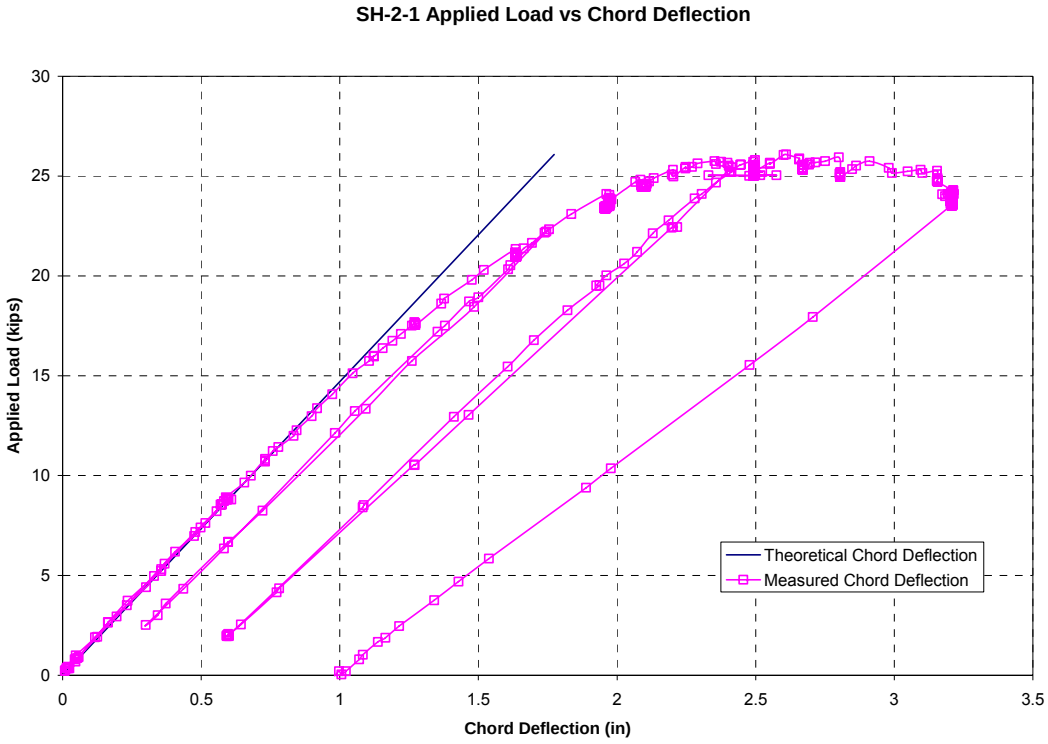

Figure E-4

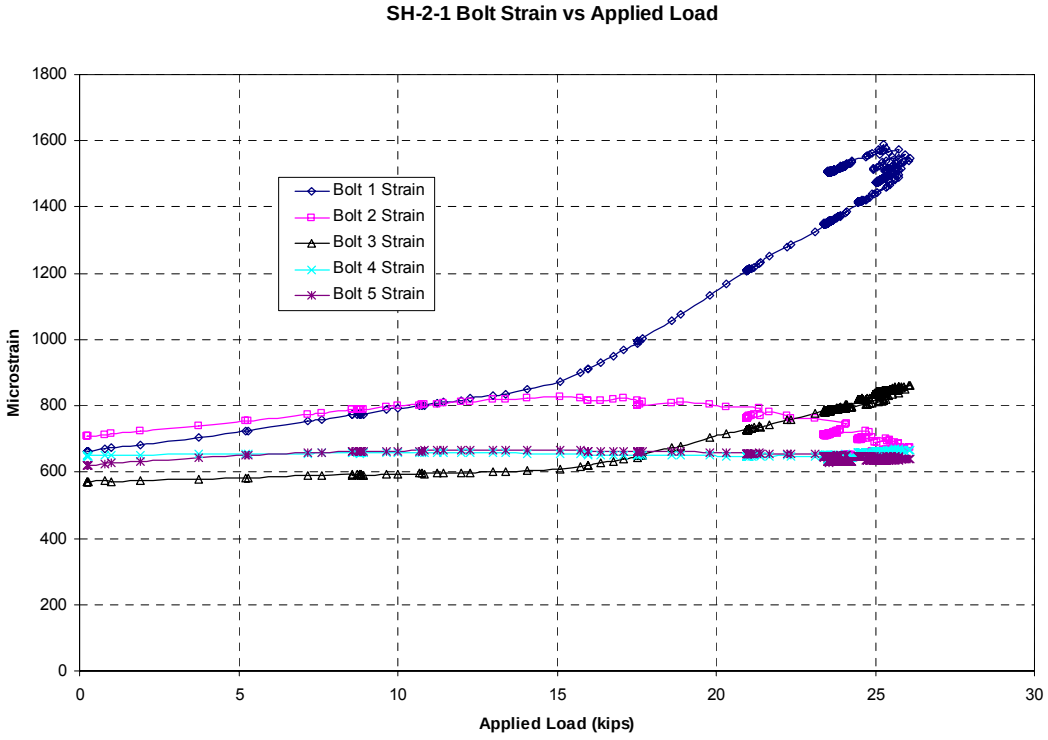

Figure E-5

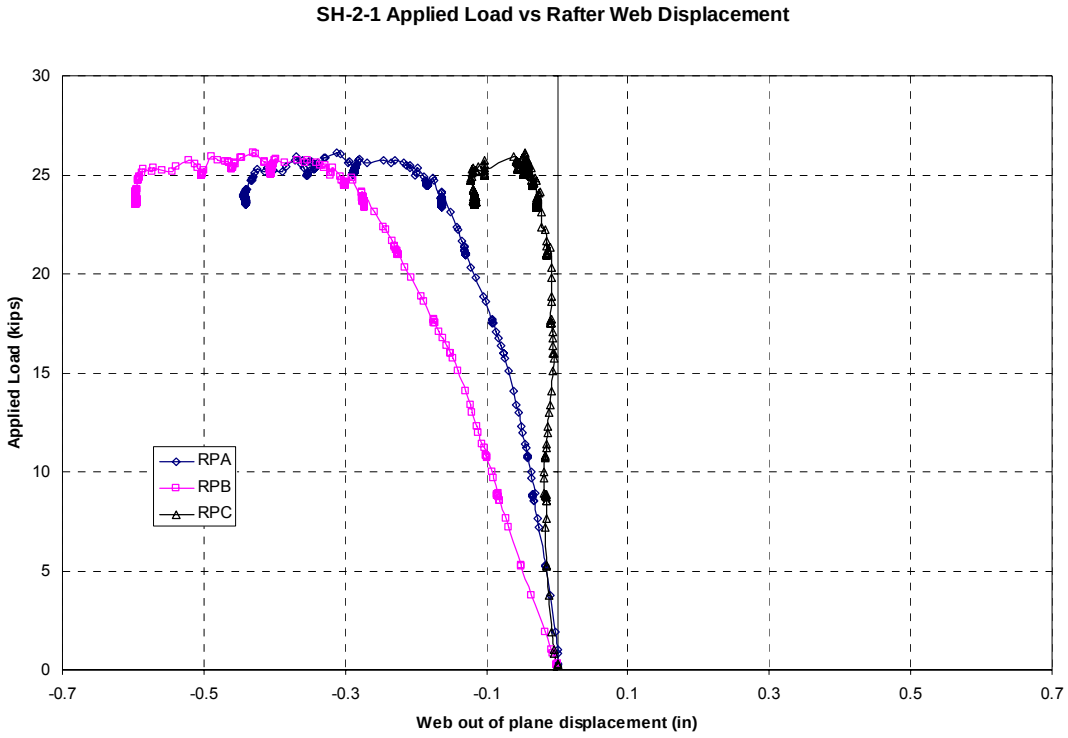

Figure E-6

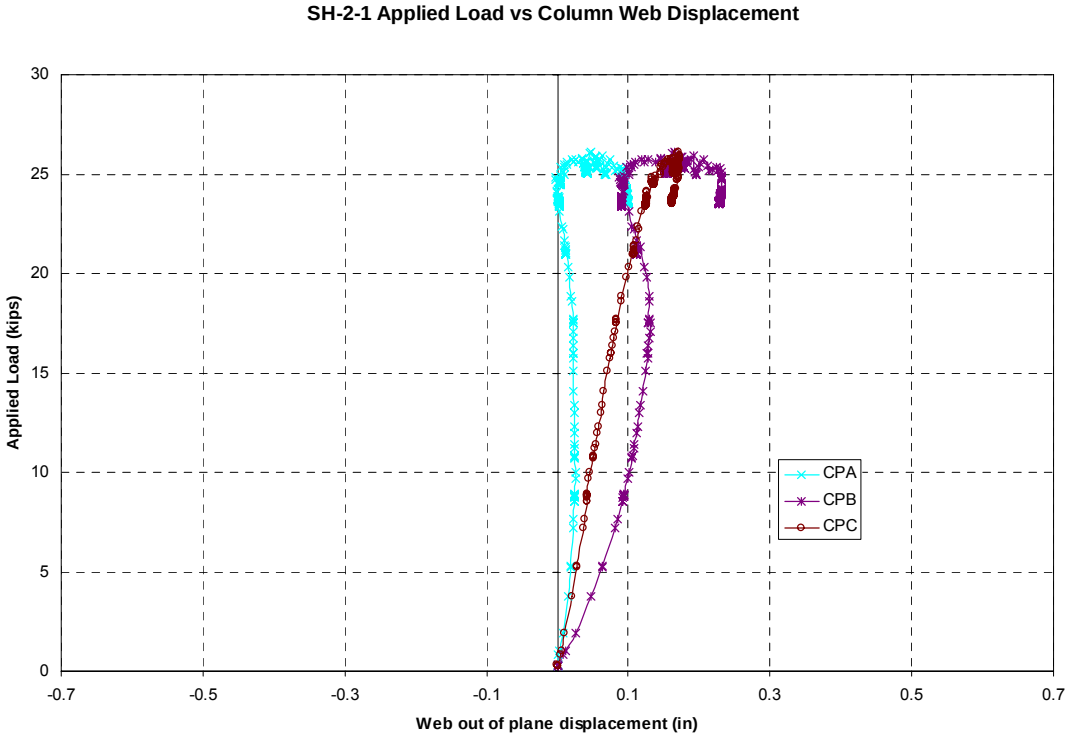

Figure E-7

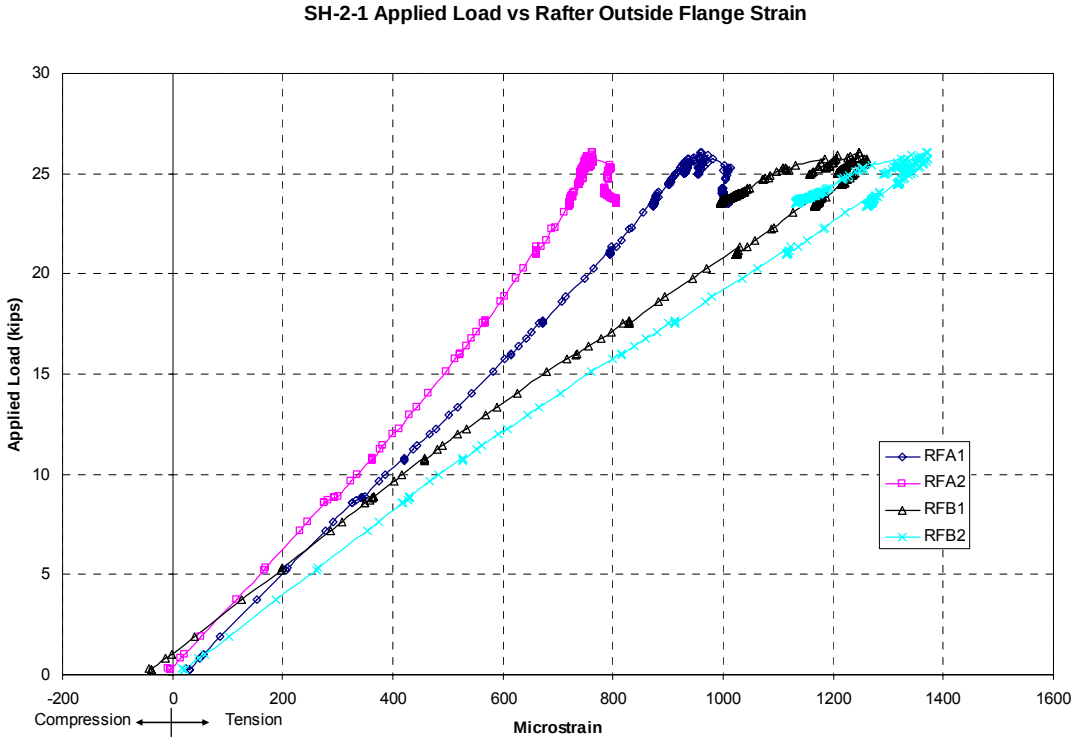

Figure E-8

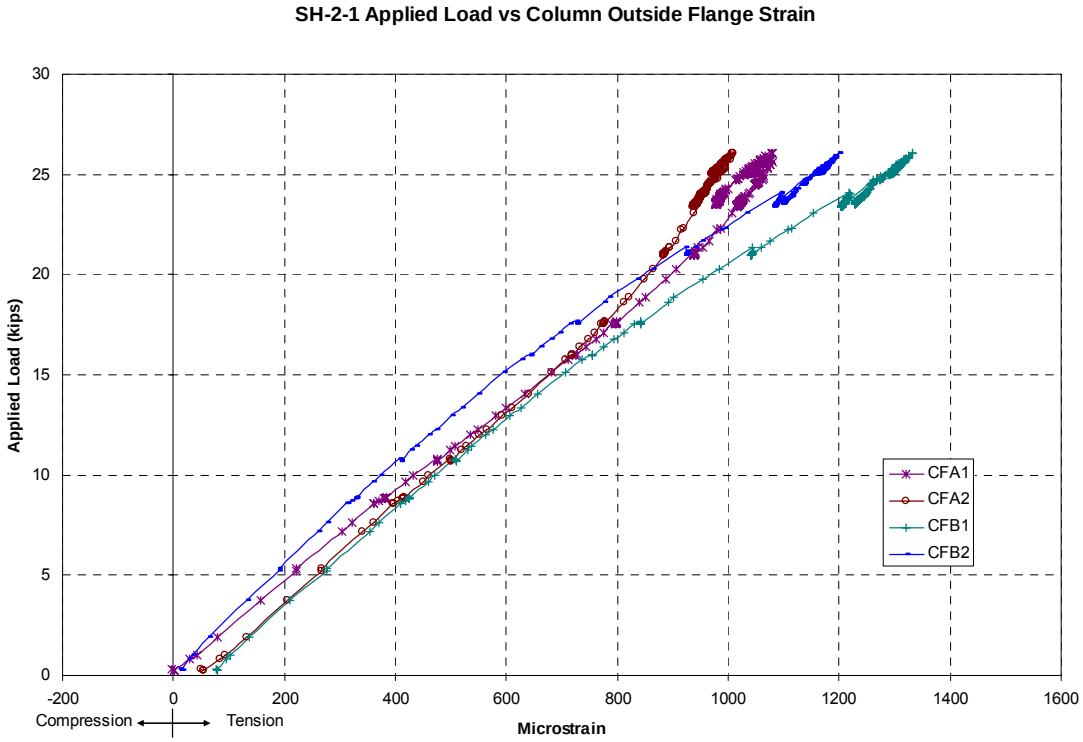

Figure E-9

APPENDIX F. TEST MH-1-1 RESULTS

PROJECT: American Buildings Company
TEST NAME: ABC-MH-1-1 (knee test 6)
TEST DATE: February 7, 2007
PURPOSE: Negative Bending Moment Test for Web Buckling w/o Stiffeners

CONNECTION DESCRIPTION:

NOMINAL YIELD STRESS: ……	55 ksi
GAGE: ……..	3 in
END PLATE WIDTH: …….	8 in
COLUMN END PLATE THICKNESS: …….	0.752 in
RAFTER END PLATE THICKNESS: …….	0.732 in

BOLT DATA:

BOLT DIAMETER: ……	3/4 in
BOLT TYPE: ……...	A490
BOLT PRETENSION: ……	14 kips

COLUMN DATA: (MEASURED)

OUTSIDE FLANGE WIDTH: …….	8 in
OUTSIDE FLANGE THICKNESS: ……	0.504 in
INSIDE FLANGE WIDTH: ……..	8 in
INSIDE FLANGE THICKNESS: …….	0.750 in
WEB DEPTH AT BASE(PERP. TO OS FLANGE): ……..	29.062 in
WEB DEPTH AT REENTRANT CORNER(PERP. TO OS FLANGE): ……	35.938 in
WEB THICKNESS: …….	0.247 in

RAFTER DATA: (MEASURED)

OUTSIDE FLANGE WIDTH: …….	8 in
OUTSIDE FLANGE THICKNESS: …….	0.497 in
INSIDE FLANGE WIDTH: ……..	8 in
INSIDE FLANGE THICKNESS: …….	0.750 in
WEB DEPTH AT BASE(PERP. TO OS FLANGE): ……...	24.938 in
WEB DEPTH AT REENTRANT CORNER(PERP. TO OS FLANGE): ……	35.625 in
WEB THICKNESS: ……..	0.247 in

EXPERIMENTAL:

MAXIMUM LOAD: ……...	86.47 kips
FAILURE LOCATION:	Column Web at Reentrant Corner
FAILURE MODE:	Web Buckling

DISCUSSION:

- Specimen unloaded at76 kips to approximately 10 kips, then reloaded.
- At approximately 83.6 kips, rafter compression flange yielding was evident.
- At 84.5 kips and 2.5 inches chord deflection, displacement control begun.

PROJECT: American Buildings Company
TEST NAME: ABC-MH-1-1 (knee test 6)
TEST DATE: February 7, 2007
PURPOSE: Negative Bending Moment Test for Web Buckling w/o Stiffeners

DISCUSSION: (CONTINUED)

- At 84.5 kips a lateral brace slipped at rafter reentrant corner; unloaded to realign braces and resumed as ABC-MH-1-2 (knee test 8).

Figure F-1 MH 1 Rafter Compression Flange Yielding

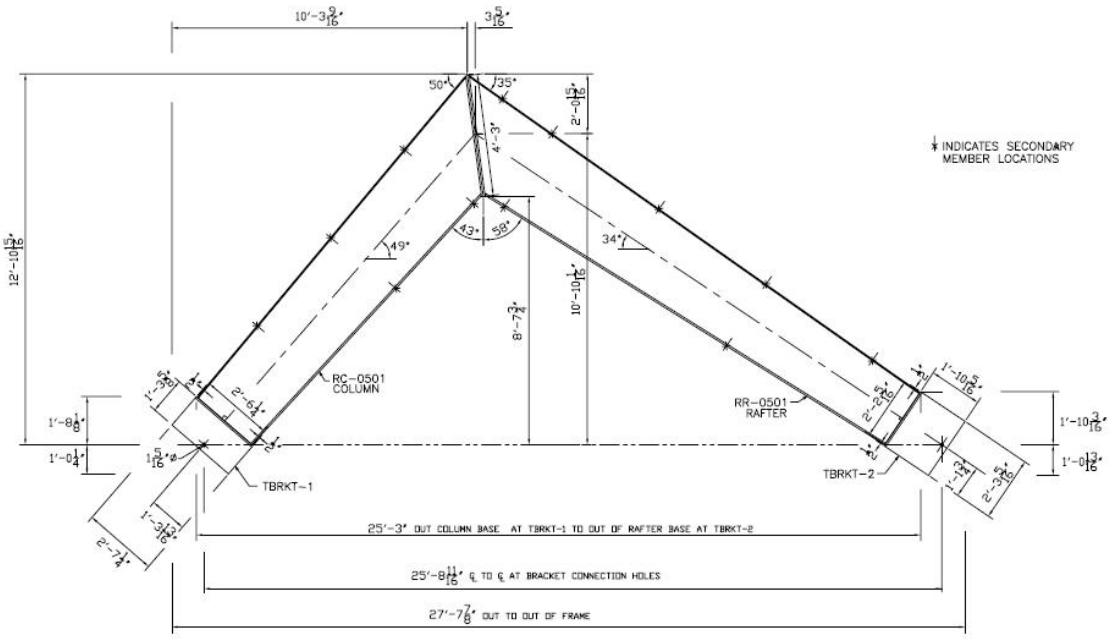

Figure F-2 MH-1 Specimen Dimensions

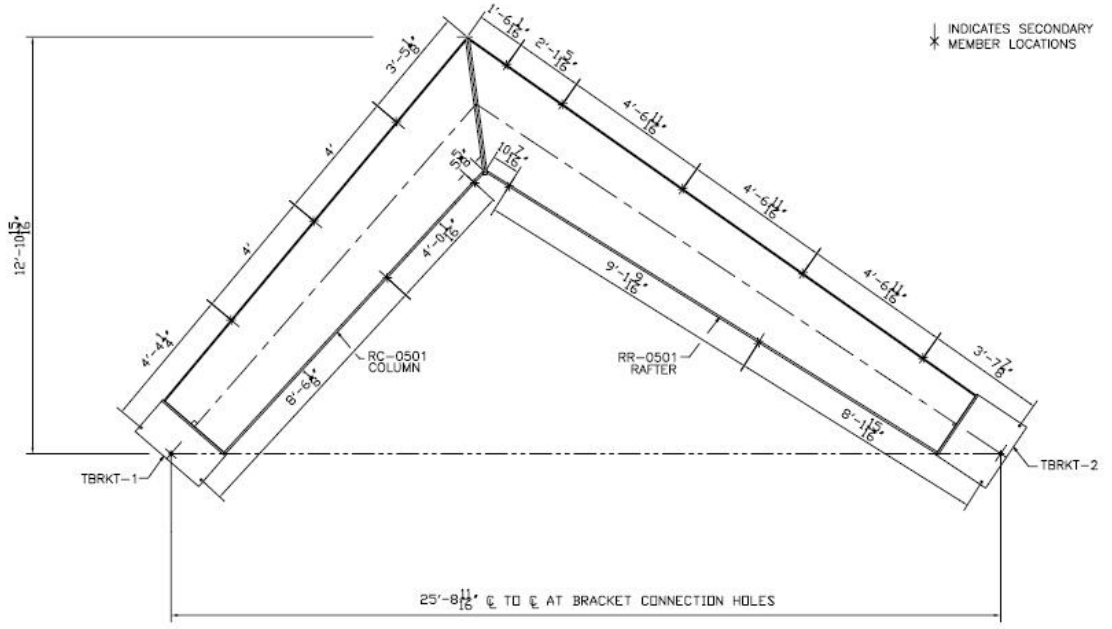

Figure F-3 MH-1 Lateral Brace Locations

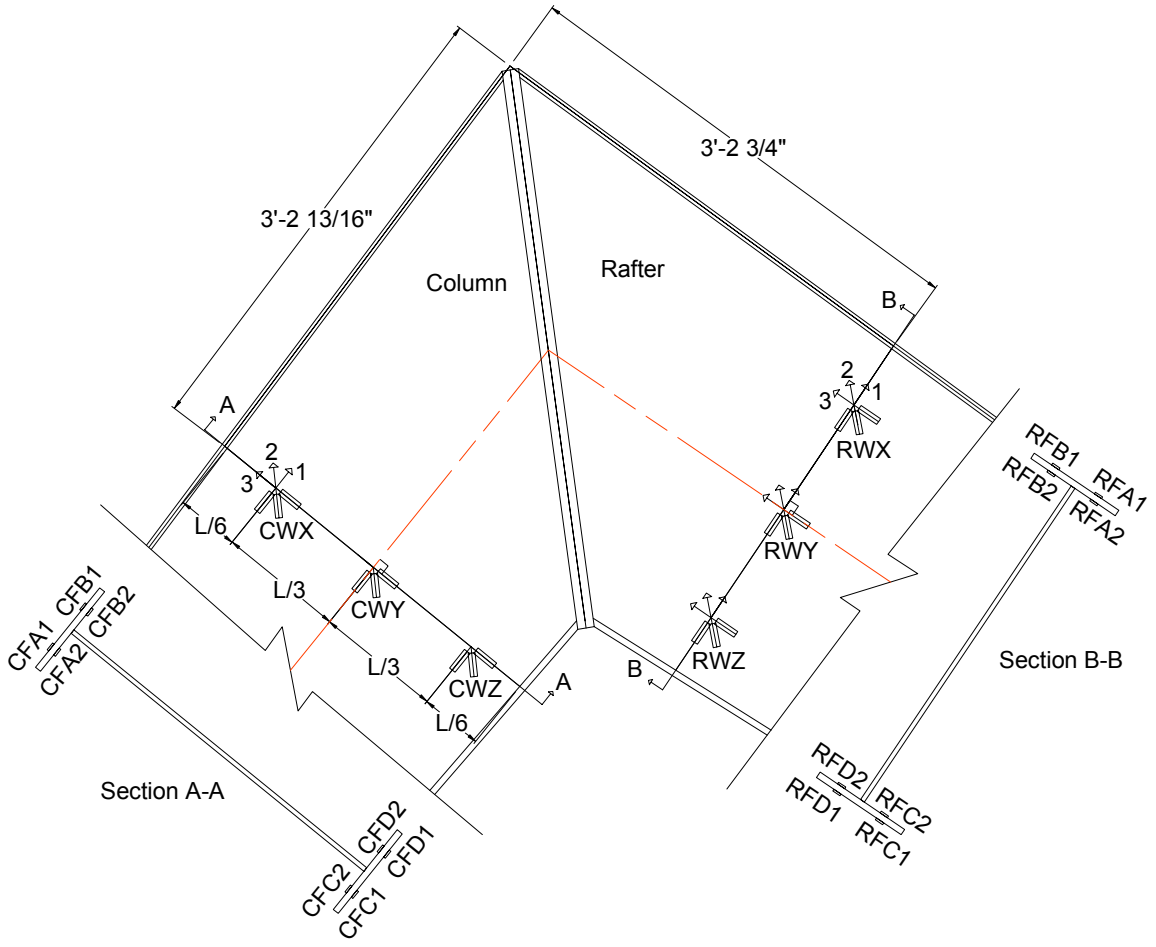

Figure F-4 MH-1 Web and Flange Strain Gages As Viewed From the South

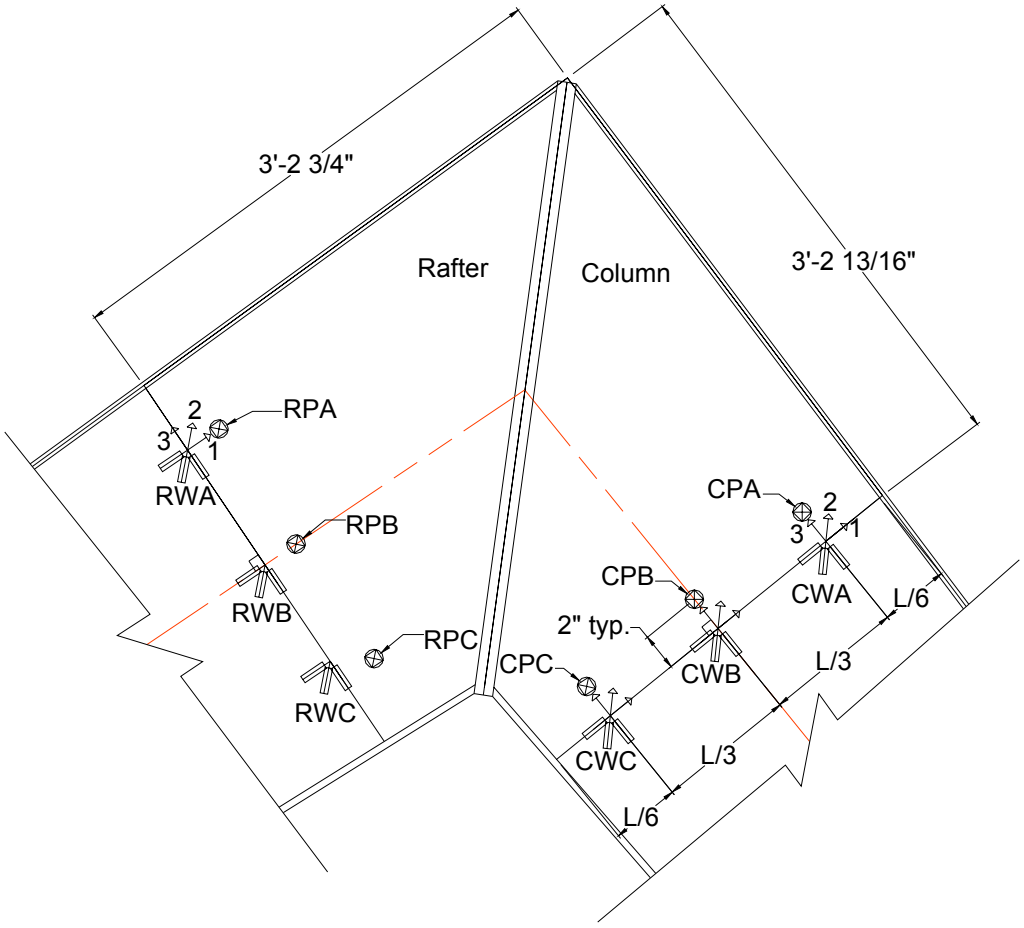

Figure F-5 MH-1 Web Strain Gages and LVDT's As Viewed from the North.

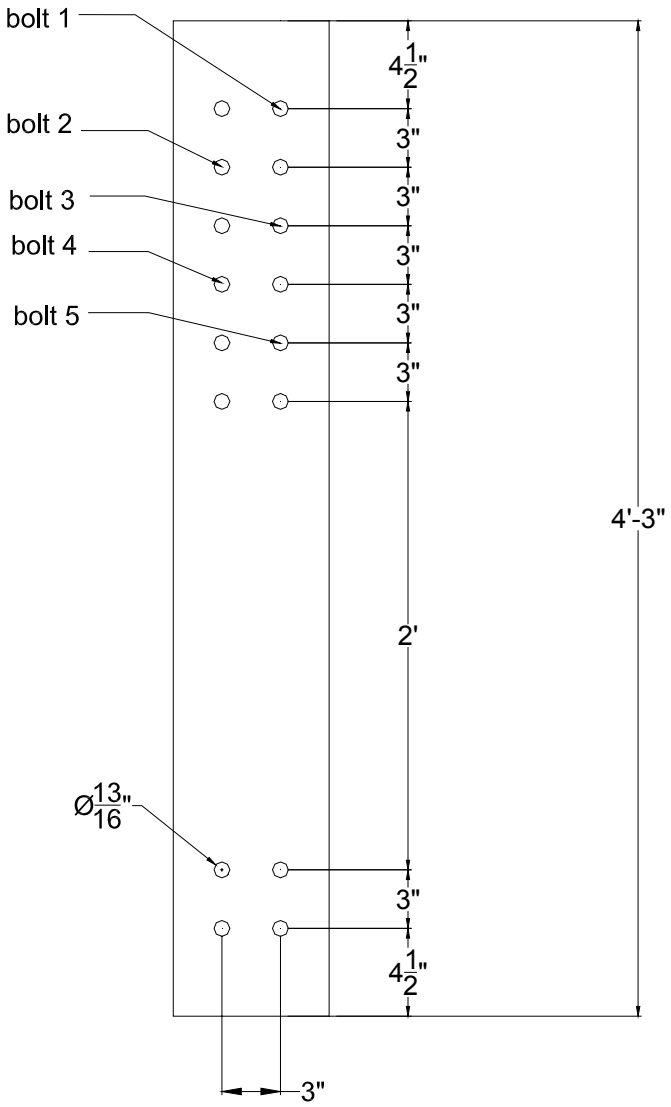

Figure F-6 MH-1 Gaged Bolt Orientation Viewed From the West

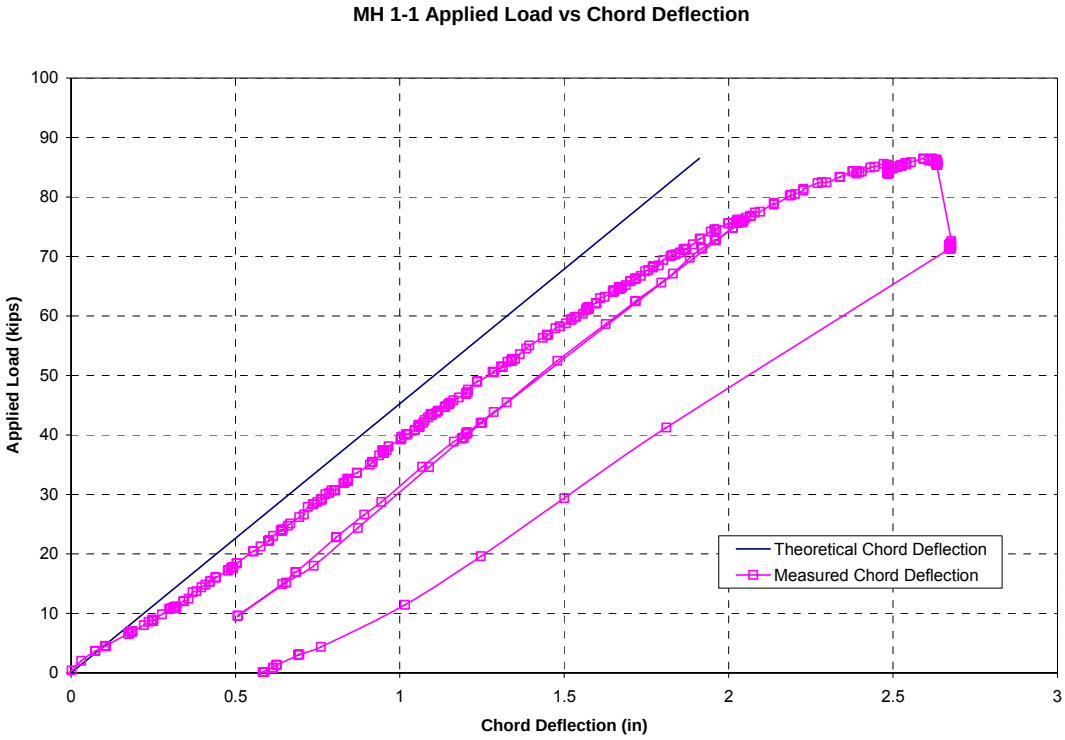

Figure F-7

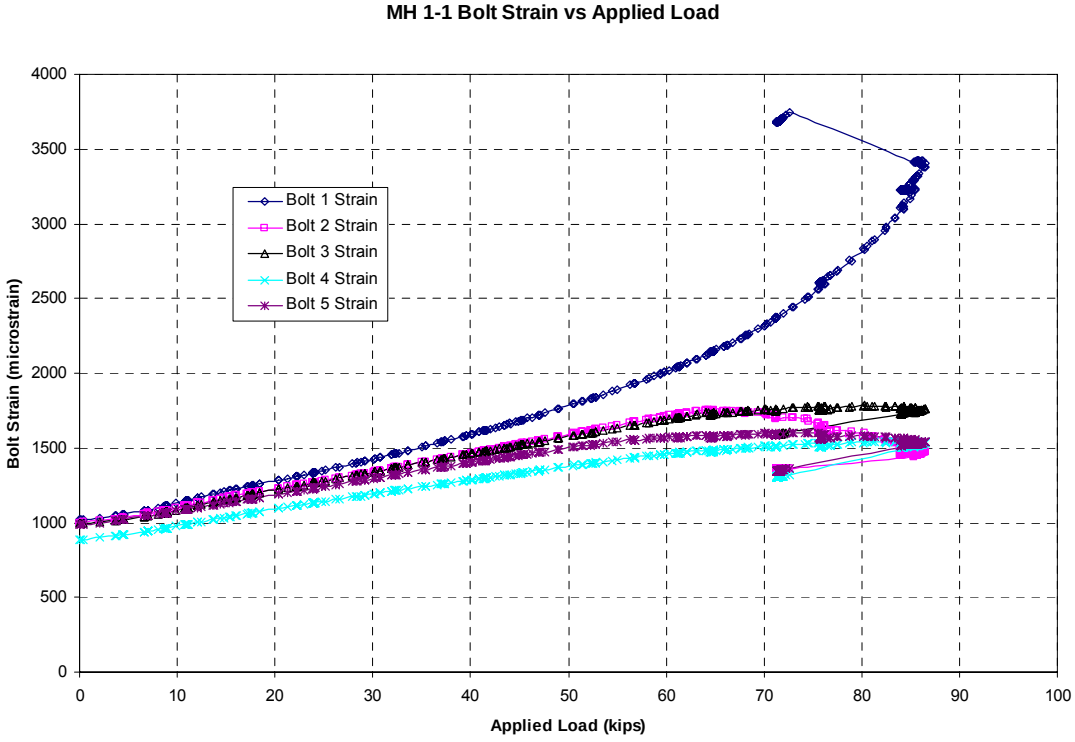

Figure F-8

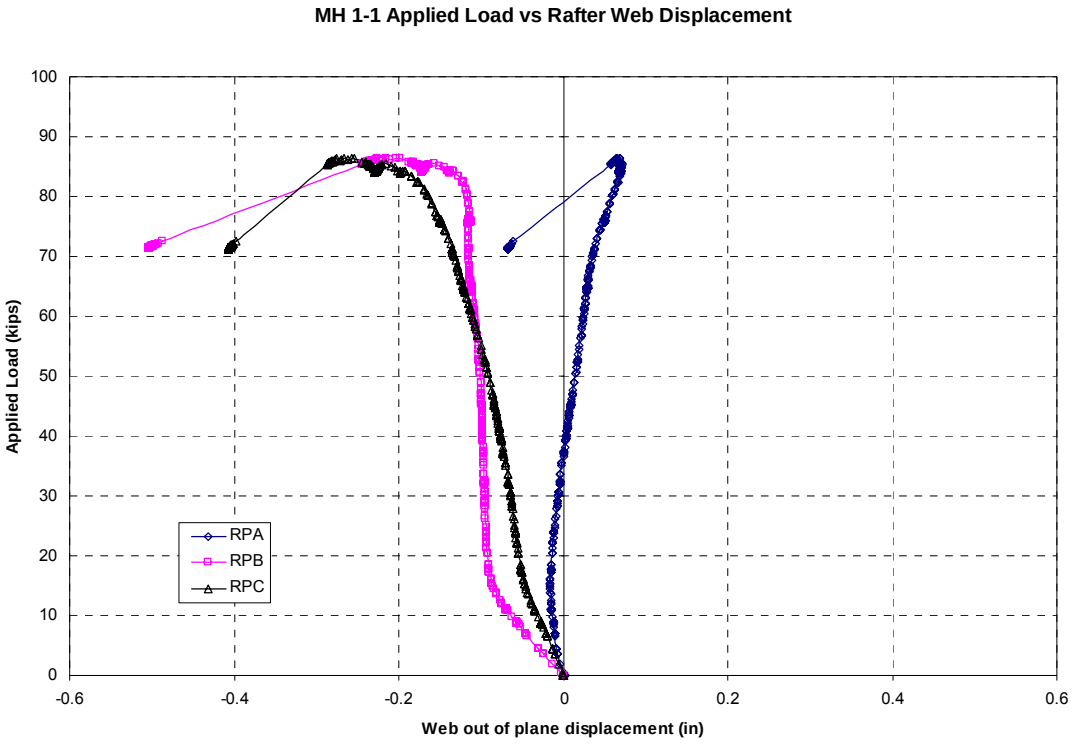

Figure F-9

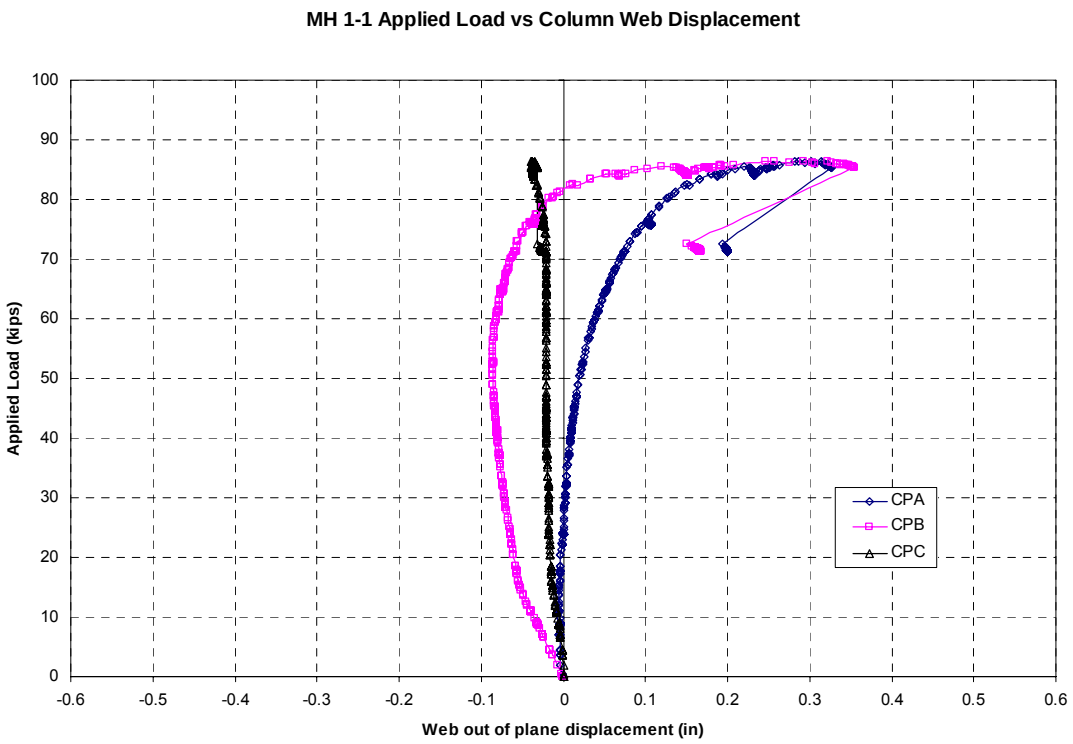

Figure F-10

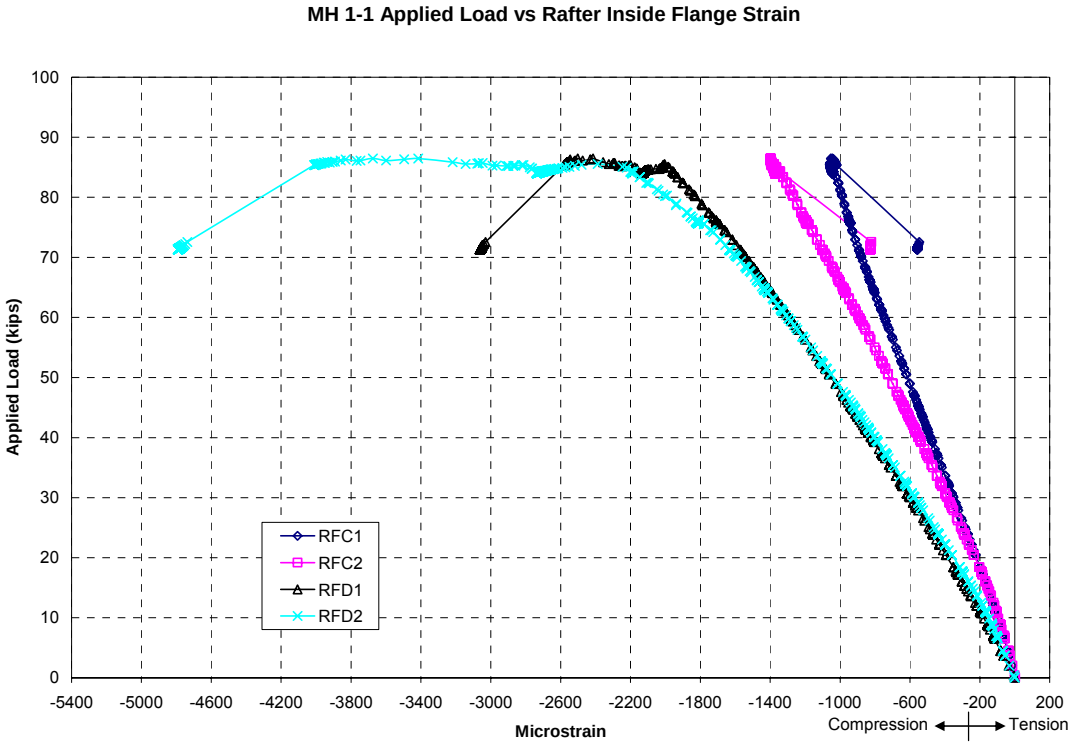

Figure F-11

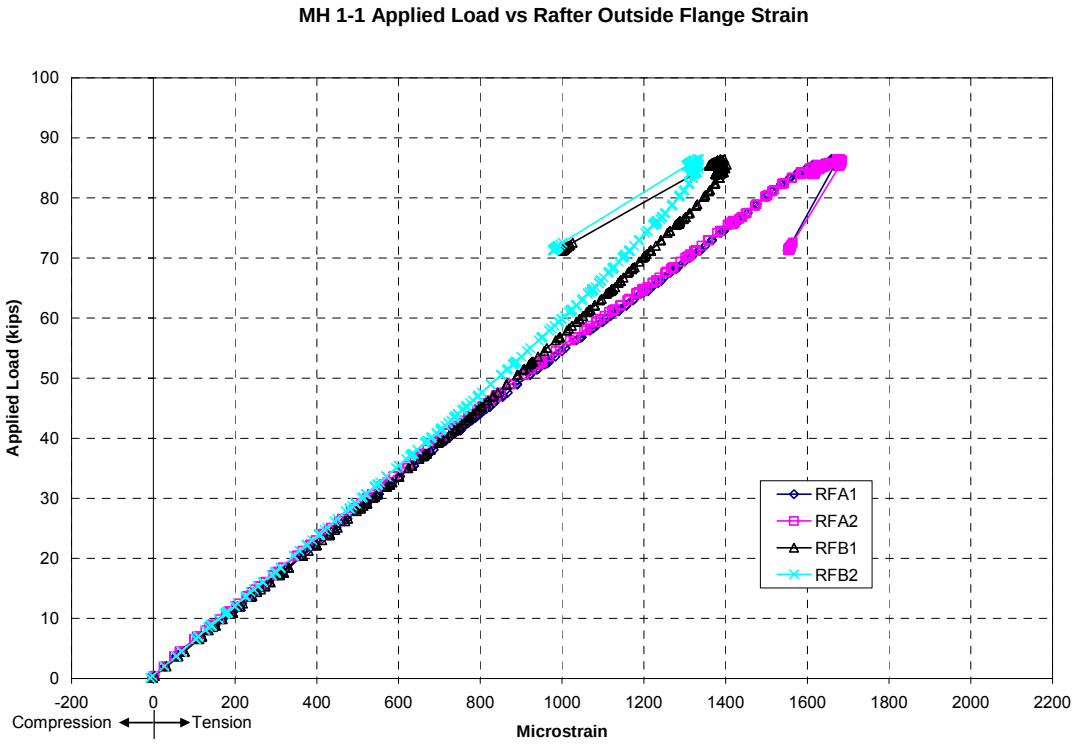

Figure F-12

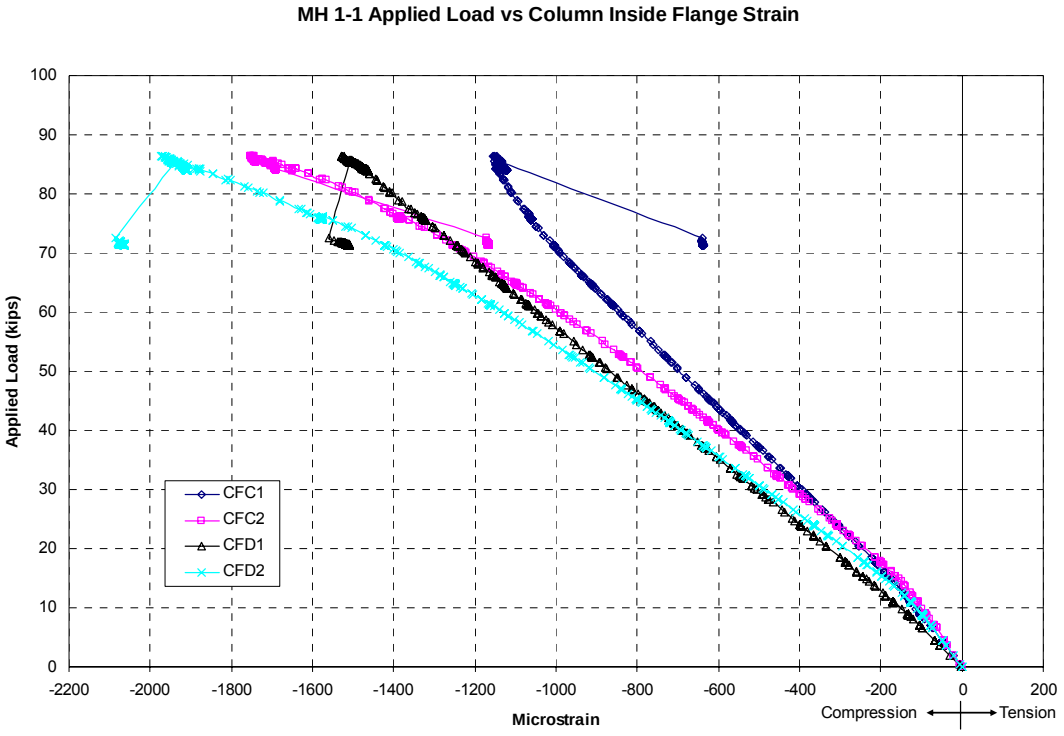

Figure F-13

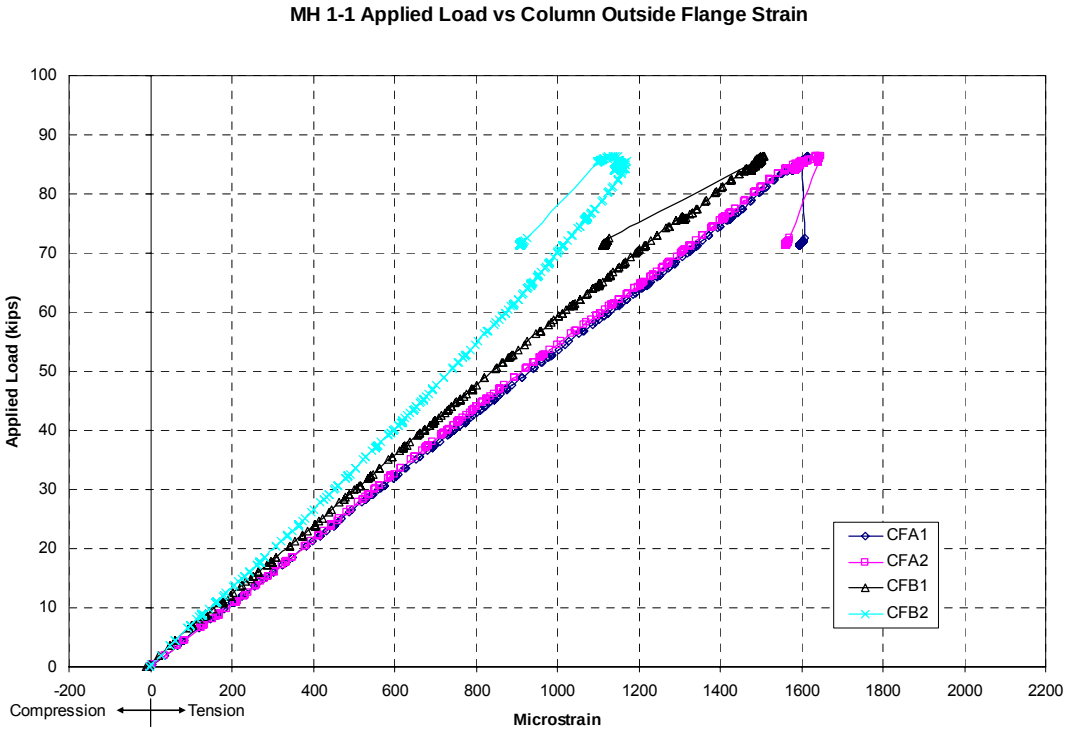

Figure F-14

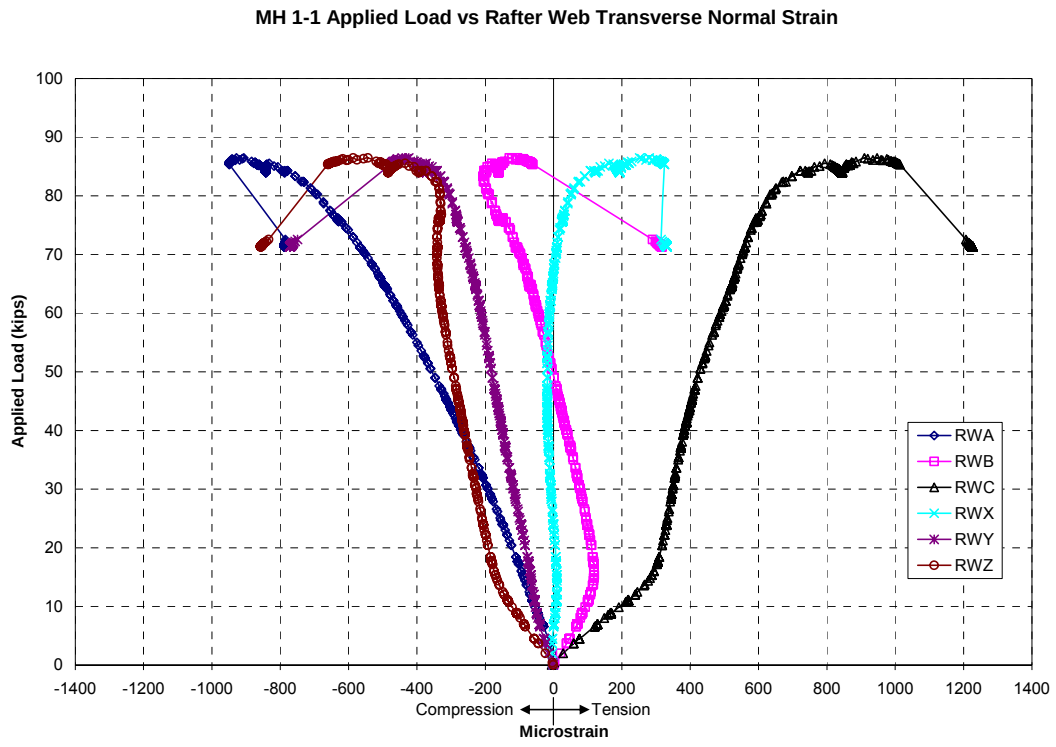

Figure F-15

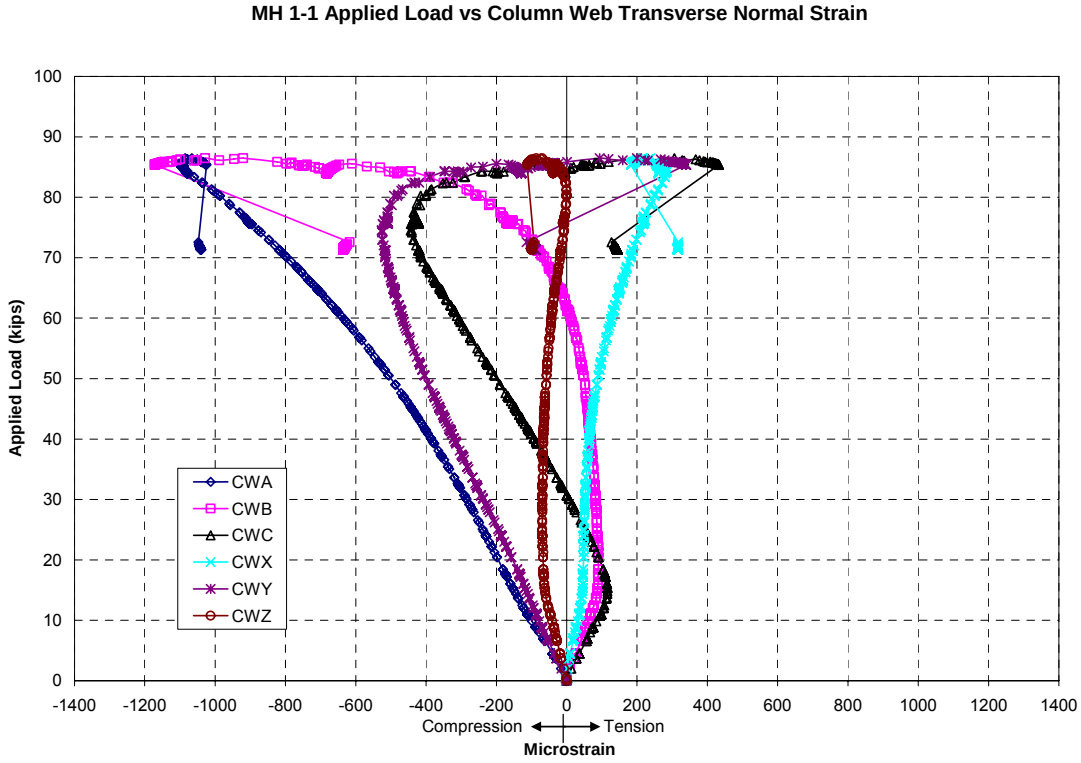

Figure F-16

APPENDIX G. TEST MH-1-2 RESULTS

PROJECT: American Buildings Company
TEST NAME: ABC-MH-1-2 (knee test 7)
TEST DATE: February 12, 2007
PURPOSE: Negative Bending Moment Test for Web Buckling w/o Stiffeners

CONNECTION DESCRIPTION:

NOMINAL YIELD STRESS: ……	55 ksi
GAGE: ……..	3 in
END PLATE WIDTH: …….	8 in
COLUMN END PLATE THICKNESS: …….	0.752 in
RAFTER END PLATE THICKNESS: …….	0.732 in

BOLT DATA:

BOLT DIAMETER: ……	3/4 in
BOLT TYPE: ……...	A490
BOLT PRETENSION: ……	14 kips

COLUMN DATA: (MEASURED)

OUTSIDE FLANGE WIDTH: …….	8 in
OUTSIDE FLANGE THICKNESS: ……	0.504 in
INSIDE FLANGE WIDTH: ……..	8 in
INSIDE FLANGE THICKNESS: …….	0.750 in
WEB DEPTH AT BASE(PERP. TO OS FLANGE): ……..	29.062 in
WEB DEPTH AT REENTRANT CORNER(PERP. TO OS FLANGE): ……	35.938 in
WEB THICKNESS: …….	0.247 in

RAFTER DATA: (MEASURED)

OUTSIDE FLANGE WIDTH: …….	8 in
OUTSIDE FLANGE THICKNESS: …….	0.497 in
INSIDE FLANGE WIDTH: ……..	8 in
INSIDE FLANGE THICKNESS: …….	0.750 in
WEB DEPTH AT BASE(PERP. TO OS FLANGE): ……...	24.938 in
WEB DEPTH AT REENTRANT CORNER(PERP. TO OS FLANGE): ……	35.625 in
WEB THICKNESS: ……..	0.247 in

EXPERIMENTAL:

MAXIMUM LOAD: ……...	77.48 kips
FAILURE LOCATION:	Column Web at Reentrant Corner
FAILURE MODE:	Web Buckling

DISCUSSION:

- At approximately 57 kips, the rafter lateral brace at the reentrant corner failed. Specimen unloaded for repair and reloaded.

PROJECT: American Buildings Company
TEST NAME: ABC-MH-1-2 (knee test 7)
TEST DATE: February 12, 2007
PURPOSE: Negative Bending Moment Test for Web Buckling w/o Stiffeners

DISCUSSION: (CONTINUED)

- Displacement control begun at 75.3 kips and 2.29 inches chord deflection.
- At 75.7 kips and 2.31 inches chord deflection, yield lines became apparent in the web at the outside flange and end plate and web buckling was also visibly apparent.
- At 75.1 kips and 2.46 inches chord deflection, lateral torsional buckling occurred in rafter between braced points.

Figure G-1 MH-1-2 Rafter Lateral Torsional Buckling

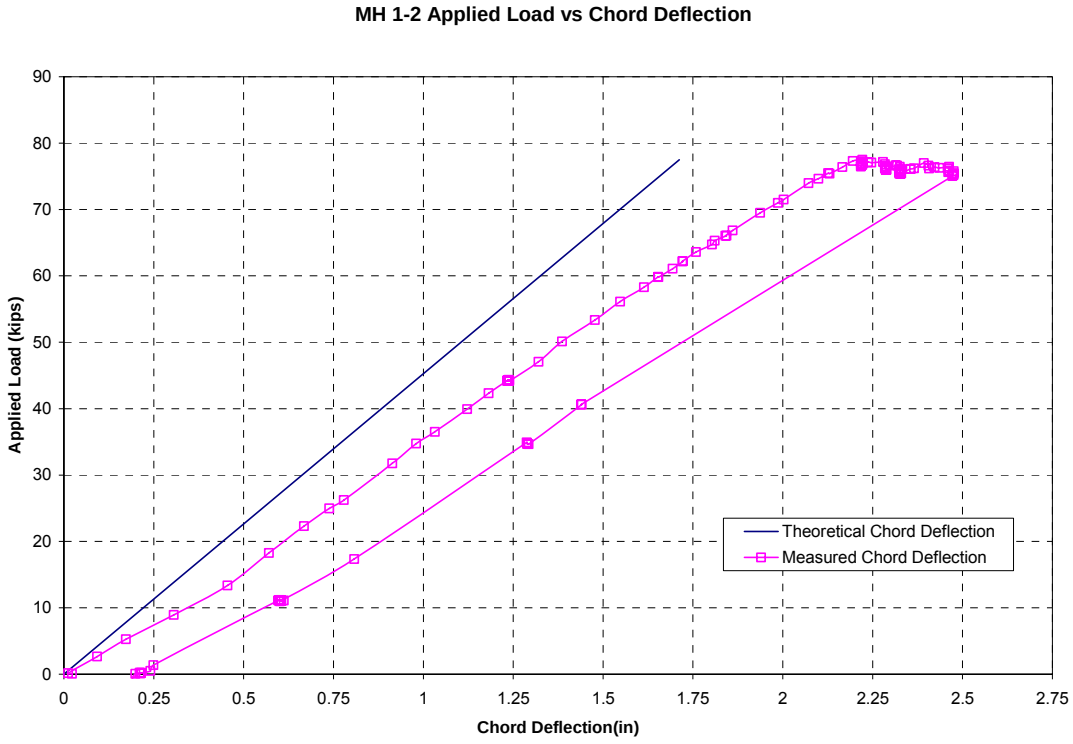

Figure G-2

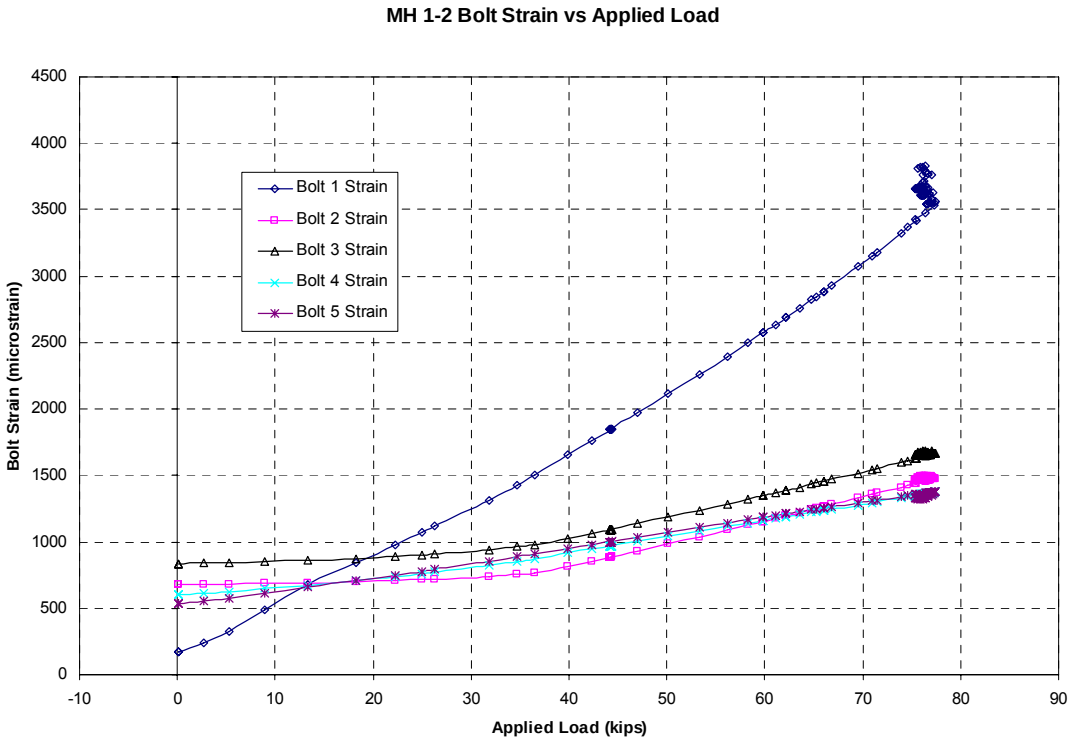

Figure G-3

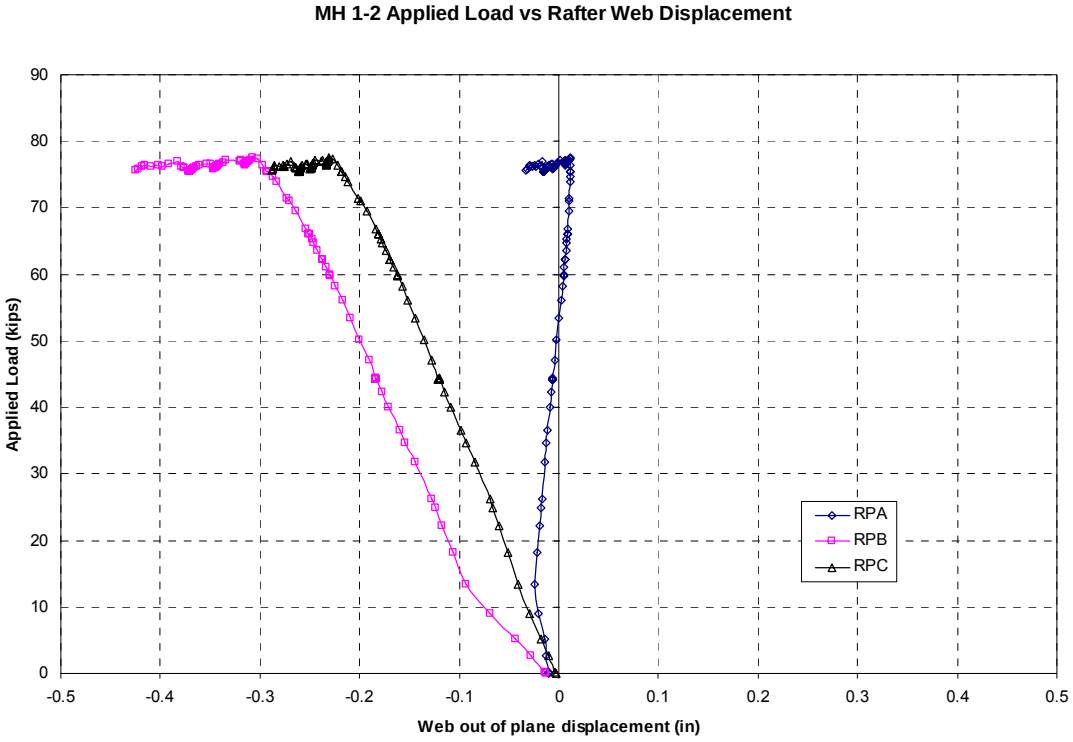

Figure G-4

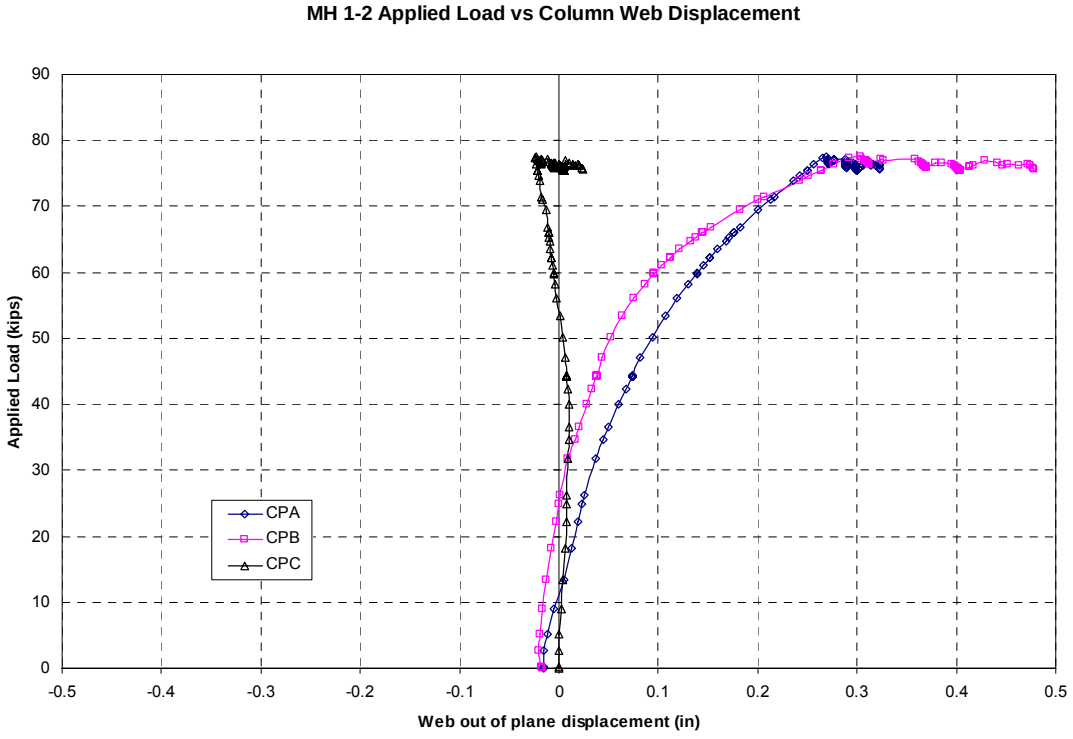

Figure G-5

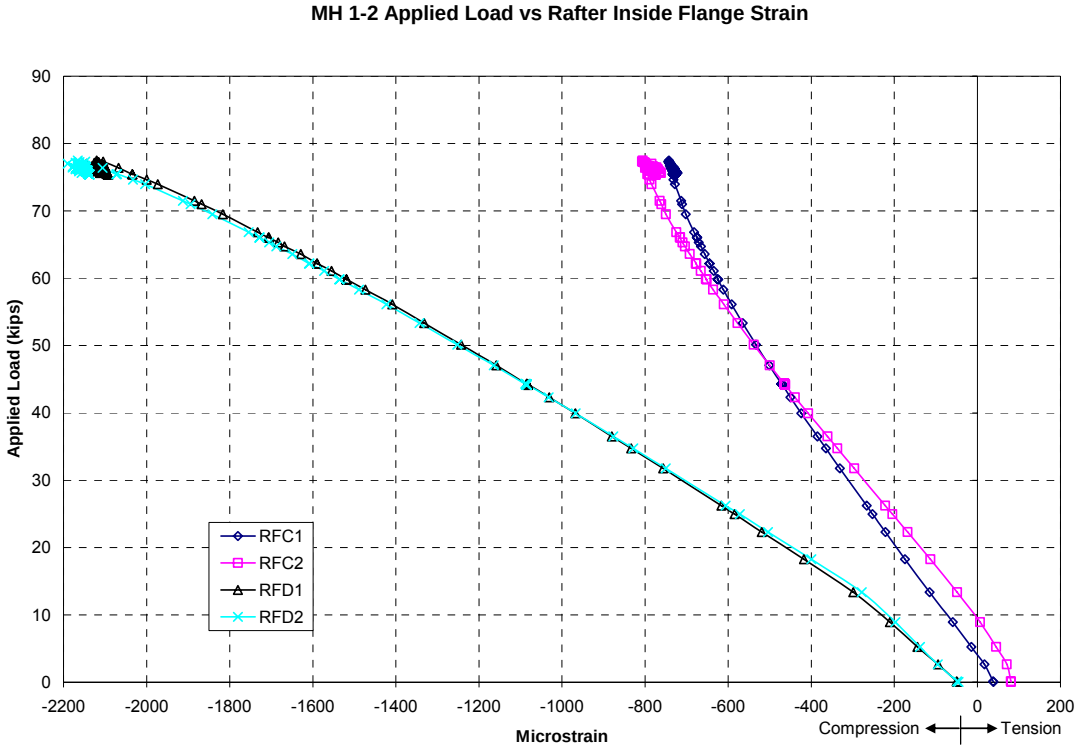

Figure G-6

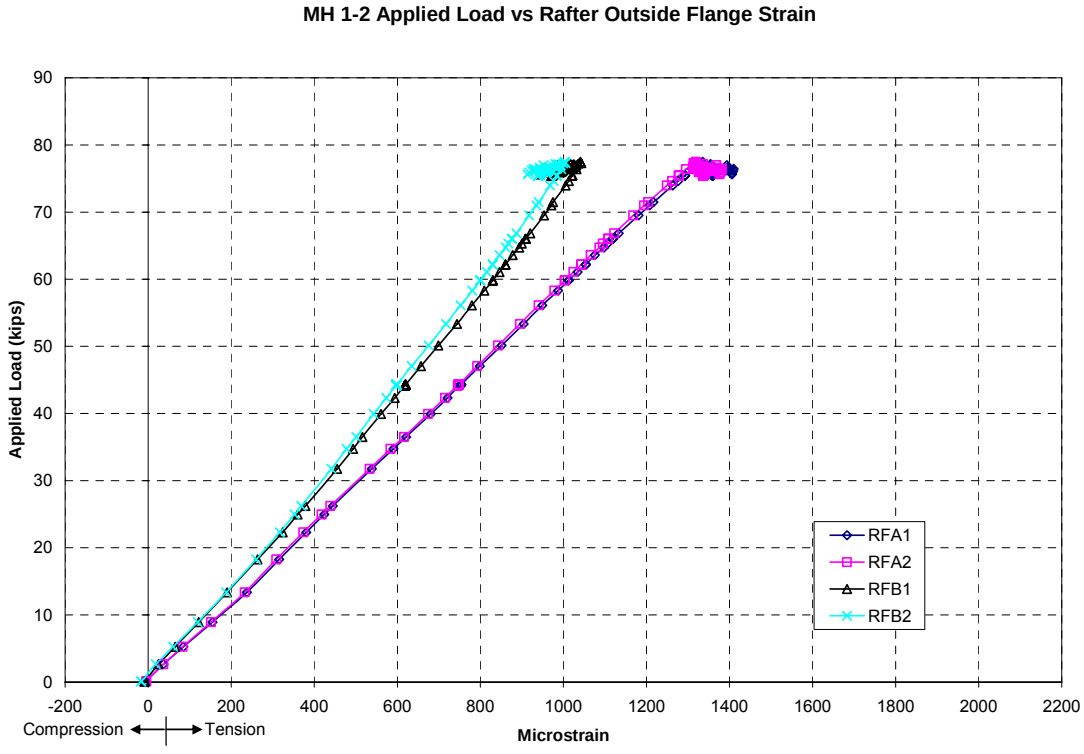

Figure G-7

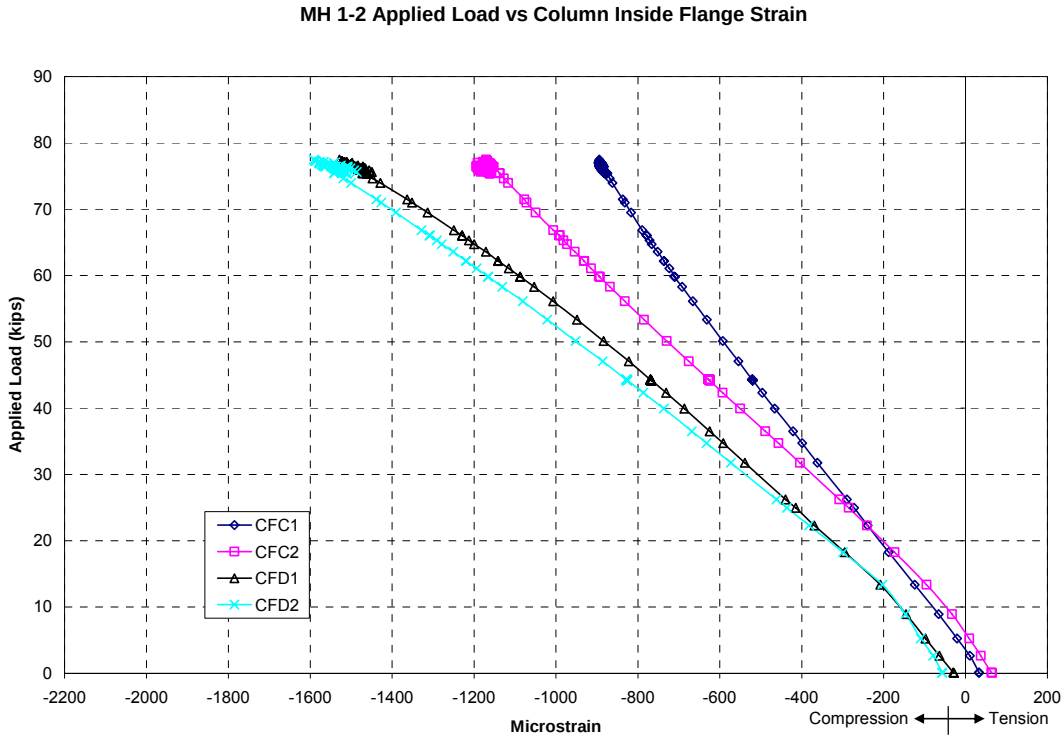

Figure G-8

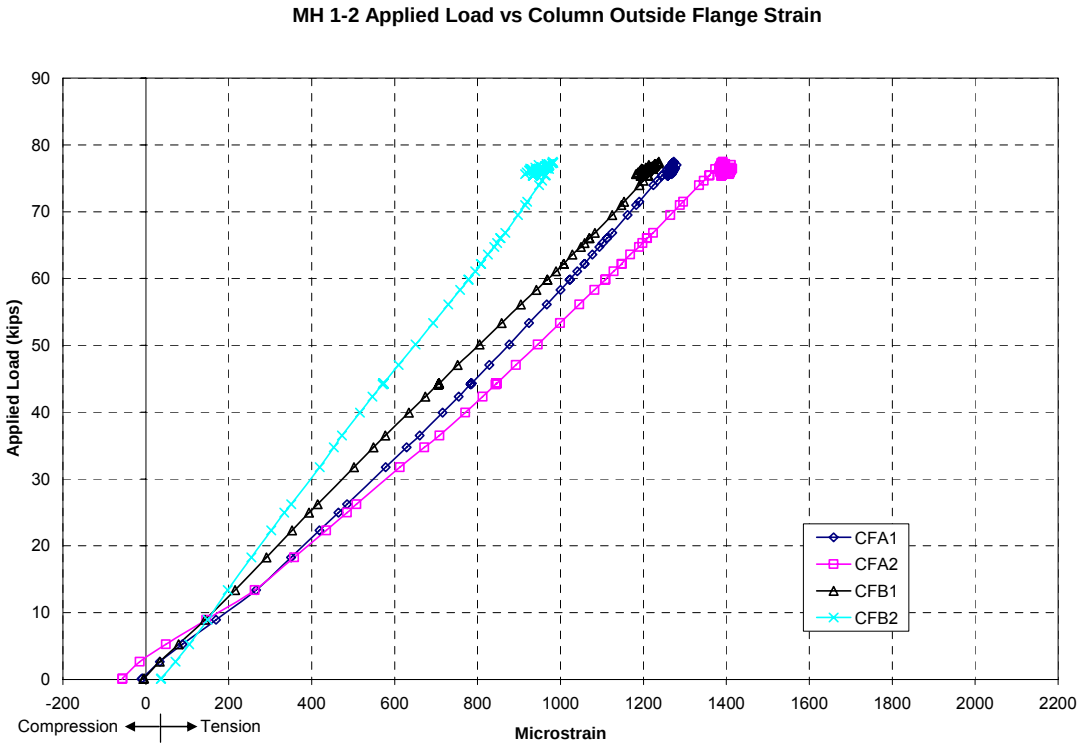

Figure G-9

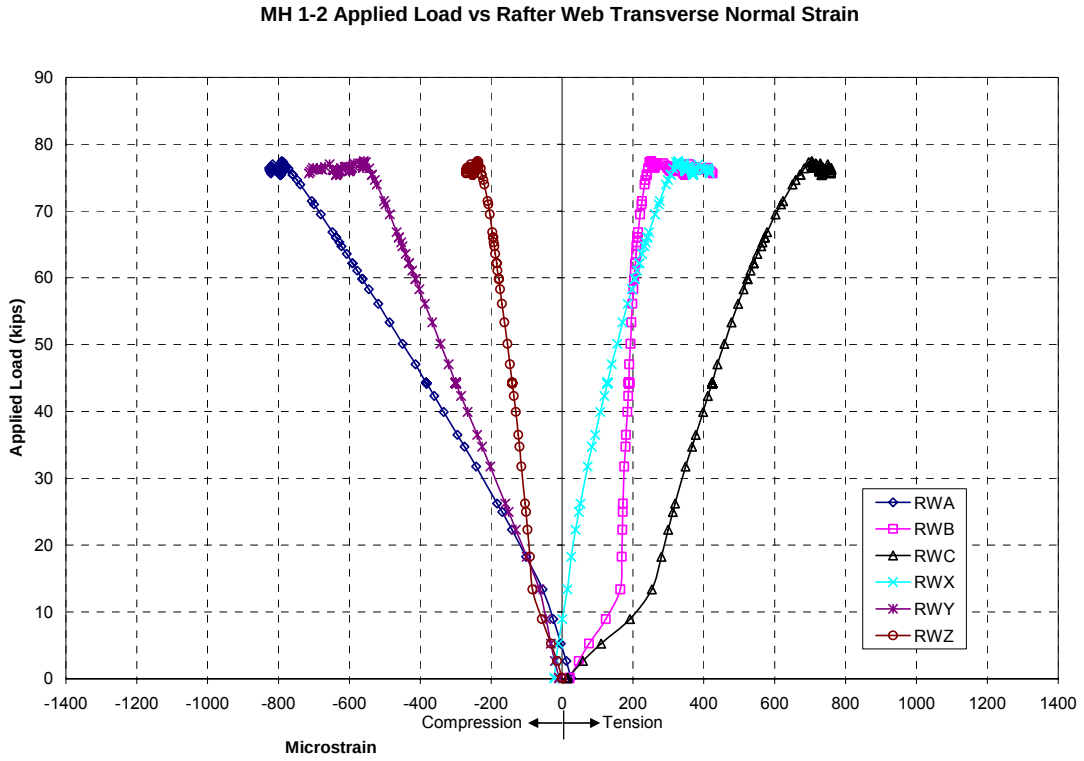

Figure G-10

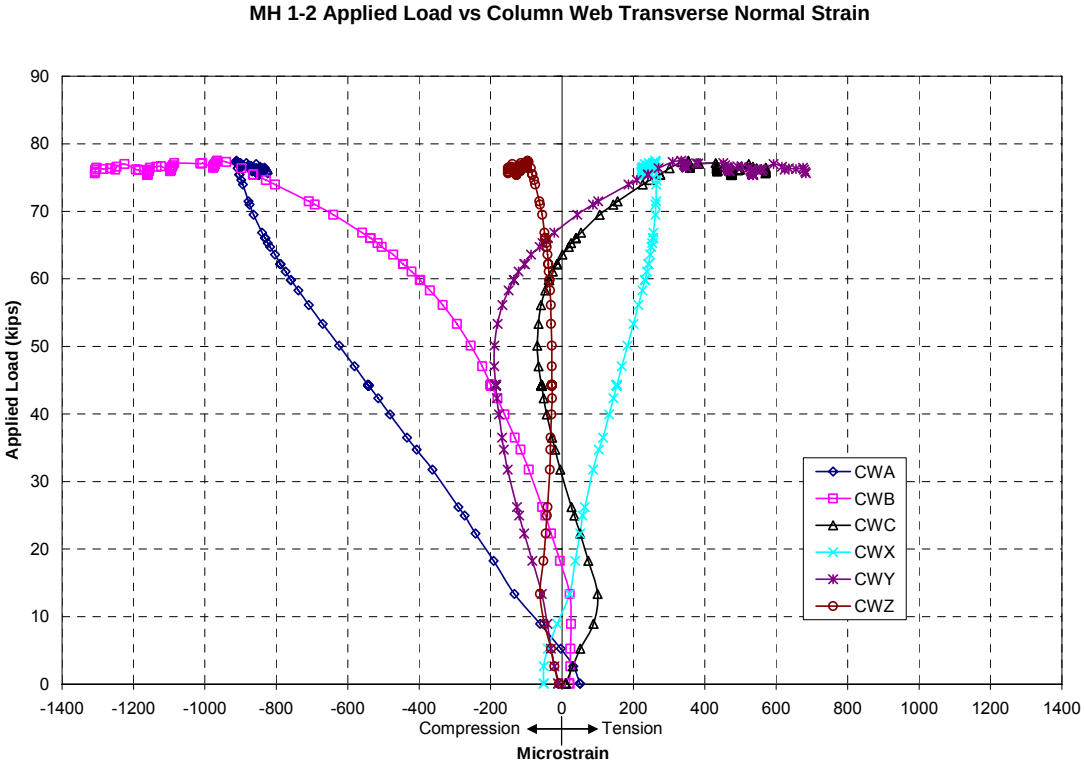

Figure G-11

APPENDIX H. TEST LH-1-1 RESULTS

PROJECT: American Buildings Company
TEST NAME: ABC-LH-1-1 (knee test 8)
TEST DATE: March 30, 2006
PURPOSE: Negative Bending Moment Test for Web Buckling w/o Stiffeners

CONNECTION DESCRIPTION:

NOMINAL YIELD STRESS: ……	55 ksi
GAGE: ……..	3 in
END PLATE WIDTH: ……	12 in
END PLATE THICKNESS (COLUMN): ……..……	0.767 in
END PLATE THICKNESS (RAFTER): …….	0.628 in

BOLT DATA:

BOLT DIAMETER: ……	3/4 in
BOLT TYPE: ……...	A490
BOLT PRETENSION: ……	14 kips

COLUMN DATA: (MEASURED)

OUTSIDE FLANGE WIDTH: …….	12 in
OUTSIDE FLANGE THICKNESS: ……	0.637 in
INSIDE FLANGE WIDTH: ……..	12 in
INSIDE FLANGE THICKNESS: …….	0.618 in
WEB DEPTH AT BASE(PERP. TO OS FLANGE): ……..	27.69 in
WEB DEPTH AT REENTRANT CORNER(PERP. TO OS FLANGE): ……	59.5 in
WEB THICKNESS: …….	0.308 in

RAFTER DATA: (MEASURED)

OUTSIDE FLANGE WIDTH: …….	12 in
OUTSIDE FLANGE THICKNESS: …….	0.627 in
INSIDE FLANGE WIDTH: ……..	12 in
INSIDE FLANGE THICKNESS: …….	0.622 in
WEB DEPTH AT BASE(PERP. TO OS FLANGE): ……...	31.19 in
WEB DEPTH AT REENTRANT CORNER(PERP. TO OS FLANGE): ……	59.75 in
WEB THICKNESS: ……..	0.308 in

EXPERIMENTAL:

MAXIMUM LOAD: ……...	162.3 kips
FAILURE LOCATION:	Rafter Web and Column Web at Reentrant Corner
FAILURE MODE:	Web Buckling

DISCUSSION:

- Unloaded at 56.14 kips, reloaded.
- At 148.9 kips, yielding was observed in rafter compression flange.
- Sudden load loss occurred at approximately 160 kips, and compression flange yielding and slight buckling observed in the rafter, adjacent to the end plate.

PROJECT: American Buildings Company
TEST NAME: ABC-LH-1-1 (knee test 8)
TEST DATE: March 30, 2006
PURPOSE: Negative Bending Moment Test for Web Buckling w/o Stiffeners

DISCUSSION: (CONTINUED)

- Displacement control begun at 156.3 kips and 1.98 inches chord deflection.
- Continued loss of load attributed to significant observed web buckling in the knee area, as well as continued rafter compression flange yielding and buckling.

Figure H-1 LH-1 Rafter Web Buckling

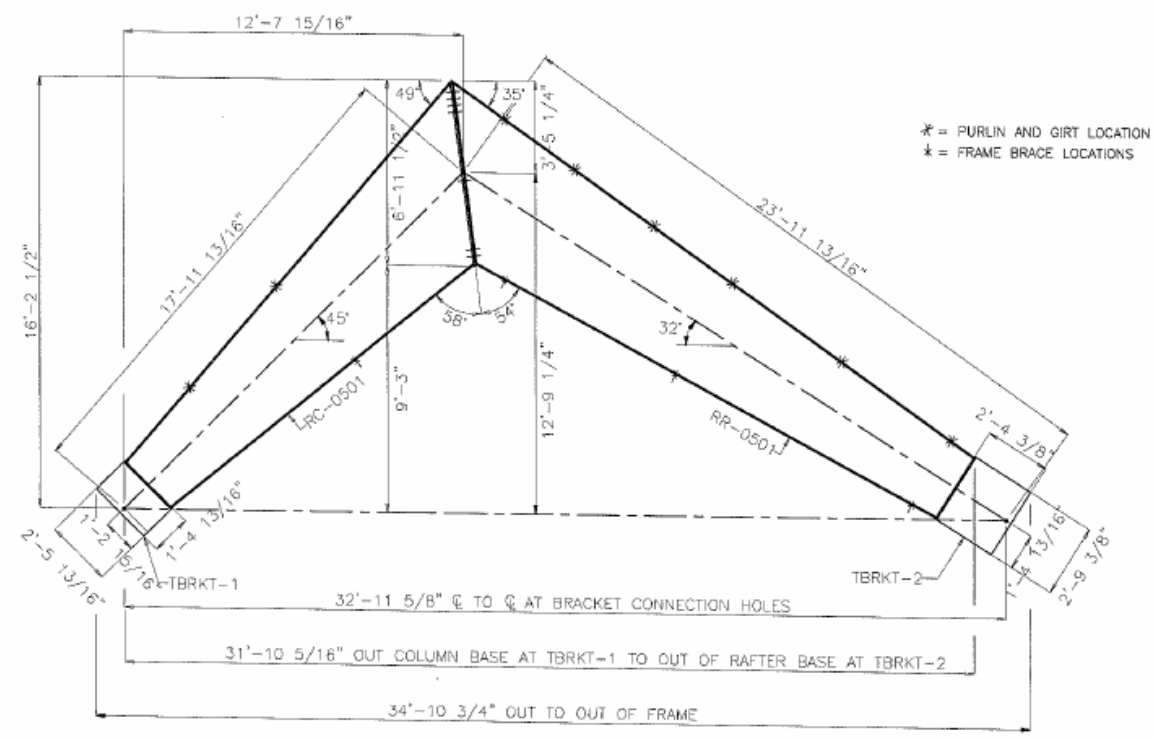

Figure H-2 LH-1 Specimen Dimensions

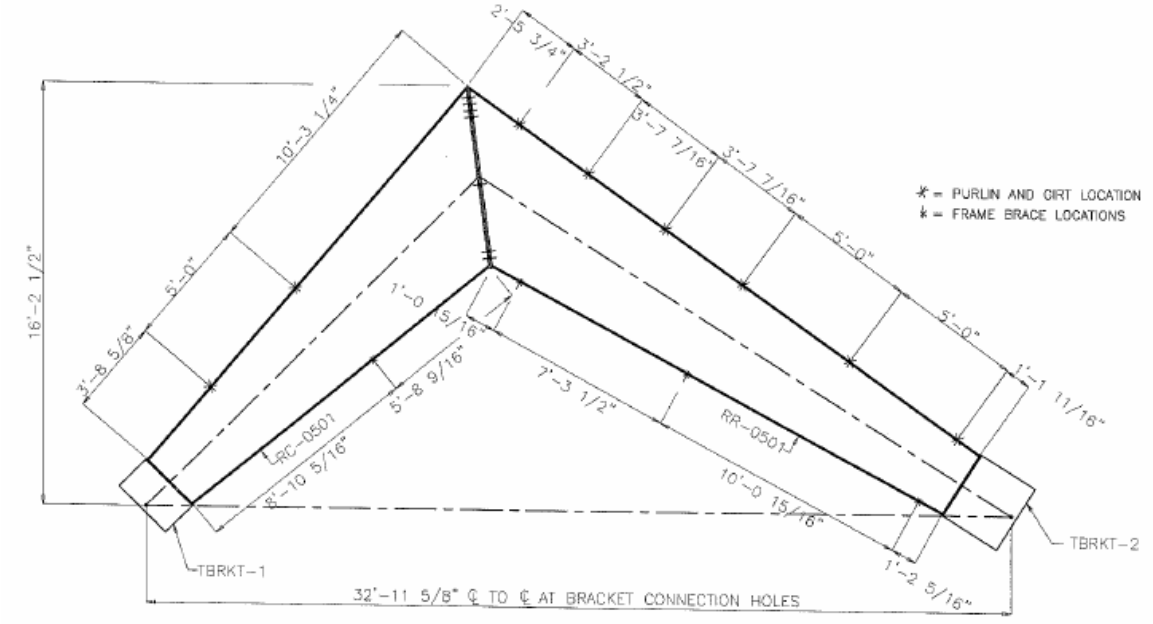

Figure H-3 LH-1 Lateral Brace Locations

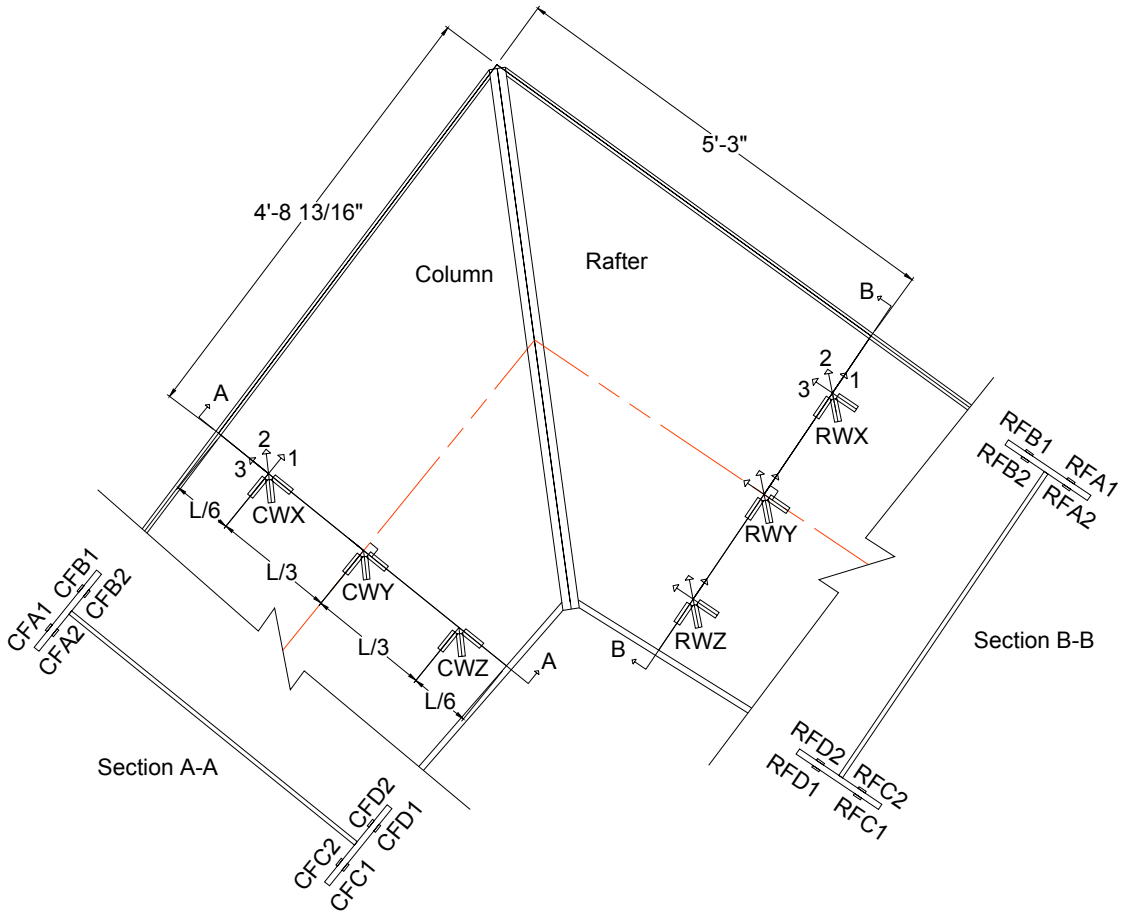

Figure H-4 LH-1 Web and Flange Strain Gages As Viewed From the South

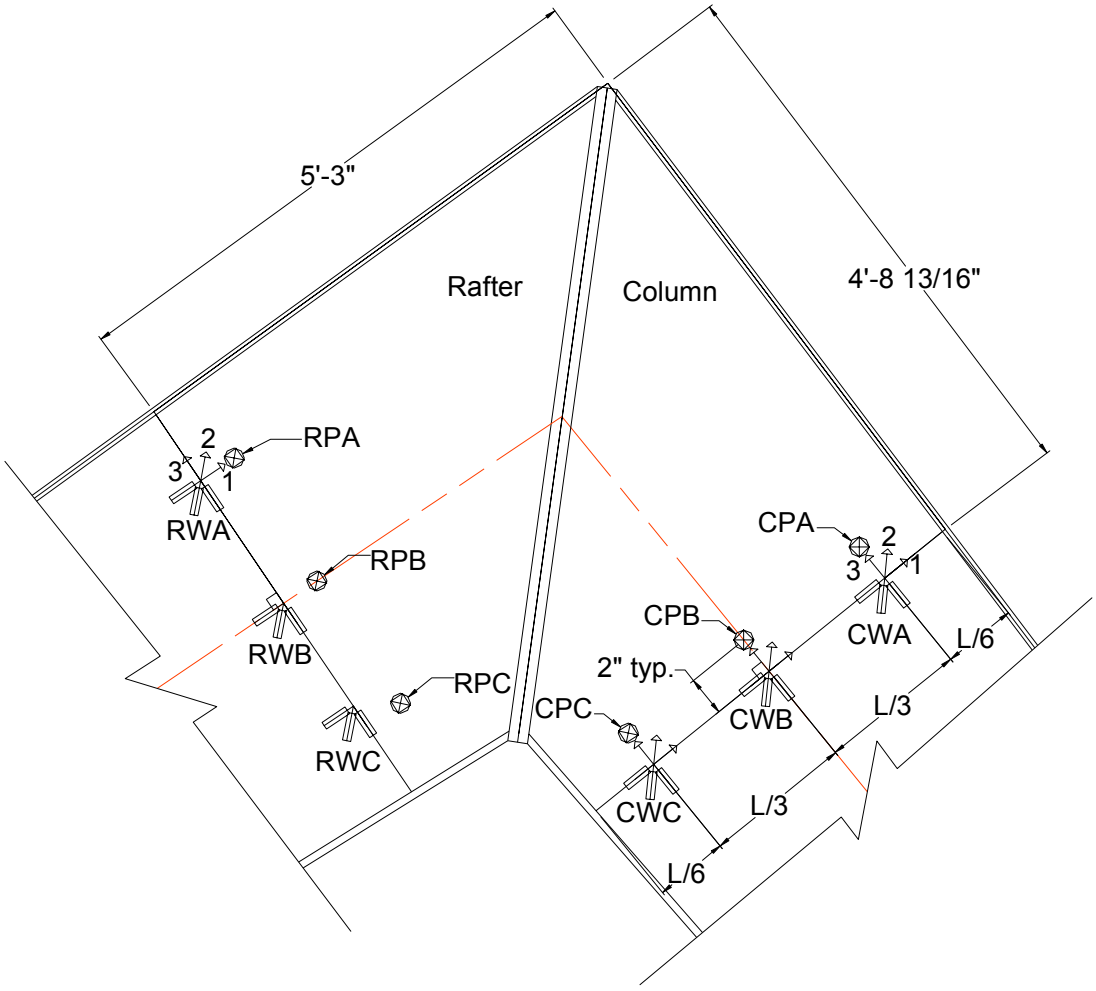

Figure H-5 LH-1 Web Strain Gages and LVDT's As Viewed from the North.

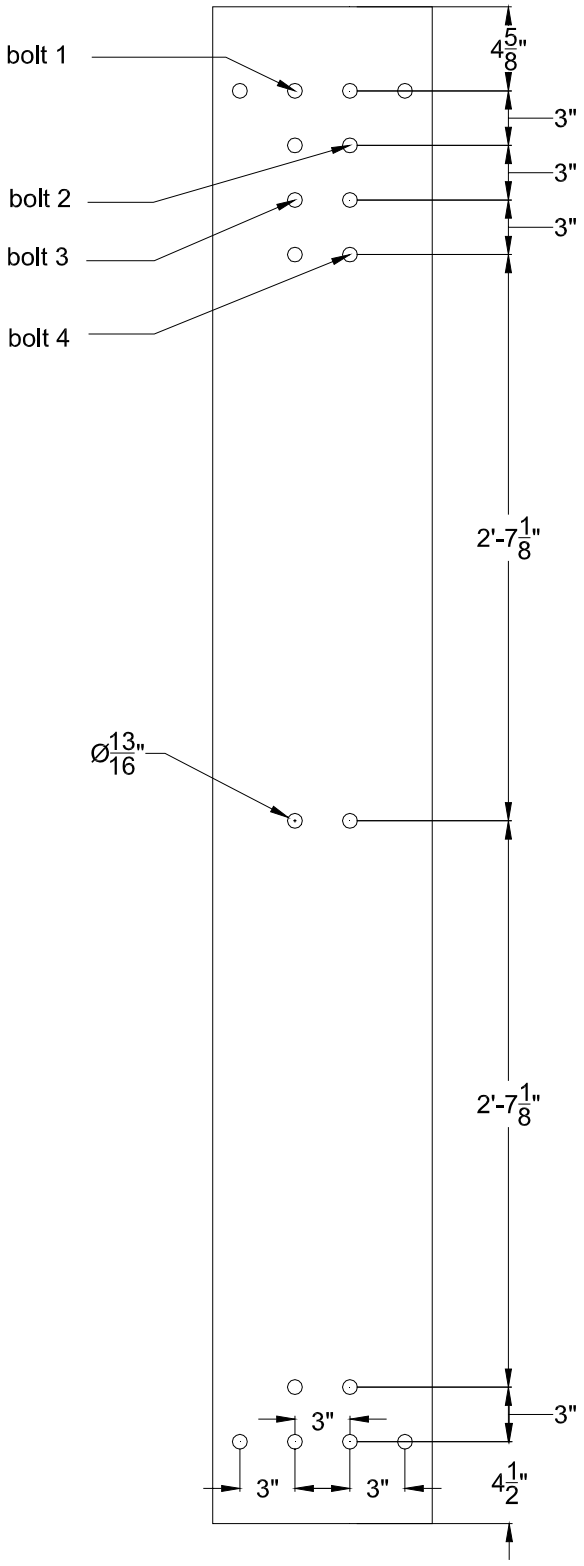

Figure H-6 LH-1 Gaged Bolt Orientation Viewed From the West

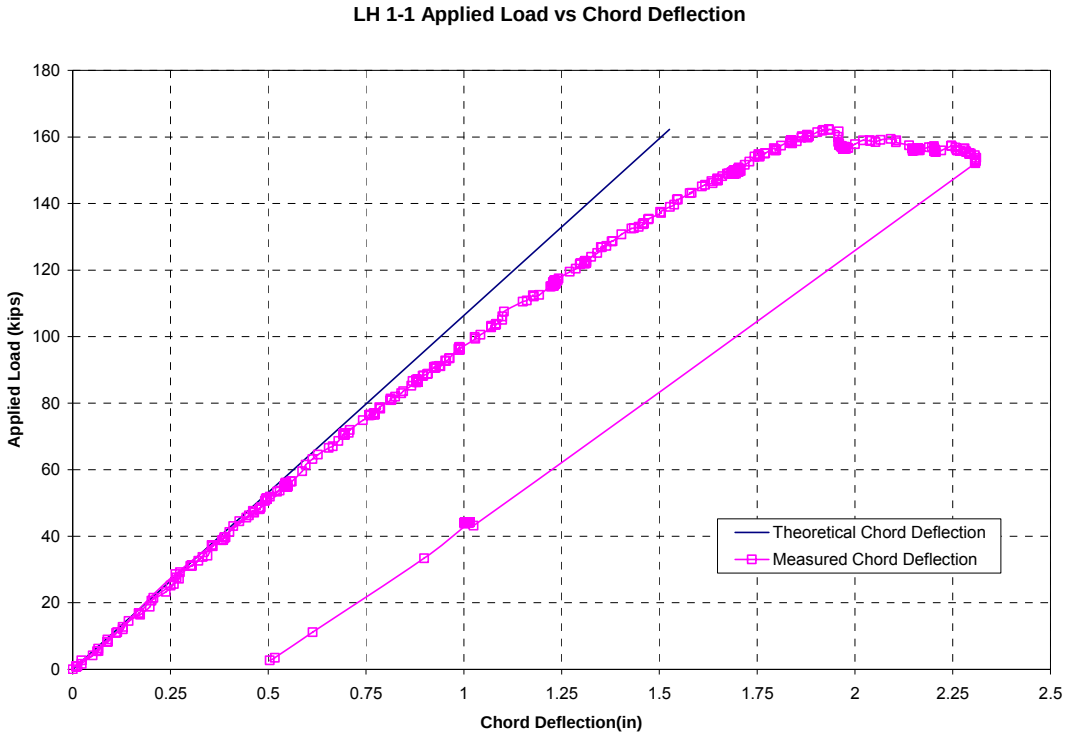

Figure H-7

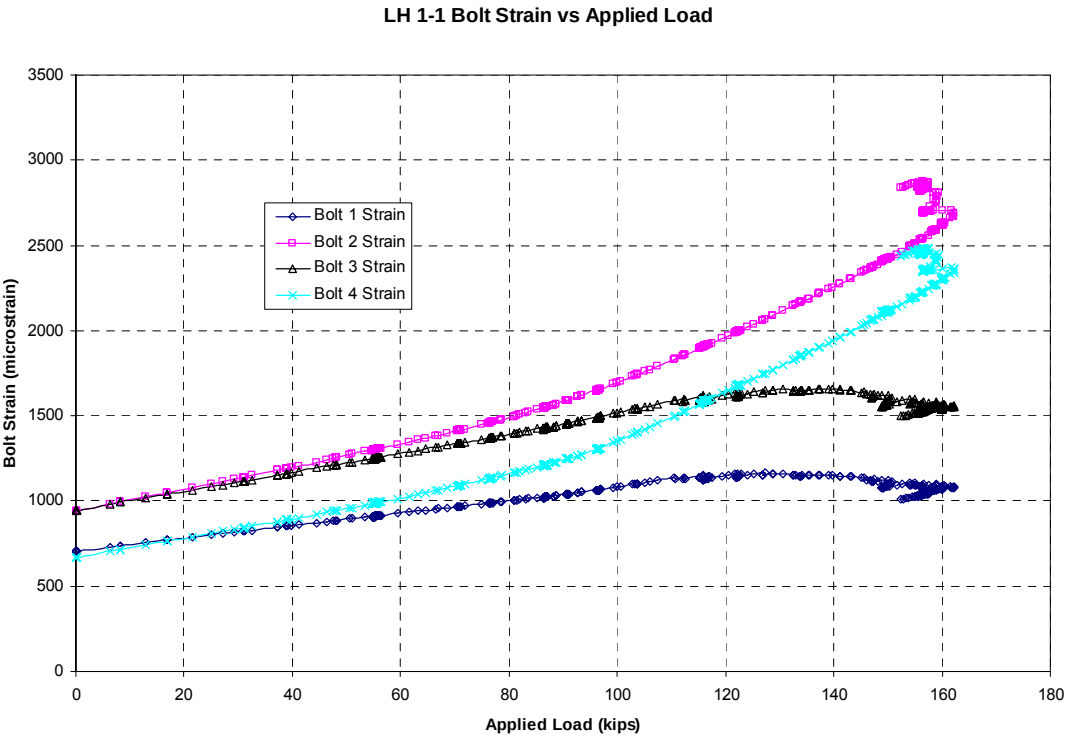

Figure H-8

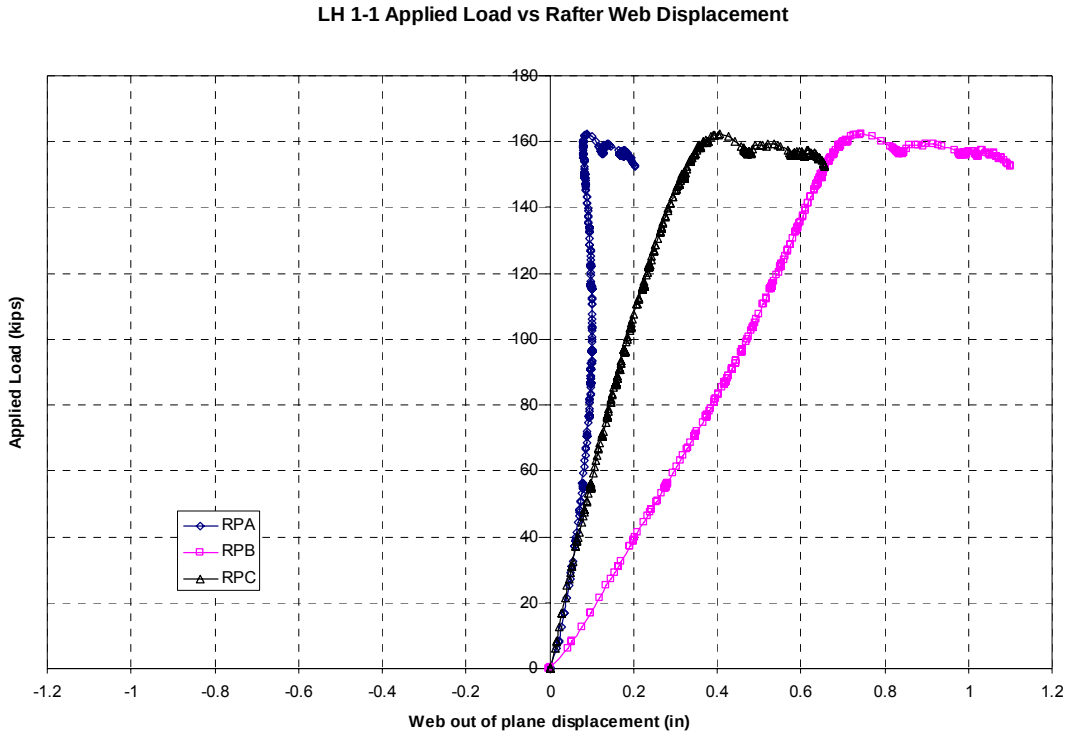

Figure H-9

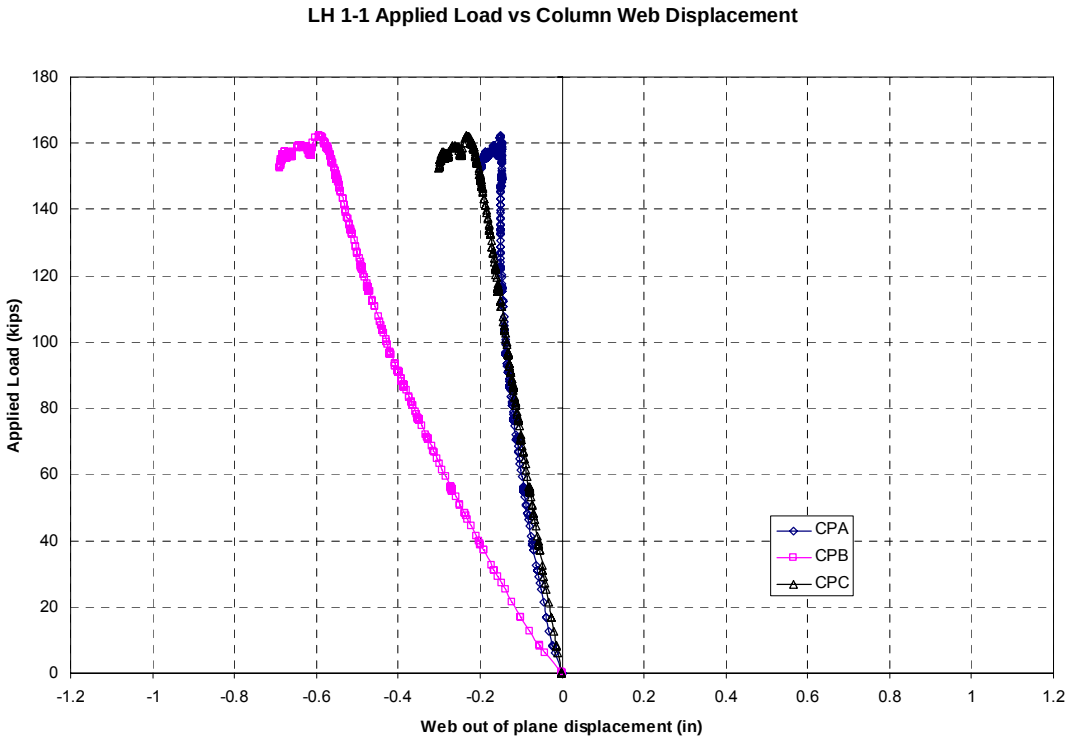

Figure H-10

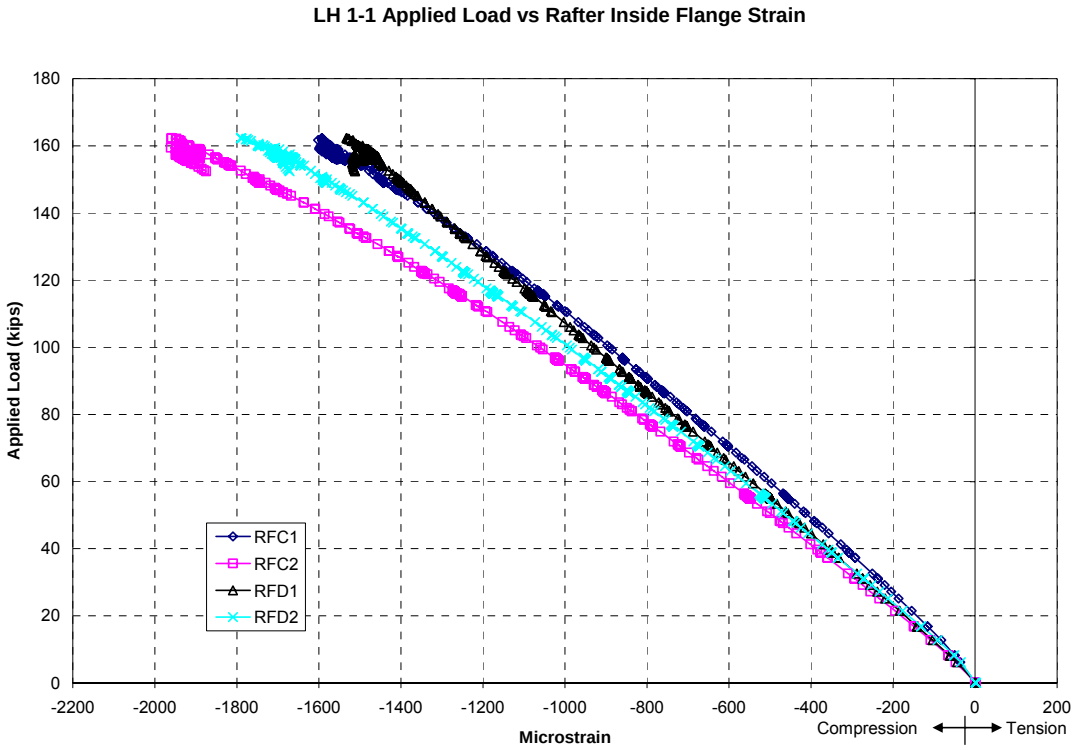

Figure H-11

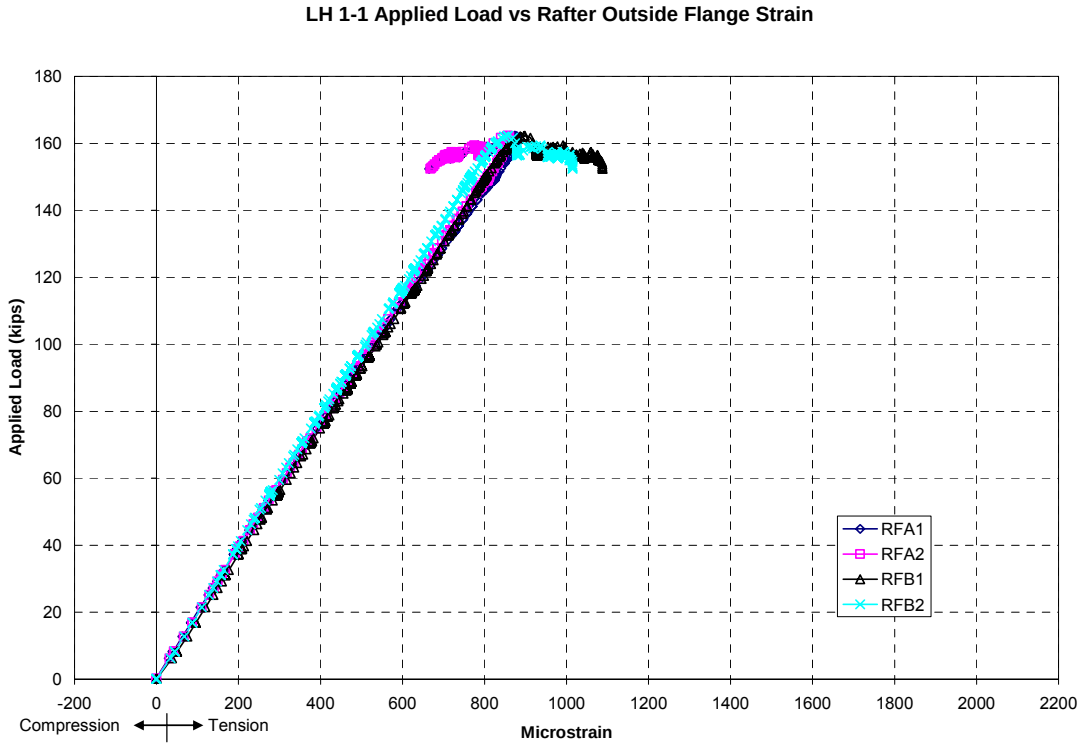

Figure H-12

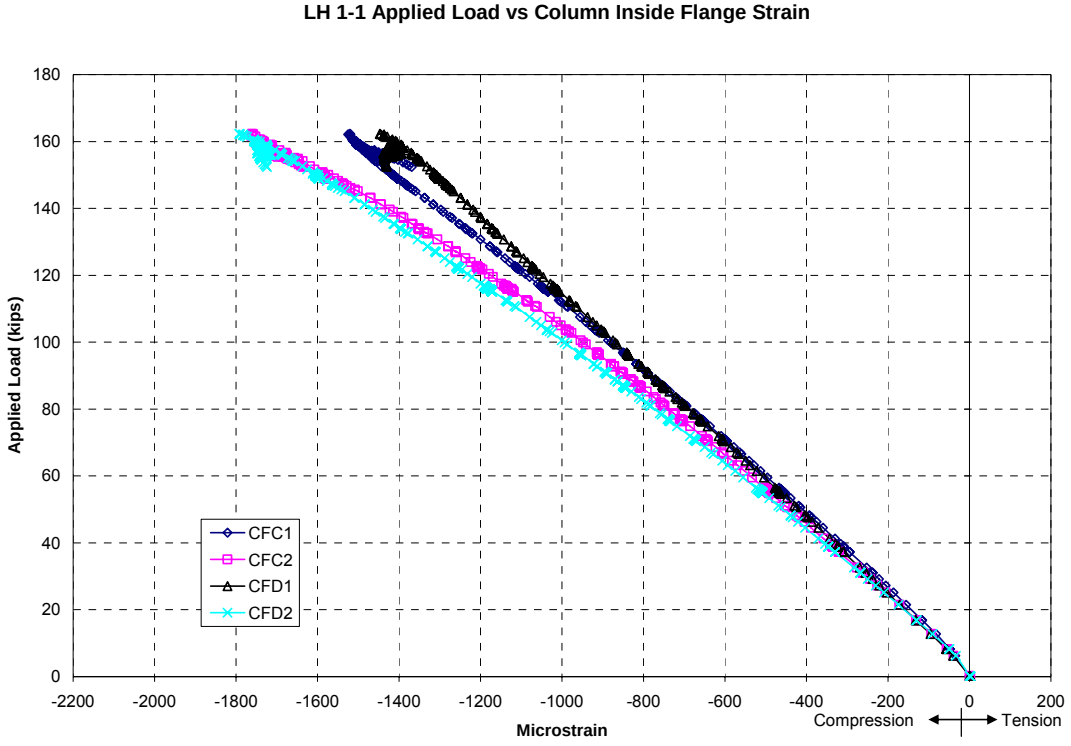

Figure H-13

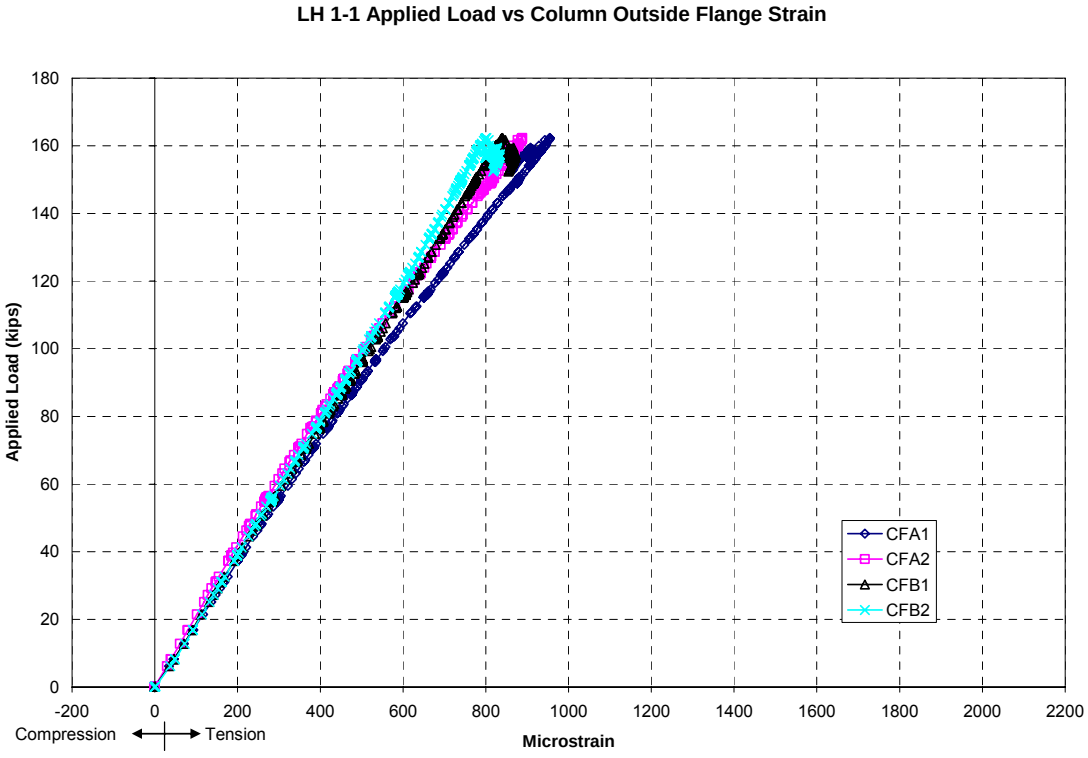

Figure H-14

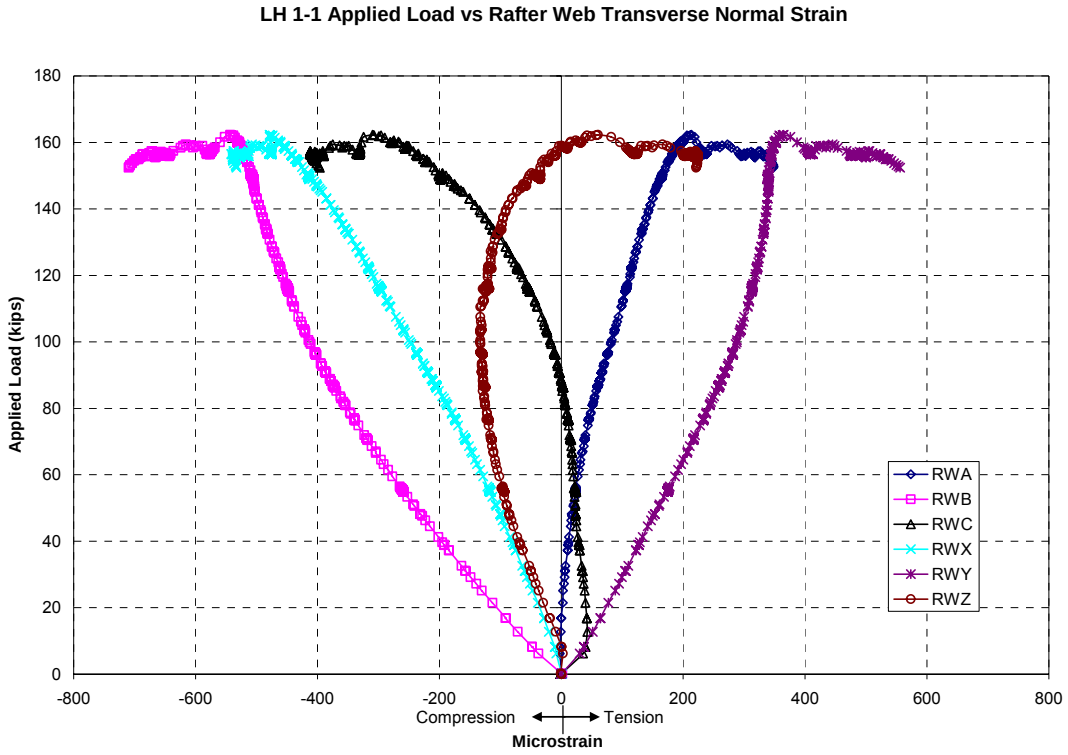

Figure H-15

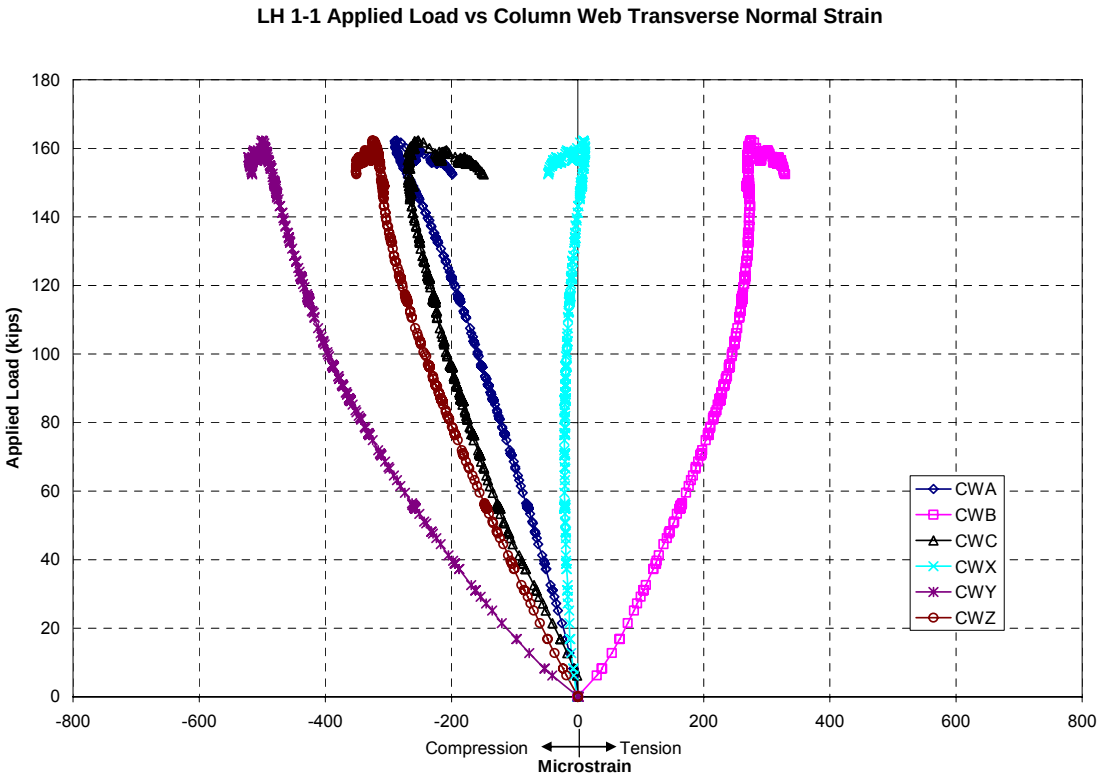

Figure H-16

APPENDIX I. SAMPLE CALCULATIONS

I.1 Shear Forces and Strength Calculations

I.1.1 Introduction

Sample calculations for the determination of modified and unmodified shear forces, and predicted shear strength are presented in this section. The provisions in Section 3.3.1 were used to determine the shear forces, and the AISC provisions for shear (AISC 2005a), which are in Section 3.3.2, were used determine shear strength. Only the column member of the LH-1 specimen is presented. The analysis cross-section measured dimensions are shown in Figure I-1 and the specimen geometry is shown in Figure I-2.

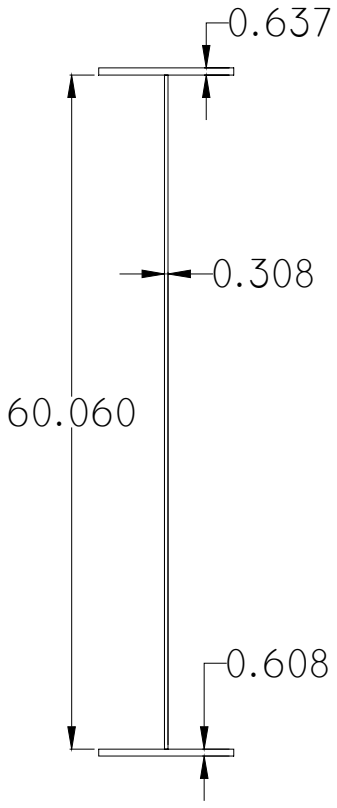

Figure I-1 Cross-Section B-B Measured Dimensions

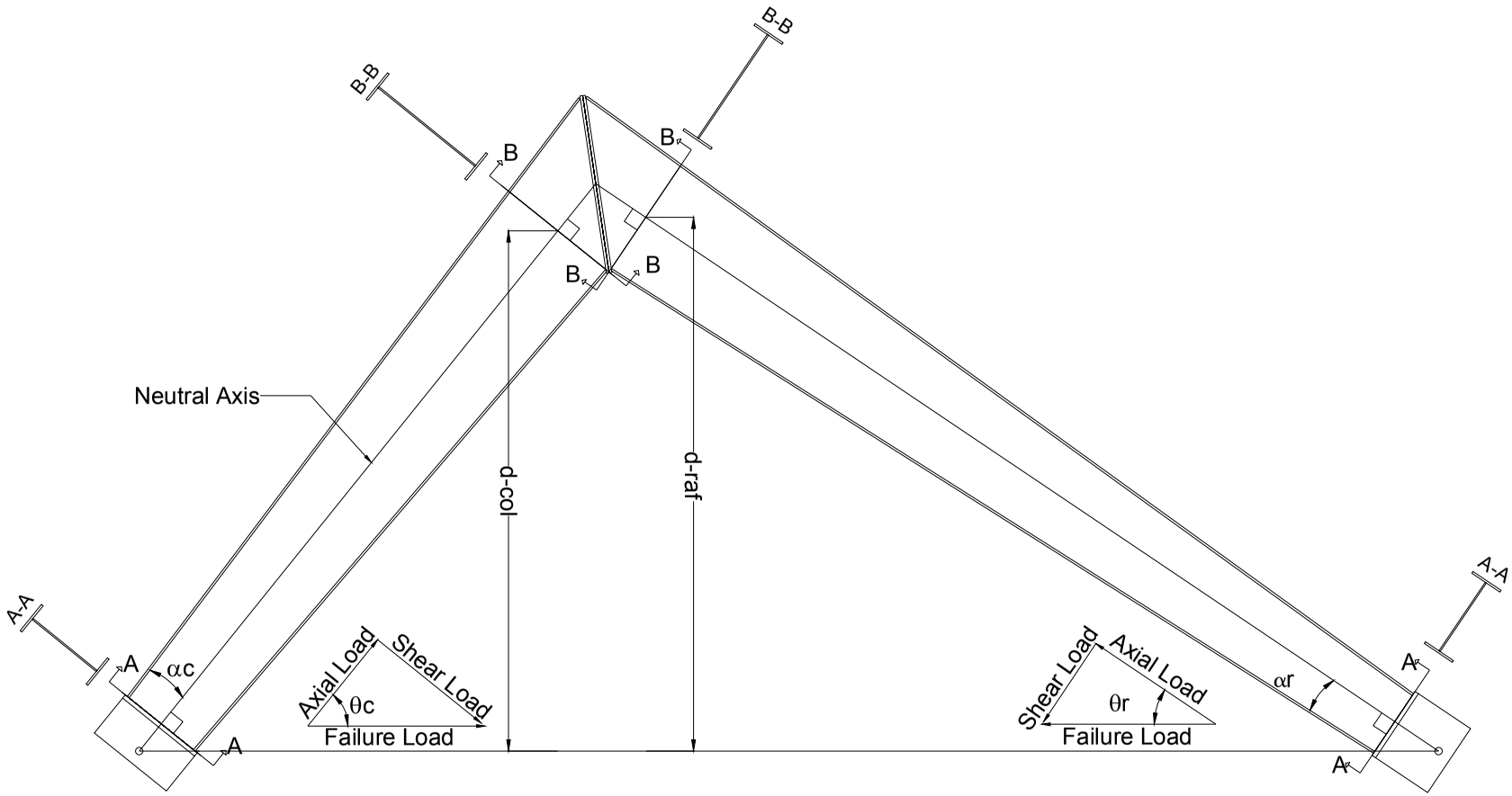

Figure I-2 LH-1 Specimen Geometry

I.1.2 LH-1 Column Properties

h	=	60.06 in.	F_{yw}	=	61 ksi
t_w	=	0.308 in.	$P_{failure}$	=	162.3 kips
b_f	=	12.0 in.	A_g	=	33.89 in^2
t_{tf}	=	0.637 in.	I_x	=	19429 in^4
t_{cf}	=	0.618 in.	S_{xt}	=	637.84 in^3
D_{col}	=	133.8 in.	S_{xc}	=	629.62 in^3
θ	=	44.69°	A_{tf}	=	7.42 in^2
α	=	5.3°	A_{cf}	=	7.64 in^2

I.1.3 Determination of Shear Forces

The experimental loads at failure are determined at section B-B by statics and the calculations reference the geometry given in Figure I-2.

Shear At Failure	Axial Load at Failure	Moment at Failure
$V = P_{failure}\sin(\theta)$	$P_a = P_{failure}\cos(\theta)$	$M = P_{failure}D_{col}$
$V = 162.3kips \cdot \sin(44.69)$	$P_a = 162.3kips\cos(44.69)$	$M = 162.3kips \cdot 133.8in$
$V = 114.14kips$	$P_a = 115.38kips$	$M = 21{,}715.74in \cdot kips$

The unmodified experimental shear force, $V_{exp,u}$ is equal to the applied shear at failure.

$$V_{\exp,u} = V = 114.14kips$$

The experimental modified shear force, $V_{exp,m}$ is determined according to Equation (3-1), Equation (3-2) and Equation (3-3), with reference to Figure I-3.

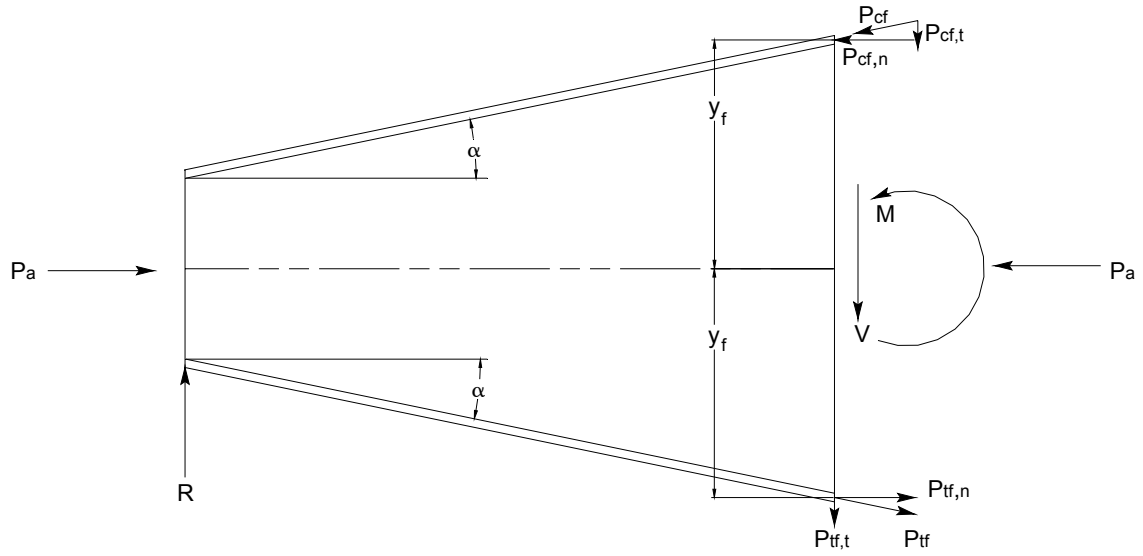

Figure I-3 Flange Contributions to Modified Web Shear at Section B-B

Compression flange axial force, P_{cf}:

$$P_{cf} = \frac{P_a A_{cf}}{A_g} + \frac{MA_{cf}}{S_{xc}\cos(\alpha)}$$

$$P_{cf} = \frac{115.38kips \cdot 7.64in^2}{33.89in^2} + \frac{21{,}715.74in \cdot kips(7.64in^2)}{629.62in^3\cos(5.3)}$$

$$P_{cf} = 26.01kips + 264.64kips$$

$$P_{cf} = 290.65kips$$

Tension Flange axial force, P_{tf}:

$$P_{tf} = -\frac{P_a A_{tf}}{A_g} + \frac{MA_f}{S_{xt}\cos(\alpha)}$$

$$P_{tf} = -\frac{115.38kips \cdot 7.42in^2}{33.89in^2} + \frac{21{,}715.74in \cdot kips(7.42in^2)}{637.84in^3 \cos(5.3)}$$

$$P_{tf} = -25.26kips + 253.70kips$$

$$P_{tf} = 228.44kips$$

Experimental modified shear force, $V_{exp,m}$:

$$V_{\exp,m} = V - \left(P_{cf} + P_{tf}\right)\sin(\alpha)$$

$$V_{\exp,m} = 114.14kips - \left(290.65kips + 228.44kips\right)\sin(5.3)$$

$$V_{\exp,m} = 66.2kips$$

I.1.4 Predicted Shear Strength

Rafter properties:

Panel length between cross-section A-A and B-B, a = 175.92 in.
Panel height at cross-section A-A, h_o = 27.53 in.
Web shear area, $A_w = h \cdot t_w = 60.06in. \cdot 0.308in. = 18.50in^2$

Calculate aspect ratio:

$$\frac{a}{h} = \frac{175.92in}{27.53in} = 6.36 > 3.0 \qquad \therefore k_v = 5.0$$

Calculate Shear Coefficient, C_v:

$$\frac{h}{t_w} = \frac{60.06in}{0.308in} = 195.0 > 1.37\sqrt{\frac{k_v E}{F_{yw}}} = 1.37\sqrt{\frac{5.0\left(29000ksi\right)}{61ksi}} = 66.79$$

$$C_v = \frac{1.51Ek_v}{\left(h/t_w\right)^2 F_y}$$

$$C_v = \frac{1.51\left(29000ksi\right)5.0}{\left(195.0\right)^2 61ksi}$$

$$C_v = 0.094$$

Calculate Shear Strength:

$$V_{pred} = 0.6F_y A_w C_v$$

$$V_{pred} = 0.6\left(61.0ksi\right)\left(18.50in^2\right)0.094$$

$$V_{pred} = 63.91kips$$

I.2 Shear Stress from Strain Data

I.2.1 Introduction

Sample calculations for the shear stresses determined from strain gage data are presented in this section. The calculation of stress in the web at the gage location nearest the compression flange of the column member from specimen SH-1 is presented. The strains were recorded at an applied load of approximately 2.6 kips, which is 10% of the failure load of 26.48 kips. The strain gages at this location are CWC and CWZ and their orientation is shown in Figure A-4 and Figure A-5 of Appendix A. It can be seen in Figure A-4 that CWZ grid 1 is parallel to the neutral axis, CWZ grid 3 is perpendicular to this axis, and CWZ grid 2 is oriented at a 45° angle to grids 1 and 3. CWZ grid 1 will be used to represent the x-axis and CWZ grid 3 will be used to represent the y-axis. This is orientation is shown in Figure I-4. The strain gage rosette CWC was oriented on the opposite face of the web such that CWC grid 1 was collinear with CWZ grid 3, CWC grid 3 was collinear with CWZ grid 1 and CWC grid 2 was collinear with CWZ grid 2.

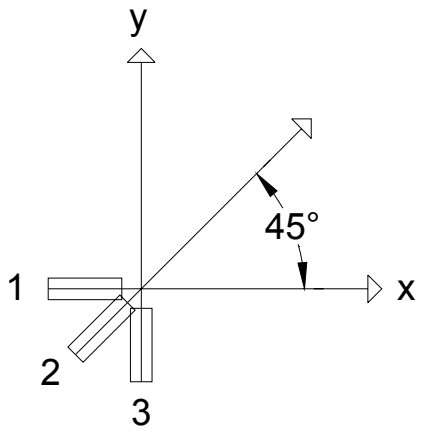

Figure I-4 Strain gage rosette CWZ

These collinear grids were averaged and the orientation of gage CWZ was used as the reference orientation for the following calculations. According to Beer et al. (2002), the shear strain γ_{xy} which is the shear strain on the element of material under the gage, in a direction perpendicular to the neutral axis is given by:

$$\gamma_{xy} = 2\varepsilon_2 - (\varepsilon_1 + \varepsilon_3) \qquad \text{(I-1)}$$

Where: ε_1 = Grid 1 strain
ε_2 = Grid 2 strain
ε_3 = Grid 3 strain

According to Hooke's law the shear stress τ_{xy} is related to the shear strain by:

$$\tau_{xy} = G\gamma_{xy} \tag{I-2}$$

Where: τ_{xy} = Shear stress
G = Shear Modulus
γ_{xy} = Shear strain

And the shear modulus, or modulus of rigidity is defined as:

$$G = \frac{E}{2(1+\nu)} \tag{I-3}$$

Where: E = Young's Modulus
ν = Poisson's ratio

I.2.2 Calculation of Shear Stress

The measured shear strains at locations CWZ and CWC were as follows, and the averages are given as CWZ′, as described in Section I.2.1:

CWZ (microstrain)	CWC (microstrain)	CWZ′ (microstrain)
ε_1= -51.23	ε_1= -1.93	ε_1= -113.65
ε_2= 145.88	ε_2= -24.49	ε_2= 60.70
ε_3= 3.87	ε_3= -176.06	ε_3= 0.973

The shear strain on the strain gaged element of web is:

$$\gamma_{xy} = 2\varepsilon_2 - (\varepsilon_1 + \varepsilon_3)$$

$$\gamma_{xy} = 2(60.70) - (-113.65 + 0.973)$$

$$\gamma_{xy} = 234.08 \text{ microstrain}$$

The modulus of rigidity is:

$$G = \frac{E}{2(1+\nu)}$$

$$G = \frac{29000ksi}{2(1+0.3)}$$

$$G = 11153.8ksi$$

The shear stress on the cross-section at the location of the gages CWC and CWZ is:

$$\tau_{xy} = G\gamma_{xy}$$

$$\tau_{xy} = 11153.8ksi(234.08\mu\varepsilon)\left(\frac{10^{-6}\varepsilon}{\mu\varepsilon}\right)$$

$$\tau_{xy} = 2.61ksi$$

It is assumed that this stress is constant over an area of web adjacent to these gages and the shear force is the product of calculated stress and a third of the web area. The total shear force in the web at the cross-section is the sum of this computed force and the forces similarly obtained at the other two strain gage rosette locations. So, for shear stress location τ_3:

$$A_{w,3} = t_w \frac{h}{3}$$

$$A_{w,3} = 0.131in\frac{21.57in}{3}$$

$$A_{w,3} = 0.942in^2$$

$$V_{w,3} = \tau_{xy} A_{w,3}$$

$$V_{w,3} = 2.61ksi(0.942in^2)$$

$$V_{w,3} = 2.46kips$$

Vita

Nicholas A. Redmond was born in Panama City, Florida in 1978 to Rockland and Sheryl. He lived for several years in Chattanooga, Tennessee and Ekalaka, Montana, before settling in Chapin, South Carolina. Upon graduating from Chapin High School in 1996 Nick moved to Columbia, SC and worked for several years in construction related fields before starting his own carpentry business in 2001. In 2003 he pursued a Bachelor of Science Degree in Civil Engineering at the University of South Carolina, and graduated with honors in 2006. Nick continued his studies at Virginia Tech that same year as a research assistant, in pursuit of a Master of Science Degree in Civil Engineering. Upon graduation he plans to relocate to Seattle, Washington and work as a structural design engineer with Magnusson Klemencic Associates.

Nick married Leah R. McComb in March of 2000, and they have a daughter, Lillian, age 4 and a son, Samuel, age 15 months.